CS (AR)-2/2008

ASSESSMENT OF GROUNDWATER QUALITY AND NITRATE TRANSPORT MODELING IN THE COASTAL AQUIFER OF KAKINADA, ANDHRA PRADESH

NATIONAL INSTITUTE OF HYDROLOGY
JAL VIGYAN BHAWAN
ROORKEE - 247 667 (UTTARAKHAND)

2008

DIRECTOR
Sri R D Singh

COORDINATOR
Dr. Bhishm Kumar

HEAD
Dr. Y R Satyaji Rao

STUDY GROUP
Dr. Y R Satyaji Rao
Dr. Bhishm Kumar

SUPPORTING STAFF
Shri T. Vijay
Shri D. Mohana Rangan

PREFACE

The use of septic-soak pit system is a common practice in India due to non-availability of organized sewer lines especially in the towns and cities. High density of septic system is one of the major sources of groundwater nitrate contamination in coastal areas. Therefore, there is a need for a comprehensive understanding of nitrate contamination from septic systems for better management of groundwater quality and public health.

Keeping in view the importance of this field problem, the Deltaic Regional Centre of NIH, Kakinada has undertaken the field study titled `**Assessment of groundwater quality and nitrate transport modeling for the coastal aquifer of Kakinada, Andhra Pradesh'**. The study has been carried out by Dr Y R Satyaji Rao, Scientist E2 and Dr Bhishm Kumar, Scientist F, with the technical support provided by Sri T. Vijaya, Sr.R.A and Sri D. Mohana Rangan, Tech Grade II.

This study is under the work program of Deltaic Regional Centre, NIH, Kakinada during the period of 2004-07.

DIRECTOR

ABSTRACT

Groundwater quality characterization revealed that the ion concentrations are in the order of $HCO_3^- > Cl^- > SO_4^{2-} > NO_3^-$ (anions) and $Na^+ > Ca^{2+} > K^+ > Mg^{2+}$ (cations2) in the study area. The Piper classification indicated that most of the groundwater samples collected from the study area are Na^+- HCO_3 type. Results of multivariate analysis (PCA) showed that salinity and nutrients are major contaminants in the study area. As the maximum observed Cl^-/HCO_3^- ratio is limited to 7.37 in the shallow groundwater, the present salinity is due to marine environment of coastal aquifer and present land use practices not from the seawater intrusion. Among nutrients, nitrates are high in groundwater (up to 421 mg/l) in the study area. The comparison between Nitrogen load from septic systems and its average groundwater quality (NO_3^-, PO_4^{3-}, EC and K^+) indicated that the shallow groundwater nitrate contamination is influenced by septic system and unsewered conditions in the study area.

RISK-N model results indicated that the % of septic systems NO_3^--N contribution into groundwater is mostly dependent on groundwater table condition and population density. The sensitivity analysis of RISK-N model indicated that intermediate vadose zone thickness, seepage from septic tank-soak pit systems, saturated zone denitrification rate, and average plot size are most influential factors in estimation of NO_3^--N from septic systems. Results of the present study can be used effectively in addressing groundwater quality problems and in decision making for better groundwater quality management and public health.

CONTENTS

LIST OF FIGURES

LIST OF TABLES

1.0 INTRODUCTION

1.1 Background

The seawater intrusion into aquifer is one of the common problems in coastal areas. The diffused seawater interface in the coastal aquifer mainly depends on recharge and groundwater table depth. Apart from seawater intrusion problems, high nitrates in groundwater have been observed in many parts of India due to green revolution (Bobba et al., 1997; Agrawal et al., 1999). Groundwater nitrates in urban areas are also increasing at an alarming rate due to inadequate household and community sanitary provisions (sewerage systems) especially in developing countries. The percentage of sewered population in India is almost negligible in most of the rural areas and is less than 50% in most of the medium and small towns. As a result, the contamination of groundwater by unsewered conditions is one of the most important environmental problems in India. The rate of wastewater generation in India during the year 1981 was estimated to be 74,529 million litre/day (i.e 27 km^3 annually), and about 110, 000 million litre/day (i.e 40 km^3 annually) in the year 2001 (MoWR, 2000). The impact of these sources is more pronounced in the urban coastal aquifers where the density of population is high and groundwater table is very shallow.

Nitrate ion is generally considered as anthropogenic source indicator of the extent of pollution of urban groundwater from domestic wastes and leaky septic tanks (Swamy and Rao, 1989; Reay, 2004; Navarro and Carbonell, 2007). BGS (1996), and Wakida and Lerner (2005) reviewed the sources of groundwater nitrate due to non-agricultural activities and highlighted that major source of groundwater contamination is due to leakage from sewers and septic tanks. High nutrients especially elevated nitrate concentrations (more than 45 mg/l) in shallow groundwater were observed in many urbanized areas (Rengaraj et al., 1996; Trauth and Xanthopoulos, 1997; Voudouris et al., 2004).

Kapoor and Viraraghavan (1997) reviewed developments in the field of nitrate removal from drinking water. Treatment processes like ion exchange, biological denitrification, chemical denitrification, reverse osmosis, electro dialysis, and catalytic denitrification can remove nitrates from water with varying degree of efficiency, cost and ease of operation. It was concluded that ion exchange and biological denitrification are more acceptable for nitrate removal than reverse osmosis. Ion exchange is more viable for groundwater while biological denitrification is preferred for surface water.

Most treatment processes are expensive and, therefore efforts are required to understand and control nitrate contamination in urban as well as in agricultural areas. Much work has been carried out to quantify nitrate leaching in agricultural areas, but very limited studies are available for urban coastal aquifers where high density of population, unsewereed and shallow water table conditions prevails. Therefore, Deltaic Regional Centre, NIH, Kakinada initiates the present

study to understand the impact of septic systems on the coastal aquifer of Kakinada, Andhra Pradesh and all the expenditure on the study is provided by the Institute only.

1.2 Scope and Objectives

Reduction in fresh water availability of drinking water has necessitated identification and quantification of pollution sources for protecting further degradation of groundwater quality. Presently many research activities aim at to establish relationship between specific land use pattern, its pollution potentials and the resulting groundwater quality. The United States Environmental Protection Agency (USEPA) established a maximum concentration limit of 10 mg/l nitrate-nitrogen (NO_3^--N) which is equivalent to 45 mg/l as total nitrate. This is the same value as specified by the World Health Organization (WHO, 1984) and Bureau of Indian Standards (BIS, 1991) in its drinking water quality guidelines, and is close to the European Economic Community (EEC) water quality directive of 11.3 mg/l (NO_3^--N) for its maximum admissible concentration.

Keeping in view the importance of growing concern of groundwater nitrate contamination in urban areas and its impact on human health/environment, and expensive treatment processes, a systematic methodology consisting of characterization of groundwater quality, assessment of nitrogen loading from septic systems and nitrate transport modeling in subsurface zone is formulated in the present study. The specific objectives of the present research are following:

- Characterization of groundwater quality in the Kakinada urban coastal aquifer using multivariate and geostatistical analysis
- Development of GIS based methodology for mapping nitrogen load from septic systems in and around Kakinada town
- Nitrate leaching estimation from septic systems using RISK-N model
- Sensitivity analysis of model parameters in estimation of nitrate leaching from septic systems

2.0 REVIEW OF LITERATURE

An intensive literature review has been carried out in the present study and briefed about health hazards of excessive nitrate concentrations in drinking water, history of septic tanks and effluent chemical characteristics. Further, state of art of the statistical techniques used for characterization of groundwater quality reviewed. The advantages and disadvantages of various models to study nitrate contamination from septic systems are also critically reviewed. The literature review details are given in the following sections.

2.1 Health effects of nitrate consumption in drinking water

Nitrate found in drinking water is reduced to nitrite (NO_2) in the gastrointestinal tract of infants during the first three months of life, and on a smaller scale by saliva in human of all ages (Canter, 1997). The presence of nitrite in the body can cause methemoglobinemia, which describes the condition in which hemoglobin is oxidized to methemoglobin. As the level of methemoglobin in the blood increases, the ability of the blood to transport and transfer oxygen is diminished. The result is oxygen starvation, known as cyanosis, which results in cellular anoxia. Young infants are most susceptible to methemoglobinemia, and the most obvious visible effects is the skin turning blue; as a result, it is commonly referred to as "blue baby syndrome'. Fortunately, the effects of methemoglobinemia can be medically treated rapidly, and there are no cumulative effects associated with repeated cases of methemoglobinemia.

Another concern of nitrate contamination is the possibility that nitrite created from nitrate in the body can act as a carcinogen. Correlations have been made, linking nitrate exposure and gastric cancer risk in Colombia, Chile, and England (Canter, 1997). However, it is not certain that nitrite causes gastric cancer because of positive correlations between gastric cancer and a number of other dietary and environmental factors in these countries. Research into the role of nitrite as a carcinogen is continuing, but the role of nitrite as a precursor to the production of carcinogenic nitrosamines has already been clearly demonstrated. The consumption of nitrate rich water also cause a large number of diseases like dizziness, abdominal disorder, vomiting, weakness, high rate of palpitation, mental disorder and even Non Hodgkin stomach cancer (Ward et al., 1996; Majumdar and Gupta, 2000). The epidemiological study carried out by Gupta et al. (1999) on nitrate in drinking water for the Jaipur region, India revealed that there is a significant interdependence among drinking water nitrate concentrations, cytochrome b_5 reductase activity and recurrent stomatitis. The water and excreta related communicable diseases were reviewed by Mara and Feachem (1999) and stated that all the deaths and loss of disability-adjusted life years occurred in developing countries are 99.9 and 99.85%, respectively.

2.2 Septic tanks

The first reported use of the household septic tank was in France in 1860 when John Louis Mouras and his friend Abbe Moigno discovered that a 'box' placed between the house and

the cesspool trapped excrement, reduced that amount of solids and produced a clarified liquid that more quickly entered the soil. In the United States, Philbrick first used the household septic in 1883 with a two-chamber tank design, utilizing an automatic siphon for intermittent effluent disposal. Since then, the septic tank is in use in most parts of the world. Septic tanks were first introduced in England by Cameron in 1895 and are still in use today in a form that would be instantly recognized by these early sanitary pioneers. The main application for septic tanks in the U.K. is in the disposal of sewage from many small communities, usually from premises, which are not connected to a public sewer. In India, mainly pit latrine, water closet and other latrine are practicing in each house. As per the census of India 2001 (Table H-10), the percentage of house latrines in the form of pit latrine, water closet, other latrines and no latrine are 10.3, 7.1, 4.5 and 78.1% respectively in rural areas. Similarly, the percentages in urban areas are 14.6, 46.1, 13.0 and 26.35 respectively. Most septic tanks discharge to land or underground strata, although some discharge to watercourses.

The satisfactory performance of septic tanks depends on a number of factors, including their design, installation, maintenance and mode of operation. For the elaborate description on septic tanks, readers may refer Kaplan (1987). Mani et al. (2007) presented design of a modified compact septic-tank and implemented for sanitation at Tsunami affected island Kodaiyampalayam, in Nagapatnam District, Tamilnadu, India, where the groundwater table is very shallow. The design of the septic tank is such that in the event of any flooding, the toilets (septic-tank) would be able to function normally once the water recedes. They also mentioned that, identifying a sanitation design in response to the community needs and in response to the local environmental conditions led to the development of a modified Compact Septic-tank.

Septic systems consist of two main redox environments, and sometimes a third depending on soil and effluent conditions. The first is the anaerobic septic tank, in which dissolved oxygen (DO) content is low and organic matter is high. As a result, microorganisms use organic C, H^+, and SO_4^{2-} as electron acceptors in the oxidation of organic matter, producing CO_2, H_2, and sulfide. Approximately 90% of the nitrogen entering the septic tank is bound in organic molecules, but nitrogen is released from these molecules as NH_4^+ during the septic tank processes. As a result, the effluent from the septic tank contains approximately 75% NH_4^+-N and 25% organic nitrogen compounds.

The second redox environment is the aerobic drain field or soak pit, located in unsaturated sediments. In this aerobic zone, O_2 acts as the electron acceptor as organic C is transformed into CO_2. The availability of O_2 also has a very important effect on the nitrogen transformation process, as NH_4^+ is quickly oxidized (nitrified) to NO_3^-. Because organic matter removal through oxidation is the primary purpose of the aerobic drain field zone or soak pit, nitrate is an inevitable by product given the soil and water conditions. In certain cases, part of the aerobic zone may 'fail' due to clogging of organic matter within the sediments, and a third redox environment is created in which anaerobic conditions prevail. In this zone, denitrification may

be an important nitrate loss mechanism if enough labile C is present. In properly functioning septic systems, however, this third anaerobic zone would not be created.

2.3 Chemical composition of septic tank effluent and its effect on groundwater quality

Butler and Payne (1995) reviewed the septic tank problems and practices in general and particularly in the U. K. They found that the main problems of septic systems are inadequate ventilation of drains, blocked drainage field, tank full of sludge, undersized tank, deliberate outflow connection made, shallow groundwater table.

Whelan and Titamnis (1982) studied chemical variability of septic effluent from five households for 15 days in Perth, Western Australia. The chemical parameters include N, P, Ca, Mg, K, Zu, Cd, Cr, Pb, Mg and Temperature, redox potential, conductivity and BOD_5. Samples from the five households differed in the values obtained but the differences were small. Little daily variation occurred in the effluent from five households. The concentration of total nitrogen (N) in the effluent was about 100 mg/l and that of phosphorous (P) was about 15 mg/l. The mean annual N and P loading in the effluent over the five households were 3.8 kg N/head/yr and 0.6 kg P/head/yr. The chemical composition of the effluent was very similar to that found in New Zealand, Canada and USA. The overview of septic systems and nitrogen transformations is nicely presented as a conceptual model by Wilhelm et al. (1994). It describes the biogeochemical evolution of domestic wastewater.

Rajasekhar et al. (1994) evaluated septic tank effluent characteristics and its impact on groundwater in the city of Tirupathi, Andhra Pradesh, India. Total 32 septic effluents samples were randomly selected in the city and analyzed for chemical and bacteriological parameters. The average values are: pH (7.2), EC (1420 microsimens/cm), TDS (1008 ppm), Suspended solids (238 mg/l), BOD_5 (276), Ammonia-N (61.5 mg/l), Organic-N (34.6 mg/l)), Nitrate-N (0.10 mg/l), Phosphates (17.8 mg/l), Chlorides (180 mg/l), Sulphate (52 mg/l), Hardness (252 mg/l), total coliform/100 ml ($1x10^7$), Fecal coliform/100 ml ($8x10^6$) and Fecal strepto-cocci/100 ml ($29x10^4$). It was stated that the septic effluents contain high pollution strength and suggested for good management system for the ultimate disposal of these effluents, which is essential to prevent groundwater pollution. The groundwater nitrate is already reached up to 150 mg/l in some places in the study area.

Schouw et al. (2002) analyzed chemical composition of human excreta in three areas of the Southern Thailand: Kuan Lang, Phattalung and Prik. The inhabitants of three areas represent people of Southern Thailand by age, sex, occupation, religion and type of residence. Information on average values of generation rate and chemical composition indicated that there was no significant variation found between the results for human excreta from the 15 individuals and further more there was no significant influence of age, sex, occupation or religion on the chemical composition. The only significant variation was that the older people excreted larger

amounts of total wet matter than the younger, which could be due to a higher water intake, in order to reduce the risk of constipation. The generation rate found was 0.0 -1.2 L urine/per capita/day and 120-400 g wet faeces/ per capita/day. The generation rate range of the elements in the excreta was 7.6 –7.9 g N/per capita/day, 1.6-1.7 g P/per capita/day, 1.8-2.7 g K/per capita/day, 1.0-1.1 g S/per capita/day, 0.75-1.5 g Ca/per capita/day, 0.25-0.4 g Mg/per capita/day, 9.0-16.0 mg Zn/per capita/day, 1.4-1.5 mg Cu/per capita/day, 0.3 mg Ni/per capita/day, 0.002-0.003 mg Cd/per capita/day, 0.07-0.14 mg Pb/per capita/day, 0.01 mg Hg/per capita/day and 0.8-1.1 mg B/per capita/day. The metals (Ca, Mg, Zn, Cu, Ni, Cd, Pb, Hg) are mainly excreted via the faeces and the remaining elements (N, P, K, S, B) are mainly excreted via the urine.

Montangero and Belevi (2007) studied the nutrients flows from the on site sanitation installations (septic tanks, pit and urine diversion latrines). Nitrogen and phosphorus separation in different output materials from these on site sanitation installations were determined. Use of expert elicitation technique proved to be effective, particularly in the context of developing countries where data is often scare but expert system readily available. In Vietnam, only 5-14 % and 11-27% of the nitrogen and phosphorus respectively are removed from septic tanks with the faecal sludge. The remaining fraction leaves the tank via the liquid effluent. Unlike septic tanks, urine diversion latrines allow immobilizing most of the nutrients either in the form of stored urine or dehydrated fecal matter.

Based on the above review, it may be concluded that the septic effluent contains most of the nitrogen in the form of ammonia-nitrogen and organic nitrogen, but is negligible in the form of nitrate-nitrogen.

2.4 Statistical analysis of groundwater quality data

The increasing problem of groundwater contamination has resulted in a need for information on groundwater quality and awareness on the importance of groundwater quality monitoring. The monitored data is often used to provide early warning of pollution events and the effectiveness of cleanup efforts. The statistical analysis of water quality data is required to detect changes in groundwater quality over time and space. Some of the important works on statistical analysis of groundwater quality data are reviewed in the following sections.

Guler et al. (2002) studied many available graphical and statistical methodologies used to classify water samples including Collins bar diagram, pie diagram, Stiff pattern diagram, Schoeller plot, Piper diagram, Q-mode hierarchical cluster analysis, k-means clustering, principal component analysis, and fuzzy k-means clustering by applying to the south Lahanton hydrologic region of southeastern California where wide variety of climatic conditions, hydrologic regimes and geologic environments existing. This study provides an opportunity to test the performance of many of the available graphical and statistical methodologies used to classify water samples.

The study revealed that the use of graphical techniques have limitations as compared with the multivariate methods for large data sets. Principal component analysis (PCA) is found to be useful for data reduction and to assess the continuity/overlap of clusters or clustering/similarities in the data. The most effective grouping was achieved by statistical clustering techniques. However, these clustering techniques do not provide any information on the chemistry of the statistical groups. The combinations of graphical and statistical techniques provide consistent and objective means to classify large number of samples while retaining the ease of classic graphical presentations.

To extract inherent hydrochemistry from large groundwater quality data sets, multivariate/factor analysis is useful for interpreting groundwater quality data and these interpretations may be related to specific hydrogeological processes in a region where groundwater sampling has been carried out. The most commonly used multivariate/factor analysis is Principal Component Analysis (PCA).

Melloul and Collin (1992) studied the use of PCA for the identification of relevant groups of water and the factors that brought a change in groundwater quality of the Dan metropolitan region of Israel's coastal plain. The variables included in PCA are major ions as well as the physical factors of depth of the well intake, filter below sea-level, distance from sea and aquifer recharge. The PCA revealed two major water types: a low-salinity, calcium bicarbonate water occurring in the phreatic portion of the coastal plain aquifer, and more saline, sodium chloride water characterizing the neighboring Cenomanian aquifer and in the confined portions of the coastal aquifer. In addition to water inputs, the quality of water is also affected by physical factors such as distance from the sea, depth of well intake filters below sea-level, proximity to streams, and the lithology of the saturated and unsaturated zones. The study recommended that the classical diagrams and the principal component approaches could be used as complimentary tools in geochemical analysis and concluded that PCA is a good tool for sorting vast quantity of data and subsequently identifying the most significant influence on sources of water quality changes.

Grande et al. (1996) successfully used PCA to study contamination in the aquifer system of Ayamonte-Huelva (Spain) and delineated two factors: saltwater intrusion and agriculture contamination. The proximity between both factors was justified for each of the contaminating processes.

Helena et al. (2000) studied temporal evolution of groundwater composition in an alluvial aquifer of the Pisuerga river, located at north-east of Valladolid (Spain) by analyzing 16 physico-chemical variables from 32 sampling sites during two field surveys by PCA. Results showed the existence of five significant Principal Components (PC's) which account 71.39% of the variance. Two principal components namely PC1 (33.25 %) and PC4 (8.71 %) are assigned 'mineralization' process originating from the chemical interaction between groundwater and the host rocks. On the other hand, variables indicative of pollution present in the other PCs are lead,

aluminium and iron in PC2 (13.45%), nitrate, cadmium and copper in PC3 (9.26%) and Zinc in PC5 (6.37%). Varimax rotation was used to detect dilution process in the study area.

Rao et al. (2001) used PCA to understand the major processes of groundwater quality in the Guntur urban area, Andhra Pradesh, India. The study concluded that the PC1 is dominated by TDS, Na^+, Cl^-, SO_4^{2-} and K^+, PC2 is by pH and CO_3^- and PC3 is by NO_3^- variables. The climate, water-rock interaction, land use and anthropogenic sources are major factors identified that influence groundwater quality in the study area.

Liu et al. (2003) applied PCA to 28 groundwater samples collected from wells in the coastal blackfoot disease area of Yun-Lin, Taiwan and analyzed for 13 hydrochemical parameters. A two-factor model is suggested and explains over 77.8% of the total groundwater quality variation. Factor 1 or PC1 (seawater salinization) includes concentration of Electrical Conductivity (EC), Total Dissolved Solids (TDS), Cl^-, SO_4^{2-}, Na^+, K^+ and Mg^{2+}, and factor 2 or PC2 (arsenic pollutant) includes concentrations of alkalinity, Total Organic Carbon (TOC) and arsenic. The maps of these factor scores delineate high salinity and arsenic zones in the study area. The over extraction of groundwater in these zones is found to be major cause of salinity and arsenic pollution.

The PCA ignores the spatial correlations between sampling points, which gives additional information. To overcome these limitations, geostatistics has been used to study both large-scale variations (the trend) and small-scale variations (spatial correlation). Geostatistical methods focus on providing the estimate of spatially distributed variables at unsampled locations as a function of a set of sample values at a limited number of locations. Therefore, PCA and geostatistical analysis can be applied together to identify contamination types and to study its spatial variations. ASCE Task Committee (1990 a) reviewed the basics of geostatistics to study the spatial variability of various variables pertaining to geohydrology. Similarly, ASCE Task Committee (1990 b) also reviewed various applications of geostatistics in geohydrology. Some important applications of geostatistics and PCA in characterization of groundwater quality are reviewed below.

Bjerg and Christensen (1992) studied the spatial small-scale variation in groundwater quality (pH, alkalinity, chloride, nitrate, calcium and potassium) of a shallow sandy aquifer within a farmland. The geostatistical analysis of these water quality parameters shows substantial horizontal variation even over short distances. Variograms for pH, alkalinity, calcium and potassium show correlation with distance up to 5 to 8 m, while nitrate and chloride seem to be uncorrelated with distance more than 0.7 m.

Istok and Rautman (1996) applied geostatistical framework for obtaining a probabilistic assessment of groundwater contamination by nitrate and herbicide in a shallow, unconfined alluvial aquifer in an agricultural area in eastern Oregon. Sample variograms fitted with nugget, and spherical models described the pattern of spatial continuity of nitrate and herbicide

concentrations, and accumulations. This case study illustrated the potential applicability and utility of probabilistic approach for the interpretation of site characterization data and the design of future data collection activities.

Ceron et al. (2000) analyzed hydrogeochemical data of alluvium aquifer of Alto Guadalenin, Southern Spain using PCA and geostatistical framework to obtain probabilistic assessment of groundwater quality. In this study, experimental and theoretical semivariograms of the selected factors are considered as regionalized variables. These variographic information and factor values in the experimental sites were used in the ordinary kriging, which provided unbiased and linear estimates of the regionalized variables. These estimates were used to compile maps of the chosen factors, which explained their spatial distribution.

Martos et al. (2001) presented statistical and geostatistical methods for studying groundwater quality variables. These methods were applied to investigate detrital aquifer of the Bajo Andarax, Spain. The study revealed that PCA is a first step for the identification of relevant types of groundwater and the processes that bring change in their quality. Analysis of their spatial distribution was performed through the calculation of experimental and theoretical variograms, which served as input for geostatistical modeling using ordinary block kriging. In this way, one can evaluate the spatial and temporal variation of the principal physico-chemical processes associated with the groundwater quality of the detrital aquifer.

Kravchenko (2003) studied the influence of spatial structure of monitoring network on accuracy of interpolation methods (ordinary point kriging and optimal inverse distance weighting). The study revealed that the strength of modeled spatial structure ranged from weak with nugget to sill ratio (N/S) of 0.6 to strong with ratio (N/S) of 0.1. Kriging with known variogram parameters performed significantly better than the Inverse Distance Weighted (IDW) for most of the studied cases. However, when variogram parameters were determined from sample variograms, kriging was as accurate as the IDW for sufficiently large data sets only, but was less precise when a reliable sample variogram could not be obtained from the data.

Flipo et al. (2007) assessed nitrate pollution in the Grand Morlin aquifers (France) by combined use of geostatistics and physically based modeling. They observed that kriging takes into account the spatial structure of point nitrate concentrations to give an estimate of nitrate concentration for each cell with an associated uncertainty due to the spatial variability of the data. In this study, the kriging results for 1977 are used to set initial conditions of the distributed model. Simulation gives nitrate concentrations for each cell for 1988. The mean annual concentrations simulated by the physically based model are in agreement with kriged concentrations. The study concluded that the combined use of geostatistics and physically based modeling facilitates accurate predictions of nitrate fate in the aquifers. In the present study, PCA and geostatistics together have been used to characterize groundwater quality in the selected study area.

2.5 Mapping of nitrogen load from septic system using GIS

Geographical Information System (GIS) provides an extensive approach to evaluate mapping characteristics that explain the spatial distribution of non-point and point source of contamination. Tsihrintzis et al. (1996) provided detailed review of GIS in water resources applications including groundwater modeling and assessment of non-point source pollution. Many researchers developed GIS based methodologies for non-point source pollution in agricultural areas (Robinson and Ragan, 1993; Shaffer et al., 1995; Mohan and Kananan, 1998; Srinivasan et al., 1998; Hession, 2000; Paz and Ramos, 2002; Babiker et al., 2004) to relate nitrate contamination in groundwater. Very limited studies have been carried out exclusively in and around urban areas to map nitrogen load from septic systems. The following are important studies in connection with mapping of pollutant loads in the urban aquifers.

Ventura and Kim (1993) introduced micro approach for urban non point source pollution assessment that takes into consideration the high degree of land use heterogeneity in urban areas. Individual land use polygons were used as the unit of analysis. GIS was implemented to generate and manage digital layers, conduct overlay and other spatial analysis, and transfer data to an empirical non point source model to estimate total pollutant loadings for each sewered or sewer junction. This study demonstrates that GIS technology is more effective for urban non-point source control, overlay analysis, databases management and cartographic display capabilities.

Nizeyimana et al. (1996) developed a procedure to map nitrogen loading from septic systems for the Pennsylvania watershed, using various hydrologic, soil and census databases. Sub watersheds were ranked and grouped into three significantly different classes (high, medium, and low) according to their nitrogen loadings. High nitrogen producing watersheds were generally located in the suburbs adjacent to larger metropolitan areas. It was observed that the reliability of nitrogen estimates and watersheds classification could be improved by conducting in depth site investigations on population, septic densities, rainfall recharge, the number of malfunction systems, soil properties, and site characteristics related to effluent renovation of septic systems. However, three nitrogen load classes (high, medium, and low) were not compared with corresponding groundwater quality in their study.

Gogu et al. (2001) developed hydrogeological GIS database that facilitates groundwater vulnerability analysis and hydrogeological modeling for the Wallon region in Belgium. It was observed that the reliability and validity of groundwater analysis strongly depend on the availability of large volumes of high quality data. The developed data base allows time and spatial queries, and stored databases can be easily used in different groundwater numerical models.

Lee et al. (2003) made an assessment of nitrate contamination in urban groundwater using statistical models and GIS. Data such as land use, location of wells and groundwater quality were collected and a database was constructed using GIS. The Optimum Radius of

Influence (ROI) of a well which affects NO_3^--N concentration in a well is about 200 m in dry season and 250 m in the rainy season for both shallow and deep wells. Landuse that affects NO_3^--N concentrations were the grass land area and the field crop area in the dry season, and the mixed residential and business area in the rainy season. In statistical methods, landuse areas are considered as non point sources that affect NO_3^--N wells, but the R^2 values from the regression analysis showed very low correlation. These results suggest that many contaminant sources exists in addition to the land uses, and that hydrogeological conditions are severely disturbed in urban areas. The study recommended to include the number of people, sewer lines and sewage disposal facilities, geological conditions and soil characteristics in GIS database to get better correlation.

Almasri and Kaluarachchi (2004) presented modeling approach based on GIS to estimate the variability of surface nitrogen loading and the corresponding nitrate leaching to groundwater. This methodology integrates all point and non point sources of nitrogen especially fertilizers and dairy applications, dairy lagoons and septic systems. The study showed that dairy manure is the main source of nitrogen followed by fertilizers. It was stated that recharge rate and denitrification rate are the most influential parameter on nitrate leaching.

As per the literature review, the sub basin wise nitrogen loading assessment is more appropriate to map the nitrogen load over a catchment. However, in coastal regions, the delineation of sub watersheds is more complex due to flat terrain, therefore as an alternative, village boundary has been chosen as unit to map the nitrogen load from septic systems. Furthermore, the databases on population, landuse, and soil types are available at village level in statistical records. Therefore, the methodology of the Nizeyimana et al. (1996) would be appropriate to map the nitrogen load from septic systems with suitable modifications as carried out in the present research work. In the present study, nitrogen loading pattern is also compared with its average groundwater quality to show qualitative validation.

2.6 Modeling nitrate leaching into subsurface from septic systems

Nitrogen fate and transport models are many but are diverse, ranging from simple leaching equations to complex mechanistic models describing each important nitrogen transformation processes. Many models are available to simulate nitrogen cycles in agricultural environments. Some of the important model approaches /applications to estimate nitrate leaching from septic systems as it is the focus in the present study, are reviewed in the following paragraphs.

Mercado (1976) studied regional nitrate and chloride pollution using single-cell model. The model integrates pollution sources on the land surface, hydrologic parameters of the aquifer and unsaturated zone, and variations of chloride and nitrate concentrations distribution in pumping wells. The study was based on assumption that the relationship between nitrogen quantities (from all sources) released in the surface and the nitrogen quantity reaching the water

table is linear. It was further assumed that all the nitrogen, leaching the water table is in the form of NO_3^- and other reactions within the aquifer are negligible.

Sikora and Corey (1976) studied fate of nitrogen and phosphorus in soils under septic tank waste disposal fields. The study concluded that nitrogen end product from observed soil moisture tensions beneath septic system in soils of different textural classes are: a) NO_3^- in sands, sandy loams and loamy sand and loams b) a mixture of NO_3^- and NH_4^+ in silt loams and some silt clay loams with a possibility of decreasing total nitrogen via denitrification, and c) NH_4^+- N in clay loams and clays. The phosphorus concentrations in septic waste, both sorption and decomposition-precipitation reactions probably determine phosphate movement. The study also concluded that from pollution standpoint, nitrogen in septic tank effluent is a greater concern than phosphorous.

Anderson et al. (1987) assessed the contamination potential from septic systems in Florida using groundwater modeling where 90% of people are using groundwater as a source of drinking water. An analytical solution to the advection-dispersion equation was developed under the assumption of a steady, 1-D flow field, 3-D hydraulic dispersion, linear contaminant retardation and first order decay. The study revealed that modeling of contaminant transport from assumed subdivision sources appeared to be a useful tool in assessing the potential for contamination of a region. Modeling results estimated that groundwater NO_3^--N exceeded allowable limit (10 mg/l) for housing densities for a 50-acre subdivision utilizing septic systems. However, some of the important processes like mineralization, nitrification, and denitrification are not considered in their study.

Harmsen et al. (1991) described model to estimate lateral and vertical separation distance necessary to prevent contamination of a well by a nearby septic tank. The model is capable of handling three dimensional, transient flows in an unconfined, homogeneous, anisotropic aquifer of infinite areal extent, under a regional horizontal hydraulic gradient. Vertical hydraulic gradients due to aquifer recharge resulting from rainfall and contaminant spreading due to hydrodynamic dispersion is ignored. The comparison of model simulations results with other numerical and analytical solutions showed good agreement. Sensitivity analysis revealed that the separation distance and minimum well depth are most sensitive to variations in the horizontal hydraulic conductivity, anisotropy ratio and horizontal regional hydraulic gradient.

Hantzsche and Finnemore (1992) developed simple mass balance equation to predict nitrate-nitrogen optimum concentrations into groundwater from septic systems. This equation incorporates only the vertical component of groundwater recharge, ignoring any dilution effect of lateral groundwater flow from up gradient areas. The predicted values are only intended to use to evaluate average area-wide groundwater nitrate-nitrogen condition. The quantification of mineralization and nitrification are not included in this equation.

Simone and Howes (1998) studied nitrogen transport and transformation in a shallow aquifer from wastewater using mass balance approach. The study revealed that ammonification and nitrification in the unsaturated zone and ammonium sorption in the saturated zone were predominant, while loss of fixed nitrogen through denitrification was minor. The major effect on nitrate transport was the oxidation of discharged organic and inorganic forms of nitrate, which was the dominant nitrogen form in transient condition.

Gusman and Marino (1999) developed physically based analytical nitrate transport model RISK-N which combines both the unsaturated and saturated zones, with fewer input parameters than any currently available models simulating the complex systems. The RISK-N model is suitable for agricultural areas and septic systems with turf grass (urban areas). The initial application of this model on corn plots provided reasonable predictions of nitrate leaching to groundwater. The sensitivity analysis of the model parameters showed that unsaturated zone soil porosity and irrigation leaching factor both have a significant effect on nitrate flux from the intermediate zone and the aquifer denitrification rate can be a significant factor to affect nitrate levels in groundwater. The applicability of RISK-N model for urban areas is yet to be tested in the field.

Tabachow et al. (2001) compared the practical utility of four models of APS (Novichikhin and Tarko, 1984), NLEAP (Shaffer et al., 1991), DAISY (Hansen et al., 1991) and RISK-N (Gusman and Marino, 1999), and concluded that physically based RISK-N model simulates nitrogen fluxes in soils, and seems to be the best suited for modeling the full complex of geochemical N cycles in fertilized systems. Oyarzun et al. (2007) tested RISK-N model in the central valley of Chile on corn plot and carried out sensitivity analysis of the model. The study revealed that the model performs well when spatially averaged values are used and the prediction error increases when the concentration in each well is considered. Sensitivity analysis showed that both the nitrate flux from the vadose zone and NO_3^--N groundwater concentrations are mainly influenced by the initial soil nitrogen levels, water input and unsaturated zone soil porosity. Further, simulated groundwater NO_3^--N levels are sensitive to changes on the saturated zone denitrification rates.

There is a limited literature on modeling nitrogen transport from septic system through unsaturated zone and saturated zone by incorporating all chemical process (rapid mineralization, slow mineralization, ammonification, nitrification, denitrification, volatization). It was found that only RISK-N model is capable of simulating nitrate leaching with all possible nitrogen transformations from septic systems by integrating saturated and unsaturated zones, however its application to real life situations are limited. Therefore, it is interesting and valuable to explore the applicability of RISK-N model along with characterization of groundwater quality and mapping of nitrogen load from septic systems in Indian scenarios particularly in urban coastal areas.

3.0 METHODOLOGY

To study the nitrate contamination in an urban coastal aquifer, a methodology has been presented, which has been grouped under three major components. These components are characterization of groundwater quality, mapping of nitrogen load from septic systems and modeling of nitrate leaching into groundwater. The descriptions and the details on these three components are given in the following sections.

3.1 Characterization of groundwater quality using multivariate geostatistical analysis

To characterize the groundwater quality, groundwater samples were analyzed for physical and chemical parameters as per the procedures adopted by Standard Methods (APHA, 1985). Physical parameters (EC, pH, Temperature) were measured with portable electrodes, chemical analysis of Ca^{2+}, Mg^{2+}, Cl^- and HCO_3^- were determined by volumetric analysis, Na^+ and K^+ were determined using Flame photometer, and SO_4^- and NO_3^- were determined using UV-Spectrophotometer. The chemical analysis is verified by computing the ion balance error of each sample. The statistical properties (minimum, maximum, mean, standard deviation and skewness coefficient) were computed for each water quality parameter, and the correlation coefficients among water quality parameters are also computed. Piper trilinear diagrams (Piper, 1944) are used to find the type of groundwater sample and Schoeller diagram was used for identification of changes in average concentration of each water quality parameter in the study area. The hydrochemical ratios of SO_4^-/Cl^- and Cl^-/HCO_3^- are computed to characterize groundwater quality for dominant sources of contamination in the study area. For multivariate analysis of groundwater quality data Principal Component Analysis (PCA) is carried out using SPSS (1999) software. This analysis has enabled in identifying major geochemical processes in the study area.

3.1.1 Principal Component Analysis (PCA)

This is the most widely used method of multivariate analysis owing to the simplicity of its algebra and its straightforward interpretation. A linear transformation is defined which transforms a set of correlated variable into uncorrelated factors. These orthogonal factors can be shown to extract successively a maximal part of the local variance of the variables. The basic problem solved by PCA is to transform a set of correlated variables into uncorrelated quantities, which could be interpreted in an ideal multi Guassian context as independent factors underlying the phenomenon (Wackernagel, 1995). The detailed description on PCA is available in Martos et al. (2001).

Let Z be the n x N matrix of data from which the means of the variables have already been subtracted. Then the corresponding N x N variance-covariance matrix, V is given by:

$$V = [\sigma_{ij}] = \frac{1}{n} Z^T Z \qquad (3.1)$$

Let Y be an n x N matrix containing in its rows the n samples of factors Y_p (p = 1,..., N), which are uncorrelated and of zero mean. The variance-covariance matrix of the factors is diagonal, owing to the fact that the covariances between factors are nil by definition:

$$D = \frac{1}{n} Y^T Y = \begin{pmatrix} d_{11} & 0 & 0 \\ 0 & \ddots & 0 \\ 0 & 0 & d_{NN} \end{pmatrix} \tag{3.2}$$

Where, the diagonal elements d_{pp} are the variances of the factors.

A matrix A is sought, N x N orthogonal, which linearly transforms the measured variables into synthetic factors:

$$Y = ZA \quad with \quad A^T A = 1 \tag{3.3}$$

Multiplying this equation from the left by $1/n$ and Y^T and replacing Y by ZA, one obtains:

$$\frac{1}{n} Y^T Y = \frac{1}{n} Y^T ZA = \frac{1}{n} (ZA)^T (ZA) = \frac{1}{n} A^T Z^T ZA = A^T \frac{1}{n} (Z^T Z) A \tag{3.4}$$

Thus,

$$D = A^T VA \implies VA = AD \tag{3.5}$$

It can be shown that the matrix Q orthonormal of eigenvetors of V offers a solution to the problem and the eigenvalues λ_p are simply the variances of the factors Y_p. Principal component analysis is basically a statistical interpretation of the eigenvalue problem:

$$VQ = QA with \quad Q^T Q = 1 \tag{3.6}$$

defining the factors as:

$$Y = ZQ \tag{3.7}$$

Another important aspect of principal component analysis is that it allows to define a sequence of orthogonal factors which successively absorb a maximal amount of variance of the data.

Take a vector y_1 corresponding to the first factor obtained by transforming the centered data matrix Z with a vector a_i calibrated to unit length:

$$y_1 = Za_1 \; with \; a_1^T a_1 = 1 \tag{3.8}$$

The variance of y_1 is :

$$\text{var}(y_1) = \frac{1}{n} y_1^T y_1 = \frac{1}{n} a_1^T Z^T Z a_1 = a_1^T V a_1 \tag{3.9}$$

To attribute a maximal part of the variance of the data to y_1, an objective function ϕ_1 with a Lagrange parameter λ_1 is defined, which multiplies the constraint that the transformation vector a_1 should be of unit norm:

$$\phi_1 = a_1^T V a_1 - \lambda_1 (a_1^T a_1 - 1) \tag{3.10}$$

Setting the derivative with respect to a_1 to zero:

$$\frac{\partial \phi_1}{\partial a_1} = 0 \quad \Leftrightarrow \quad 2Va_1 - 2\lambda_1 a_1 = 0 \tag{3.11}$$

λ_1 is an eigen value of the variance-covariance matrix and a_1 is equal to the eigenvector q_1 associated with this eigenvalue:

$$Vq_1 = \lambda_1 q_1 \tag{3.12}$$

A second vector y_2, orthogonal to the first, is of interest:

$$\mathrm{cov}(y_2, y_1) = \mathrm{cov}(Za_2, Za_1) = a_2^T V a_1 = a_2^T \lambda_1 a_1 = 0 \tag{3.13}$$

The function ϕ_2 to maximize incorporates two constraints: the fact that a_2 should be unit norm and the orthogonality between a_2 and a_1. These constraints bring up two new Langrange multipliers λ_2 and μ:

$$\phi_2 = a_2^T V a_2 - \lambda_2 (a_2^T a_2 - 1) + \mu a_2^T a_1 \tag{3.14}$$

Setting the derivative with respect to a_2 to zero:

$$\frac{\partial \phi_2}{\partial a_2} = 0 \quad \Leftrightarrow \quad 2Va_2 - 2\lambda_2 a_2 + \mu a_1 = 0 \tag{3.15}$$

$$\underbrace{2a_1^T V a_2}_{0} - 2\lambda_2 \underbrace{a_1^T a_2}_{0} + \mu \underbrace{a_1^T a_1}_{1} = 0 \tag{3.16}$$

since μ is nil (the constraint is not active), equation 3.16 reduces to:

$$Va_2 = \lambda_2 a_2 \tag{3.17}$$

Again λ_2 turns out to be eigenvalue of the variance-covariance matrix and a_2 is the corresponding eigenvector q_2. Continuing in the same way, one can find the rest of the N eigenvalues and eigenvectors of V as an answer to the maximization problem. The components are subsequently rotated orthogonally using the Varimax method to obtain a more significant distribution of the weights of the different variable on the components (Davis, 1986).

3.1.2 Geostatistics

The theoretical fundamentals of the geostatistical methods are described in various textbooks (Journel and Huijbergts, 1978; Isaaks and Srivastava, 1989). From hydrogeochemical

point of view, these methods perform analysis for the spatial continuity and temporal variation of the hydrochemical variables. For this, the spatial variability of hydrochemical variables is determined by calculating experimental and theoretical variograms (variographic analysis), and by mapping these variables using ordinary block kriging.

The experimental variogram is defined as follows (Martos et al., 2001):

$$\gamma^*(h) = \frac{1}{2N(h)} \sum_{i=1}^{N(h)} [Z(x_i) - Z(x_i + h)]^2 \qquad (3.18)$$

where N(h) is the number of pairs of sample points separated by h, which have measured values of the regionalized variable $Z(x)$; x_i is a sample point with i = 1,..., n. The theoretical variograms chosen for modeling may be a mixture of nugget and spherical models. Fig 3.1 shows the skeleton diagram of theoretical variogram parameters.

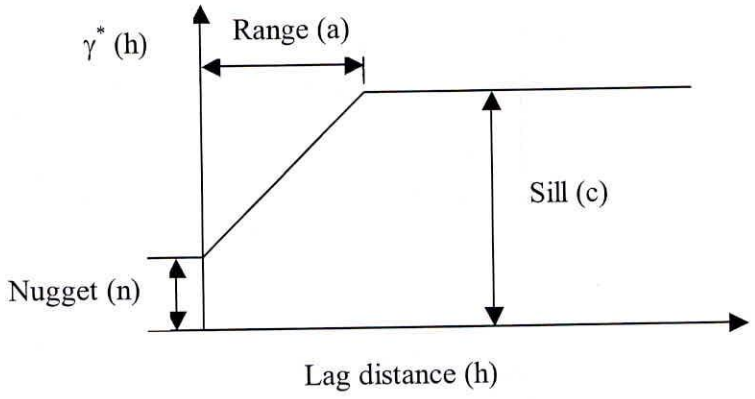

Fig. 3.1 Definition sketch of a model variogram

$$\textit{nugget} \quad \left| \begin{array}{l} \gamma(h) = 0 \\ \gamma(h) = c_1 \end{array} \quad c_1 \text{ constant } h > 0 \right| \Rightarrow cNug \qquad (3.19)$$

$$\textit{spherical} \quad \left| \begin{array}{l} \gamma(h) = c_2\left(\dfrac{3h}{2a} - \dfrac{h^3}{2a^3}\right) \\ \gamma(h) = c_2 \quad h > a \end{array} \quad a, c_2 \text{ constant } 0 \le h \le a \right| \Rightarrow cSph(a) \qquad (3.20)$$

a = range; c = sill

To map the variables considered, the geostatistical estimation method of ordinary block-kriging on a regular grid was utilized. The linear kriging estimate, $Z^*(x_0)$, was used to obtain the value of the regionalized variable at any sampling point, x_0 (considered as the mean value

assigned to the block), using the data values from the neighboring sample points x_α and combining them linearly with weights.

$$Z^*(x_0) = \sum_{\alpha=1}^{n} w_\alpha Z(x_\alpha) \tag{3.21}$$

The sum of weights should be one, because in the extreme case when all data are equal to a constant, the estimated value should also be equal to this constant.

It is assumed that the data are part of a realization of an intrinsic random function with a variogram $\gamma(h)$. The unbiasedness is warranted with unit sum weights:

$$E[Z^*(x_0) - Z(x_0)] = E\left[\sum_{\alpha=1}^{n} w_\alpha Z(x_\alpha) - Z(x_0) - Z(x_0).\underbrace{\sum_{\alpha=1}^{n} w_\alpha}_{1}\right] = \sum_{\alpha=1}^{n} w_\alpha E[Z(x_\alpha) - Z(x_0)] = 0 \tag{3.22}$$

because the expected values of the increments are zero.

The estimation variance $\sigma_E = \mathrm{var}\left[Z^*(x_0) - Z(x_0)\right]$ is the variance of the linear combination:

$$Z^*(x_0) - Z(x_0) = \sum_{\alpha=1}^{n} w_\alpha Z(x_\alpha) - 1.Z(x_0) = \sum_{\alpha=0} w_\alpha Z(x_\alpha) \tag{3.23}$$

with $\sum_{\alpha=0} w_\alpha = 0$

Thus the condition that the weights numbered from 1 to n sum up to one also implies that the use of the variogram is authorized in the computation of the variance error. The estimation variance is

$$\sigma_E^2 = E\left[\left(Z^*(x_0) - Z(x_0)\right)^2\right] = -\gamma(x_0 - x_0) - \sum_{\alpha=1}^{n}\sum_{\beta=1}^{n} w_\alpha w_\beta \gamma(x_\alpha - x_\beta) + 2\sum_{\alpha=1}^{n} w_\alpha \gamma(x_\alpha - x_0) \tag{3.24}$$

By minimizing the estimation variance with the constraint of the weights, one obtains the ordinary kriging system:

$$\begin{pmatrix} \gamma(x_1 - x_1) & \cdots & \gamma(x_1 - x_n) & 1 \\ \vdots & \ddots & \vdots & \vdots \\ \gamma(x_n - x_1) & & \gamma(x_n - x_n) & 1 \\ 1 & \cdots & 1 & 0 \end{pmatrix} \begin{pmatrix} w_1 \\ \vdots \\ w_n \\ \mu \end{pmatrix} = \begin{pmatrix} \gamma(x_1 - x_0) \\ \vdots \\ \gamma(x_n - x_0) \\ 1 \end{pmatrix} \tag{3.25}$$

where w_α are the weights to be assigned to the data values and where μ is the Lagrange parameter. The left hand side of the system describes the dissimilarities between the data points,

while the right hand side shows the dissimilarities between each data point and the estimation point x_0.

Performing the matrix multiplication, the ordinary kriging system can be rewritten in the form:

$$\begin{cases} \sum_{\beta=1}^{n} w_\beta \gamma(x_\alpha - x_\beta) + \mu = \gamma(x_\alpha - x_0) & \forall \alpha = 1,.....,n \\ \sum_{\beta=1}^{n} w_\beta = 1 \end{cases} \tag{3.26}$$

The estimation variance of ordinary kriging is

$$\sigma^2 = -\mu - \gamma(x_0 - x_0) + 2\sum_{\alpha=1}^{n} w_\alpha \gamma(x_\alpha - x_0) \tag{3.27}$$

Ordinary Kriging is an exact interpolator in the sense that if x_0 is identical with a data location then the estimated value is identical with the data value at that point

$$Z^*(x_0) = Z(x_\alpha) \qquad if \quad x_0 = x_\alpha \tag{3.28}$$

The experimental and theoretical variograms were computed with an adaptation of the 2-D geostatistical module from GMS (2000) software in the present research work.

3.2 Quantification of nitrogen load from septic systems using GIS

The methodology described by Nizeyimana et al. (1996) was used for assessing the nitrogen load from septic systems. It is assumed that each house has septic systems in the study area. However, to account variant condition, a correction factor has been applied to the number of persons using septic systems because in rural areas people are using other methods like out houses. The village map and its attributes data of population, soil type, number of houses, % of malfunctioning of septic system in each soil type were prepared in GIS environment using Geomedia (2000) and Arcview (2000) software.

The average number of persons per housing unit was calculated by dividing the number of persons in each polygon (village/town) by the total number of housing units. The nitrogen load produced by each person in a year is computed by multiplying total nitrogen content of typical septic effluent with per capita usage of wastewater per year. The annual nitrogen load produced by village is computed by multiplying total number of people using septic systems, nitrogen load produced by each person in a year and % of malfunctioning of septic systems in each soil type (Matelski, 1975 and Hoover et al., 1981). It is assumed that all nitrogen released as a result of septic system failure reach groundwater without loss due to various biogeochemical processes. Costas-Carlos and Gomez-Gomez (1998) also advocated this assumption. The Indian guidelines for proper septic tank construction, BIS (1996) also recognize the fact that the septic

tank treatment is not efficient in coastal regions. The estimated village wise nitrogen load was further divided into low, medium and high zones using Fuzzy c-means clustering technique. Babuska (1998) has given a detailed description of fuzzy c-means clustering technique (FCM), however a brief description is given below.

3.2.1 Fuzzy c-Means Clustering (FCM)

Fuzzy clustering of numerical data forms the basis of many classification and system modeling algorithms. It can be used as a tool to obtain a partitioning of data where the transitions between the subsets are gradual rather than abrupt. Clustering techniques are among the unsupervised (learning) methods, since they do not use prior class identifiers. The purpose of clustering is to identify natural groupings of data from a large data set to produce a concise representation of a system's behavior. If the data sets for two different periods are available, the 2-D FCM clustering may be applied on this data set. The 2-D FCM is a data clustering technique wherein each data point belongs to a cluster to some degree that is specified by a membership grade. This technique was originally introduced by Bezdek (1981), an improvement on earlier clustering methods.

A large family of fuzzy clustering algorithms is based on minimization of the fuzzy c means functional formulated as (Bezdek, 1981):

$$J(Z;U,V) = \sum_{i=1}^{c}\sum_{k=1}^{N}(\mu_{ik})^{m}\left\|z_k - v_i\right\|^2 A \tag{3.29}$$

where, Z is the n x N matrix, and objective of clustering is to partition the data set into c clusters.

$$U = [\mu_{ik}] \in M_{fc} \tag{3.30}$$

is a fuzzy partition matrix of Z, and contains values of the i^{th} membership function (M_{fc}) of fuzzy subset A_i of Z.

$$V = [v_1, v_2, ..., v_c], \quad v_i \in \Re^n \tag{3.31}$$

is a vector of cluster prototypes (centers), which have to be determined,

$$D_{ikA}^2 = \left\|z_k - v_i\right\|^2 A = (z_k - v_i)^T A (z_k - v_i) \tag{3.32}$$

is a squared inner product distance norm, and

$$m \in [1, \infty) \tag{3.33}$$

is a weighting exponent, which determines the fuzziness of the resulting clusters. The measure of dissimilarity in Equation (3.29) is the squared distance between each data points z_k and the cluster prototype (means) v_i. This distance is weighted by the power of the membership degree of that point $(\mu_{ik})^m$. The value of cost function (Equation 3.29) can be seen as a measure of the total variance of z_k from v_i. The minimization of the c-means functional (Equation 3.29) represents a nonlinear optimization problem that can be solved by simple Picard iteration through the first-order conditions for stationary points of (Equation 3.29), known as the fuzzy c-means (FCM) algorithm, which is given below.

Given the data set Z, the number of clusters, $1 < c < N$, the weighing exponent $m > 1$, the termination tolerance $\varepsilon > 0$ and the norm inducing matrix A are chosen. The partition matrix is initialized randomly, such that $U^{(0)} \in M_{fc}$. It is repeated for $l = 1, 2, \ldots\ldots$

Step 1: Compute the cluster prototypes (means):

$$v_i^{(l)} = \frac{\sum_{k=1}^{N} (\mu_{ik}^{(l-1)})^m z_k}{\sum_{k=1}^{N} (\mu_{ik}^{(l-1)})^m}, \quad 1 \le i \le c. \tag{3.34}$$

Step 2: Compute the distances:

$$D_{ikA}^2 = (z_k - v_i^{(l)})^T A (z_k - v_i^{(l)}), \quad 1 \le i \le c, \qquad 1 \le k \le N. \tag{3.35}$$

Step 3: Update the partition matrix:

if $D_{ikA} > 0$ *for* $1 \le i \le c, \quad 1 \le k \le N,$

$$\mu_{ik}^{(l)} = \frac{1}{\sum_{j=1}^{c} (D_{ikA} / D_{jkA})^{2/(m-1)}} \tag{3.36}$$

otherwise

$$\mu_{ik}^{(l)} = 0 \ \ if \ \ D_{ikA} > 0, \ \ and \ \ \mu_{ik}^{(l)} \in [0,1] \ \ with \sum_{i=1}^{c} \mu_{ik}^{(l)} = 1 \tag{3.37}$$

$$\text{until } \left\| U^{(l)} - U^{(l-1)} \right\| < \varepsilon. \tag{3.38}$$

Matlab (2000) software with fuzzy logic toolbox (Ver., 2.0) was used to perform 2D-FCM algorithm on nitrogen loads computed for the years 1991 and 2004.

3.3 Nitrate leaching estimation from septic systems using RISK-N model

RISK-N (Gusmen and Marino, 1999) is a physically based analytical nitrate transport model, which links up both unsaturated and saturated zones. The model is capable of simulating both (1) irrigated agriculture and (2) septic tank systems with turf grass. The later is especially important because no physically-based nitrogen cycling models were developed to simulate the combined effect of both septic tanks and fertilized turf grass found in suburban settings. However, in the present research work, the estimation of nitrate leaching from septic systems alone is considered to suit the field conditions. The major processes considered in the RISK-N model for the septic system are shown in Figure 3.2. In simulating nitrogen processes, the RISK-N model separates the unsaturated soil into the upper zone, lower zone, drain field zone and intermediate-vadose zone. Transport in each unsaturated soil zone is simulated on the premise of complete mixing of nitrogen concentrations, which is achieved by spatially averaging the nitrogen convective-dispersive partial differential equations. In the saturated zone, this complete mixing assumption is not used. Instead, the two-dimensional convective-dispersive equation is solved analytically. In addition to convection, nitrate in groundwater may be influenced by diffusion, dispersion and denitrification. Rainfall is the main driving variable controlling infiltration, and subsequently leaching of nitrate from the soil. The model allows the use of either (1) seasonal rainfall averages, or (2) rainfall may vary from year-to-year with a stochastic model. The term 'seasonal' refers to the time periods specified by the user for the simulation, from 1 (annual) to 12 (monthly), or any other number in between. A simplified approach for soil water transport is considered in the RISK-N model. All water fluxes are taken as one-directional, steady state, and calculated as monthly averages.

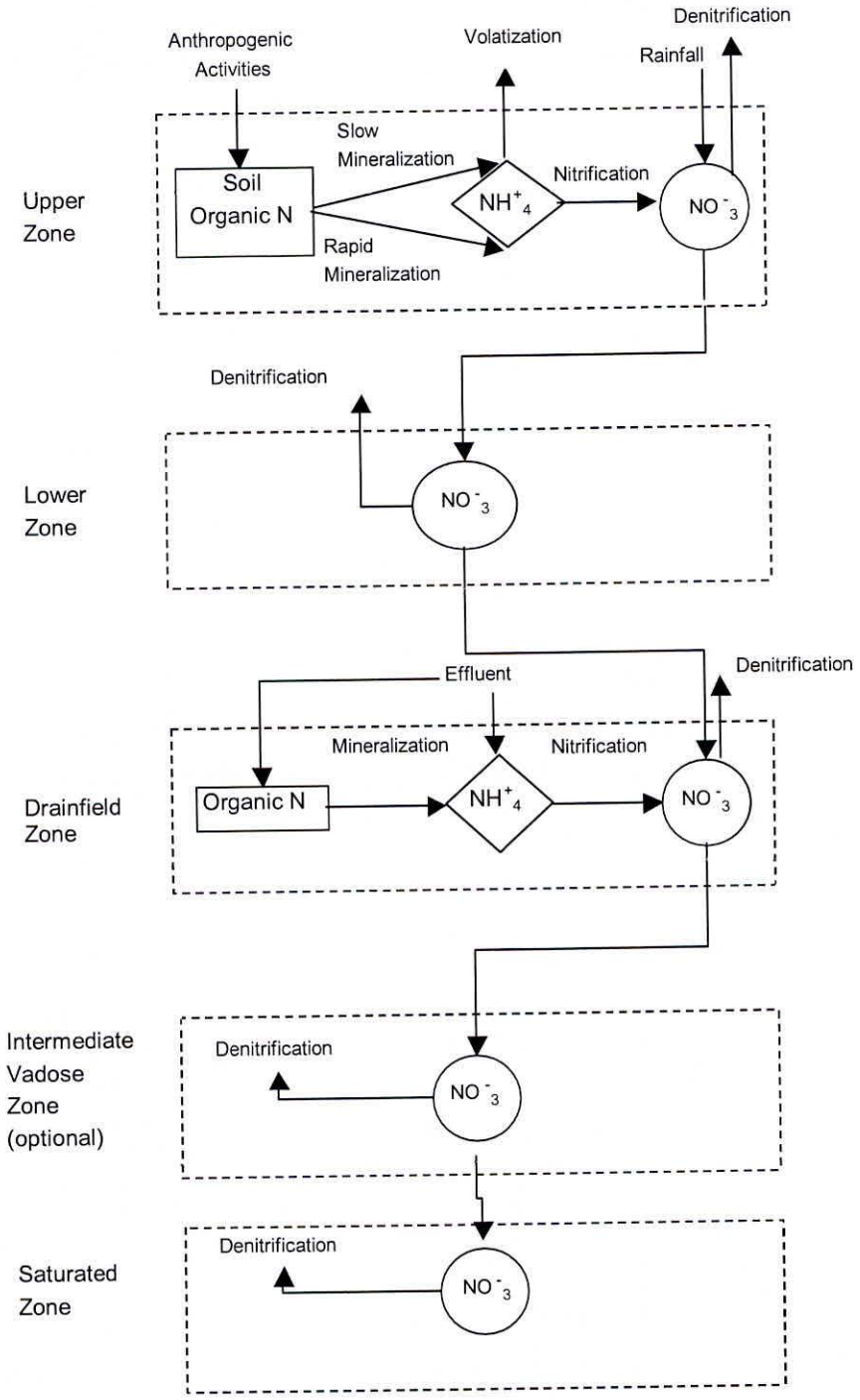

Fig. 3.2 Flow chart showing RISK-N model processes (Modified from Gusmen and Marino, 1999)

3.3.1 Soil water transport equations

Infiltration into the upper zone can be expressed as (since there is no applied irrigation water in urban environment):

$$q_{ur} = p - r \tag{3.39}$$

where,

p = precipitation rate (m/year);

r = runoff rate (m/year);

Percolation from the upper zone is given by:

$$q_{ur}^{*} = q_{ur} - F_{ur} L_s, \quad q_{ur}^{*} = 0, \text{ if } L_s > q_{ur} \tag{3.40}$$

where,

L_s = Losses due to septic systems or soak pits (m/year);

$$L_s = K_{septic} * ET_o \tag{3.41}$$

K_{septic} = septic coefficient for evaporation

ET_o = Class A Pan Evaporation (m)

F_{ur} is the fraction of Evapotranspiration taken from the upper zone. A non linear root water extraction model is explained by Ojha and Rai (1996). If no crop is grown in a season, then F_{ur} is set equal to one.

Percolation from the lower zone is given by:

$$q_{lr}^{*} = q_{ur}^{*} - (1 - F_{ur}) L_s, \quad q_{ur}^{*} = 0, \text{ if } L_s > q_{ur} \tag{3.42}$$

Percolation into the drainfield is given by:

$$q_d^{*} = q_{lr}^{*} + p_d \tag{3.43}$$

Where,

p_d = the rate of percolation added by the septic drain field (m/yr)

$$p_d = \frac{Flow_{eff} N_{person} F_{house}}{A_{lot}} \left(\frac{365}{10^7} \right) \tag{3.44}$$

Where,

$Flow_{eff}$ = is the septic tank effluent flow (liter/person/day),

N_{person} = is the number of persons per household,

F_{house} = is the fraction of houses occupied,

A_{lot} = is the average plot size per household (ha), and $365/10^7$ is a unit conversion factor.

Percolation from the intermediate vadose zone is given by:

$q_v^* = q_d^*$ for septic system application (3.45)

Percolation into the saturated zone is given by

$q_s = q_v^*$ for septic system with intermediate vadose zone (3.46)

3.3.2 Nitrogen inputs and processes in RISK-N model

Soil organic nitrogen

The soil organic N is conceptually divided into active and passive fractions. The active portion includes organic N involved in the process of mineralization, and is divided into rapid and slow mineralization fractions. The rapidly mineralizing N consists of recent additions of manure and crop residue containing organic N. The slow fraction consists of resident soil N still mineralizing, as well as the remaining organic N from past manure and crop residue applications.

Wet and dry deposition

The RISK-N model assumes that the N concentration in rainfall is a constant value of 3 ppm as NH_4^+-N. Local departures from this average value are often found in proximity to ammonia sources such as cattle feedlots, burnyards, and poultry houses. Rainfall near these sources may contain twice the nitrogen concentration as predicted from the regional averages. The 3 ppm default value may be changed when using RISK-N in such areas. The rate of dry deposition defaults to zero in RISK-N, but may also be changed by the user, if desired.

Ammonia volatization

The majority of ammonia losses take place during the first 10 hrs to 1 week following fertilizer application, although it may continue over the next several weeks. A constant fraction approach is used in the RISK-N model. For manure, 20% of the urea/ammonium N is assumed to be lost due to volatilization. For mineral fertilizer, this percentage is lowered to 10 %.

Mineralization

In its model-calculated rates of mineralization, the RISK-N model does not take into account the effects of the C:N ratio. However, the user has the option of specifying seasonal net mineralization rates. The rate of mineralization varies greatly with soil temperature. In India, mineralization is one of the significant factor, due to high soil temperatures than colder regions. The equations used by the RISK-N model to determine the mineralization rates for the rapid and slow organic N pools are as given below.

The first order rate (day^{-1}) for the rapid fraction is a function of soil temperature, T (^0C):

$$k_{mr}(T) = 5.6 * 10^{12} \exp[-9800/(T + 273)]F_{wm} \quad (3.47)$$

while the rate (day^{-1}) for mineralization of the slow fraction is

$$k_{ms}(T) = 4.0 * 10^{9} \exp[-8400/(T + 273)]F_{wm} \quad (3.48)$$

where,

T = Soil temperature;

F_{wm} = water content factor for mineralization and is given by

where, $F_{wm} = \theta / f_c \quad if\ \theta > f_c;\ F_{wm} = f_c / \theta \quad if\ f_c > \theta$ (3.49)

where,

θ = soil water content (m^3/m^3) and

f_c = water content at field capacity (m^3/m^3)

Nitrification

RISK-N uses a first order kinetic to simulate nitrification. The user may supply the nitrification rate constant as input if nitrification inhibitors are used, or else the model uses a default value of k = 1/day.

Denitrification

Denitrification rates in the RISK-N model may either be user supplied from the research data or literature or they are calculated by the model using an algorithm described below. When model calculated rates are used, the user has the option to simulate or ignore denitrification in the intermediate vadose zone; denitrification rates are always calculated for the upper, lower and drain field zones, where the organic C is normally available in sufficient quantities. For the saturated zone, the user must specify a rate constant for denitrification, if any; the model does not calculate a value given the high level of uncertainty. The method for determining the denitrification rate coefficients in the unsaturated zones is as follows.

Denitrification rate k_d (k_{dur}, k_{dlr}, k_{dd}, k_{dv} are in upper, lower, drain field and vadose zones respectively) is given by

$$k_d = k_{15} F_{wd} F_t \quad (3.50)$$

where,

k_{15} = rate coefficient for dentrification at 15^0C, equal to 0.01 (day^{-1});

F_{wd} = soil water content (m^3/m^3)

where,

$$F_{wd} = \exp\{0.304 + 2.94(\theta^u_{sat} - \theta^u) - 47(\theta^u_{sat} - \theta^u)^2\} \quad \text{for upper zone} \tag{3.51}$$

$$F_{wd} = \exp\{0.304 + 2.94(\theta^l_{sat} - \theta^l) - 47(\theta^u_{sat} - \theta^u)^2\} \quad \text{for lower zone} \tag{3.52}$$

$$F_{wd} = \exp\{0.304 + 2.94(\theta^d_{sat} - \theta^d) - 47(\theta^u_{sat} - \theta^u)^2\} \quad \text{for drain field zone} \tag{3.53}$$

$$F_{wd} = \exp\{0.304 + 2.94(\theta^v_{sat} - \theta^v) - 47(\theta^u_{sat} - \theta^u)^2\} \quad \text{for vadose zone} \tag{3.54}$$

where, θ^u_{sat}, θ^l_{sat}, θ^d_{sat}, θ^v_{sat} is the soil water content at saturation in upper, lower, drainfield and vadose zones, respectively (m^3/m^3).

F_t = the temperature factor

where,

$$F_t = 0.67\exp[0.43(T_{sat} - 10)] \quad if \quad T_{sat} \le 10^0\,C \text{ and} \tag{3.55}$$

$$F_t = \exp[0.08(T_{sat} - 15)] \quad if \quad T_{sat} > 10^0\,C \tag{3.56}$$

where,

T_{sat} =Temperature at saturation (°C)

3.3.3 Governing equations for upper zone

Slow mineralization in upper zone

Assuming an instantaneous incorporation of applied organic N into the upper zone, the slow mineralization of organic N is described by:

$$\frac{dC_s^{'}}{dt} + k_{ms}C_s^{'} = \frac{(F^s_{man}M_{man} + F^s_{res}M_{res})}{H_{ur}}\delta(t - t_0) \tag{3.57}$$

its solution is given by:

Boundary conditions of upper zone:

(At soil surface z = 0 and H_{ur} = 0; At the bottom of upper zone z = H_{ur})

$$C_s^{'}(t) = \left[C_s^{'}(t_0) + \frac{(F^s_{man}M_{man} + F^s_{res}M_{res}}{H_{ur}}\right]e^{-k_{ms}(t-t_0)} \tag{3.58}$$

Where,

$C_s'(t)$ = slowly mineralizing N concentration in upper zone from residue of soil organic N (g N/m^3);

K_{ms} = rate coefficient for net mineralization of slowly mineralizing organic N ($year^{-1}$);

$C_s'(t_0)$ = initial slowly mineralizing N concentration in upper root zone from manure / septic systems and / or residue (g $/m^3$);

F_{man}^s = slowly mineralization fraction of manure N (default value: 0.25);

M_{man} = total manure N applied (g N/m^2);

F_{res}^s = slowly mineralizing fraction of residue N (default: 0.45);

H_{ur}= Depth of upper zone (m)

The total slowly mineralizing organic N concentration C_s is given by

$$C_s(t) = C_s'(t) + C_s^{soil} \tag{3.59}$$

Where,

C_s^{soil} = slowly mineralizing N resident in the soil, (g N/m^3), is approximated as a constant value.

Rapid minerilisation in upper zone

A portion of both residue and manure N is in the form of rapidly mineralizing N compounds. Assuming an instantaneous incorporation of the organic N into the upper root zone, rapid mineralization of organic N, C_r may be explained as:

$$\frac{dC_r}{dt} + k_{mr}C_r = \frac{(F_{man}^r M_{man} + F_{res}^r M_{res})}{H_{ur}}\delta(t - t_0) \tag{3.60}$$

its solution is given by:

$$C_r(t) = \left[C_r(t_0) + \frac{(F_{man}^r M_{man} + F_{res}^r M_{res}}{H_{ur}} \right] e^{-k_{mr}(t-t_0)} \tag{3.61}$$

where,

$C_r(t)$ = rapidly mineralizing N concentration in upper zone (g N/m^3);
t = time since N application (year);
t_0 = time taken for N application (year);
$C_r(t_0)$ = initial rapidly mineralizing N concentration in upper zone (g N/m^3);
F_{man}^r = rapidly mineralization fraction of manure N (RISK-N default value: 0.25);
F_{res}^r = rapidly mineralization fraction of residue N (default: 0.5);
M_{res} = mass of residue added to soil (g N/m^2);

H_{ur} = depth of upper zone (m)

$\delta()$ = Dirac delta function

Ammonium mass balance in upper zone

The relation between adsorbed and solution NH_4^+-N concentration is modeled using a linear-equilibrium isotherm, which dictates instantaneous portioning between the two phases as strong adsorption. This non-leaching assumption for NH_4^+ is found in the majority of nitrogen cycling and leaching models. Thus, the ammonia concentration in the soil solution $\overline{C}_{al}$, may be described by the equation:

$$\overline{C}^u_{as} = K_{dur}\overline{C}_{al} \tag{3.62}$$

where,

K_{dur} = distribution coefficient (m^3 soil solution /g soil)

$\overline{C}^u_{as}$ = ammonium concentration in absorbed phase (g NH_4^+-N/g soil); and

$\overline{C}_{al}$ = ammonium concentration in soil solution (g NH_4^+-N/m^3 soil solution). Ammonium mass flux at the bottom of upper zone, z = H_{ur}, is taken to be negligible given the usual rapid rate of nitrification and is given by:

$$\theta_{ur}R_{ur}\frac{d\overline{C}_{al}}{dt}\theta_{ur}k_n\overline{C}_{al} = k_{mr}C_r(t) + k_{ms}C_s(t) + \frac{q_{ur}}{H_{ur}}C_{a0}(t) \tag{3.63}$$

its solution is given by (Gusman and Marino, 1999):

$$\overline{C}_{al}(t) = e^{-(k_n/R_{ur})(t-t_0)}\overline{C}_{al}(t_o) + (1/\theta_{ur}R_{ur})\int_{t_0}^{t} e^{-(k_n/R_{ur})(t-\tau)}[k_{mr}C_r(\tau) + k_{ms}C_s(\tau) + (q_{ur}C_{a0}(\tau)/H_{ur})]d\tau \tag{3.64}$$

where, R_{ur} is the upper root zone retardation factor and is given by:

$$R_{ur} = 1 + \left(\frac{\rho_{ur}K_{dur}}{\theta_{ur}}\right) \tag{3.65}$$

where,

ρ_{ur} = soil bulk density in upper root zone (g soil/m^3 soil)

K_{dur} = first order rate coefficient for nitrification ($year^{-1}$) in the upper zone

θ_{ur} = Volumetric water content in upper root zone (m^3 soil solution/m^3 soil);

k_n = first order rate coefficient for nitrification ($year^{-1}$) ;

$C_{a0}(\tau)$ = Ammonium concentration at soil surface (g NH_4^+-N/m^3 soil solution);

τ = "Dummy" time variable for integration.

$q_{ur}C_{a0}(t)$ = Ammonium from fertilizer applications and dry deposition instantly mobilized by q_{ur} at the surface is given by:

$$q_{ur}C_{a0}(t) = [M_a + Dep_a^{dry}\Delta t_0]d(t-t_0) + (p-r)C_{ap} \quad (3.66)$$

where,

C_{ap} = ammonium concentration in precipitation (g NH_4^+-N/m^3);

Dep_a^{dry} = constant rate of dry deposition (NH_4^+-N/m^2 / year);

Δt_0 = duration of the previous season;

M_a = the mass of ammonium applied (g NH_4^+-N/m^2)

where,

$$M_a = (1 - F_{amm}^{volat})M_{amm} + (F_{man}^{a} - F_{man}^{volat})M_{man} \quad (3.67)$$

where,

F_{amm}^{volat} = fraction of applied ammonium / urea fertilizer lost to quick volatilization (default: 0.2);

M_{amm} = amount of ammonium/urea fertilizer applied (g NH_4^+-N/m^2);

F_{man}^{a} = ammonium/urea fraction of manure N (default 0.5);

F_{man}^{volat} = fraction of applied manure N lost to quick volatilization (default 0.2); and

M_{man} = amount of total manure N applied (g N/m^2).

Nitrate mass balance in upper zone

The nitrate concentration in the upper zone $\overline{C}_n^{ur}$ (g NO_3^--N/m^3 soil solution) may be described as

$$\frac{d\overline{C}_n^{ur}}{dt} + \left[\frac{q_{ur}^*}{\theta_{ur}H_{ur}} + k_{dur}\right]\overline{C}_n^{ur} = k_n\overline{C}_{al}(t) + \frac{(q_{ur}C_{n0}(t) - U_{ur})}{\theta_{ur}H_{ur}} \quad (3.68)$$

its solution is given by (Gusman and Marino, 1999):

$$\overline{C}_n^{ur}(t) = e^{-\alpha_n(t-t_0)}\overline{C}_n^{ur}(t_0) + \int_{t_0}^{t} e^{-\alpha_n(t-\tau)}\left[k_n\overline{C}_{al}(\tau) + \frac{(q_{ur}C_{n0}(\tau) - U_{ur})}{\theta_{ur}H_{ur}}\right]d\tau \quad (3.69)$$

where,

$$\alpha_n = \frac{q_{ur}^*}{\theta_{ur}H_{ur}} + k_{dur} \quad (3.70)$$

where,

$\overline{C}_n^{ur}(t_0)$ = initial nitrate concentration in upper zone (g NO_3^--N/m^3 soil solution);

$\overline{C}_{al}(\tau)$ = ammonium concentration from eqn. 3.64 (g NH_4^+- N/m^3 soil solution);

$C_{n0}(\tau)$ = nitrate concentration at soil surface (g NO_3^--N/m^3 soil solution);

K_{dur} = first order rate coefficient for dentrification in upper root zone (year $^{-1}$); and

U_{ur} = plant uptake in upper root zone (g NO_3^--N/m^3 soil /year)

where,

$$q_{ur}C_{n0}(t) = M_n\delta(\tau - t_0) + iC_{ni} \tag{3.71}$$

where,

M_n = mass of fertilizer nitrate applied (g NO_3^--N/m^2);

C_{ni} = nitrate concentration in applied irrigation water (g NO_3^--N/m^3)

i = irrigation rate (m/yr)

3.3.4 Governing Equations for lower zone

Nitrate mass balance in lower zone

The nitrate concentration in the lower zone, $\overline{C}_n^{lr}$ (g NO_3^--N/m^3 soil solution), may be described as:

$$\frac{d\overline{C}_n^{lr}}{dt} + \left[\frac{q_{lr}^*}{\theta_{lr}H_{lr}} + k_{dlr}\right]\overline{C}_n^{lr} = \left[\frac{q_{ur}^*\overline{C}_n^{ur}(t) - U_{lr}}{\theta_{lr}H_{lr}}\right] \tag{3.72}$$

its solution is given by (Gusman and Marino, 1999):

$$\overline{C}_n^{lr}(t) = e^{-\beta_n(t-t_0)}\overline{C}_n^{lr}(t_0) + \int_{t_0}^{t} e^{-\beta_n(t-\tau)}\left[\frac{q_{ur}^*\overline{C}_n^{ur}(\tau) - U_{lr}}{\theta_{lr}H_{lr}}\right]d\tau \tag{3.73}$$

where,

$$\beta_n = \frac{q_{lr}^*}{\theta_{lr}H_{lr}} + k_{dlr} \tag{3.74}$$

where,

$C_n(t)$ = average nitrate concentration in upper root zone;

θ_{lr} = volumetric water content in lower root zone (m);

k_{dlr} = first order rate coefficient for denitrification in lower root zone ($year^{-1}$);

U_{lr} = plant uptake rate in lower root zone (g NO_3^--N/m^3 soil /year)

3.3.5 Governing equations for drain field zone

Ammonia mass balance in drain field zone

The two phase advective-dispersive equation for ammonium concentration in the sub-drain field zone is given by:

$$\theta_d R_d \frac{\partial C_{al}}{\partial t} = \frac{\partial}{\partial z}\left(\theta_d D_a \frac{\partial C_{al}}{\partial z}\right) - q_d^* \frac{\partial C_{al}}{\partial z} - k_{nd}\theta_d C_{al} + k_{mo}C_{on} \tag{3.75}$$

in which θ_d volumetric water content in the sub-drainfield zone, D_a porous media dispersion coefficient for ammonia (m^2/yr), R_d is retardation factor for ammonium in the subdrain field

zone (m), k_{mo} is the rate coefficient for net mineralization of the septic drain field organic N (yr^{-1}), k_{nd} the first order coefficient for nitrification in the sub drainfield zone (1/yr), and C_{on} is the septic drainfield organic N concentration (gm of N/m^3 of soil). Using the linear-equilibrium isotherm and the solution of equation 3.75 integrated over the sub-drainfield zone depth is:

$$\theta_d R_d \frac{d}{dt}\int_{h_{lr}}^{h_{lr}+H_d} C_{al}(z,t)dz = \left(\theta_d D_a \frac{\partial C_{al}(h_{lr}+(H_d,t))}{\partial z} - q_d^* C_{al}(h_{lr}+(H_d,t))\right)$$

$$-\left(\theta_d D_a \frac{\partial C_{al}(h_{lr},t)}{\partial z} - q_d^* C_{al}(h_{lr},t)\right) - k_{nd}\theta_d \int_{h_{lr}}^{h_{lr}+H_d} C_{al}(z,t)dz + H_d k_{mo} C_{on}(t) \qquad (3.76)$$

the above equation is rewritten as:

$$\overline{C}_{al}^{d}(t) = e^{-\mu_a(t-t_0)}\overline{C}_{al}(t_0) + \Phi_o\left\{e^{-k_{mo}(t-t_0)} - e^{-\mu_a(t-t_0)}\right\} + \Phi_d\left\{1 - e^{-\mu_a(t-t_0)}\right\} \qquad (3.77)$$

where,

$$\Phi_o = \frac{k'_{mo}(C_{on}(t_0) - \omega_{on})C_{d0}}{\mu_a - k_{mo}} \qquad (3.78)$$

where,

$$k_{mo}(T) = 5.6 * 10^{12} \exp[-9800/(T+273)]F_{wd} \qquad (3.79)$$

$$k'_{mo} = \frac{k_{mo}}{\theta_d R_d} \qquad (3.80)$$

R_d is the retardation factor and is given by:

$$R_d = 1 + \left(\frac{\rho_d K_{dd}}{\theta_d}\right) \qquad (3.81)$$

ρ_d = Soil bulk density in drainfield zone (g soil/m^3 soil);
K_{dd} = distribution coefficient (m^3 soil solution/g soil)
C_{d0} = total N concentration in sub drain field effluent (g/m^3)

The rate of change for the organic N concentration in the sub-drainfield zone is given by:

$$\frac{dC_{on}}{dt} = -k_{mo}C_{on} + ON_0 \qquad (3.82)$$

in which ON_o is the rate that organic N is added to the subdrain field zone (gm of N/m^3 of soil /yr) given by:

$$ON_0 = \frac{p_d F_{ond} C_{d0}}{H_d} \tag{3.83}$$

The solution is given by:

$$C_{on}(t) = C_{on}(t_0)e^{-k_{mo}(t-t_0)} + \omega_{on} C_{do}(1 - e^{-k_{mo}(t-t_0)}) \tag{3.84}$$

$$\omega_{on} = \frac{p_d F_{ond}}{H_d k_{mo}} \tag{3.85}$$

where,

C_{on} = septic drain field organic N concentration (gm of N/m^3 of soil),
k_{mo} = the rate coefficient for net mineralization of the septic drainfield zone organic N (1/yr),
H_d = average thickness subdrain field zone
F_{ond} = The fraction of septic tank effluent in organic N form
where,

$$F_{ond} = 1 - F_{ad} \tag{3.86}$$

where,

F_{ad} = the fraction of septic drainfield N in the NH_4^+ form;

$$\mu_a = \frac{k_{nd}}{R_d} \tag{3.87}$$

$$\Phi_d = \frac{(\omega_a + k'_{mo}\,\omega_{on})C_{d0}}{\mu_a} \tag{3.88}$$

where,

$$\omega_a = \frac{p_d F_{ad}}{\theta_d R_d H_d} \tag{3.89}$$

Nitrate mass balance in drain field zone

The advective-dispersive equation below the septic drainfield is written as

$$\frac{\partial(\theta_d C_n)}{\partial t} = \frac{\partial}{\partial z}\left(\theta_d D_n \frac{\partial C_n}{\partial z}\right) - q_d^* \frac{\partial C_n}{\partial z} - k_{dd}\theta_d C_n + k_{nd}\theta_d C_{al} \tag{3.90}$$

in which θ_d is the volumetric water content in the sub-drainfield zone (m^3 of soil solution/ m^3 of soil), k_{dd} is the first-order rate coefficient for denitrification in the sub-drainfield zone (yr^{-1}), and k_{nd} is the first-order rate coefficient for nitrification in the sub-drainfield zone. Equation 3.90 is integrated over the depth of subdrainfield zone from $z = h_{lr}$ to $z = h_{lr} + H_d$ resulting in

$$\frac{d}{dt}\int_{h_{lr}}^{h_{lr}+H_d} C_n(z,t)dz = \left(D_n \frac{\partial C_n(h_{lr}+(H_d,t))}{\partial z} - \frac{q_d^*}{\theta_d} C_n(h_{lr}+(H_d,t)) \right)$$

$$-\left(D_n \frac{\partial C_n(h_{lr},t)}{\partial z} - \frac{q_d^*}{\theta_d} C_n(h_{lr},t) \right) - k_{dd}\int_{h_{lr}}^{h_{lr}+H_d} C_n(z,t)dz + k_{nd}\int_{h_{lr}}^{h_{lr}+H_d} C_{al}(z,t)dz \qquad (3.91)$$

its solution is given by:

$$\begin{aligned}\overline{C}_n^d(t) = \overline{C}_n^{lr}(t_0)e^{-\mu_n(t-t_0)} &+ \Pi\left\{e^{-\mu_a(t-t_0)} - e^{-\mu_n(t-t_0)}\right\} + \Pi_d\left\{1 - e^{-\mu_n(t-t_0)}\right\} \\ &+ \Pi_o\left\{e^{-k_{mo}(t-t_0)} - e^{-\mu_n(t-t_0)}\right\} + \Pi''\left\{e^{-\chi_n(t-t_0)} - e^{-\mu_n(t-t_0)}\right\} \\ &+ \Pi_n\left\{e^{-\beta_n(t-t_0)} - e^{-\mu_n(t-t_0)}\right\} + \Pi_a\left\{e^{-k'_n(t-t_0)} - e^{-\mu_n(t-t_0)}\right\} \\ &+ \Pi_r\left\{e^{-k_{mr}(t-t_0)} - e^{-\mu_n(t-t_0)}\right\} + \Pi_s\left\{e^{-k_{ms}(t-t_0)} - e^{-\mu_n(t-t_0)}\right\} \\ &+ \Pi'\left\{1 - e^{-\mu_n(t-t_0)}\right\}\end{aligned} \qquad (3.92)$$

where,

$$k_n^{'} = \frac{k_{nur}}{R_{ur}} \qquad (3.93)$$

$$A_r = \frac{k_{mr}^{'} C_r^0}{(k_n^{'} - k_{mr})} \qquad (3.94)$$

$$k_{mr}^{'} = \frac{k_{mr}}{\theta_{ur} R_{ur}} \qquad (3.95)$$

$$A^{'} = \frac{(k_{ms}^{'} C_s^{soil} + Dep_t)}{k_n^{'}} \qquad (3.96)$$

$$A_s = \frac{k_{ms}^{'} C_s^0}{(k_n^{'} - k_{ms})} \qquad (3.97)$$

$$k_{ms}^{'} = \frac{k_{ms}}{\theta_{ur} R_{ur}} \qquad (3.98)$$

$$A_a = \overline{C}_{al}(t_0) - A_r - A^{'} - A_s + M_a^{'} \qquad (3.99)$$

$$M_a^{'} = \frac{M_a}{\theta_{ur} H_{ur} R_{ur}} \qquad (3.100)$$

$$M_n^{'} = \frac{M_n}{\theta_{ur} H_{ur}} \tag{3.101}$$

$$Dep_t = \frac{\left[(p-r)C_{ap} + Dep_a^{dry}\right]}{\theta_{ur} H_{ur} R_{ur}} \tag{3.102}$$

$$B_a = \frac{k_n A_a}{(\beta_n - k_n^{'})} \tag{3.103}$$

$$B_r = \frac{k_n A_r}{(\beta_n - k_{mr})} \tag{3.104}$$

$$B_s = \frac{k_n A_s}{(\beta_n - k_{ms})} \tag{3.105}$$

$$B^{'} = \frac{(k_n A^{'} + C_{ni}^{'} - U_{ur}^{'})}{\beta_n} \tag{3.106}$$

$$C_{ni}^{i} = \frac{iC_{ni}}{H_{ur}\theta_{ur}} \tag{3.107}$$

$$U_{ur}^{'} = \frac{U_{ur}}{H_{ur}\theta_{ur}} \tag{3.108}$$

$$B_n = \overline{C_n}(t_0) - B_a - B_r - B_s - B^{'} + M_n^{'} \tag{3.109}$$

$$\chi_n = \frac{q_{lr}^{*}}{\theta_{lr} H_{lr}} + k_{dlr} \tag{3.110}$$

$$\gamma_n = \frac{q_{ur}^{*}}{\theta_{lr} H_{lr}} \tag{3.111}$$

$$E_n = \frac{\gamma_n B_n}{(\chi_n - \beta_n)} \tag{3.112}$$

$$E_a = \frac{\gamma_n B_a}{(\chi_n - k_n^{'})} \tag{3.113}$$

$$E_r = \frac{\gamma_n B_r}{(\chi_n - k_{mr})} \tag{3.114}$$

$$E_s = \frac{\gamma_n B_s}{(\chi_n - k_{ms})} \tag{3.115}$$

$$E' = \frac{(\gamma_n B' - U'_{lr})}{\chi_n} \tag{3.116}$$

$$U'_{lr} = \frac{U_{lr}}{H_{lr}\theta_{lr}} \tag{3.117}$$

$$\mu_n = \frac{q^*_d}{\theta_d H_d} + k_{dd} \tag{3.118}$$

Where, k_{dd} is the is the first order rate coefficient for dentrification

$$\omega_n = \frac{q^*_{lr}}{\theta_d H_d} \tag{3.119}$$

$$\Pi = \frac{k_{nd}\Phi_a}{(\mu_n - \mu_a)} \tag{3.120}$$

where,

$$\Phi_a = \overline{C_{al}}(t_0) - \Phi_o + \Phi_d \tag{3.121}$$

$$\Pi_o = \frac{k_{nd}\Phi_o}{(\mu_n - k_{mo})} \tag{3.122}$$

$$\Pi_d = \frac{k_{nd}\Phi_d}{(\mu_n)} \tag{3.123}$$

where, k_{nd} is the first order rate coefficient for nitrification (1/year)

$$\Pi'' = \frac{\omega_n E''}{(\mu_n - \chi_n)} \tag{3.124}$$

$$E'' = \overline{C_n}(t_0) - E_n - E_a - E_r - E_s - E' \tag{3.125}$$

$$\Pi_n = \frac{\omega_n E_n}{(\mu_n - \beta_n)} \tag{3.126}$$

$$\Pi_a = \frac{\omega_n E_a}{(\mu_n - k'_n)} \tag{3.127}$$

$$\Pi_r = \frac{\omega_n E_r}{(\mu_n - k_{mr})} \tag{3.128}$$

$$\Pi_s = \frac{\omega_n E_s}{(\mu_n - k_{ms})} \tag{3.129}$$

$$\Pi' = \frac{\omega_n E'}{(\mu_n)} \tag{3.130}$$

Finally equation 3.92 is simplified to

$$\overline{C}_n^d(t) = \Pi''' e^{-\mu_n (t-t_0)} + \Pi e^{-\mu_a (t-t_0)} + \Pi_o e^{-k_{mo}(t-t_0)} + \Pi_d + \Pi'' e^{-\chi_n (t-t_0)}$$

$$+ \Pi_n e^{-\beta_n (t-t_0)} + \Pi_a e^{-k_n^{'}(t-t_0)} + \Pi_r e^{-k_{mr}(t-t_0)} + \Pi_s e^{-k_{ms}(t-t_0)} + \Pi' \tag{3.131}$$

where,

$$\Pi''' = \overline{C}_n^{lr}(t_0) - \Pi - \Pi_o - \Pi_d - \Pi'' - \Pi_n - \Pi_a - \Pi_r - \Pi_s - \Pi' \tag{3.131}$$

3.3.6 Governing equations for intermediate vadose zone

Nitrate mass balance in intermediate vadose zone

Denitrification is assumed to be the only N transformation process in the intermediate-vadose zone, so the nitrate advective-dispersive equation is written as

$$\frac{\partial(\theta_v C_n)}{\partial t} = \frac{\partial}{\partial z}\left(\theta_v D_n \frac{\partial C_n}{\partial z}\right) - q_v^* \frac{\partial C_n}{\partial z} - k_{dv}\theta_v C_n \tag{3.132}$$

in which θ_v is the volumetric water content in the intermediate-vadose zone (m^3 of soil solution/m^3 of soil), C_n = nitrate-nitrogen solution concentration (mg/l), D_n = porous media dispersion coefficient for nitrate (m^2/yr), q_v^*= percolation from the intermediate vadose zone (m/yr) and k_{dv} is the first-order rate coefficient for denitrification in the intermediate-vadose zone (yr^{-1}).

For a model application through the septic system the nitrate leaching from the subdrainfield zone enters the intermediate vadose zone. Equation 3.132 integrated over the depth of the intermediate vadose zone from $z = h_d$ *to* $z = h_d + H_v$ resulting the nitrate concentration in intermediate vadose zone is given by:

$$\frac{d}{dt}\int_{h_d}^{h_d+H_v} C_n(z,t)dz = \left(D_n \frac{\partial C_n(h_d + H_v, t)}{\partial z} - \frac{q_v^*}{\theta_v} C_n(h_d + H_v, t)\right)$$

$$-\left(D_n\frac{\partial C_n(h_d,t)}{\partial z}-\frac{q^*_{lr}}{\theta_v}C_n(h_d,t)\right)\quad -k_{dv}\int_{h_d}^{h_d+H_v}C_n(z,t)dz\ + \tag{3.133}$$

The solution of the above equation is given by Gusmen and Marino (1999):

$$\begin{aligned}\overline{C}^v_n(t)=\overline{C}^d_n(t_0)e^{-\eta_n(t-t_0)}&+\Lambda'''\left\{e^{-\mu_n(t-t_0)}-e^{-\eta_n(t-t_0)}\right\}\\&+\Lambda\left\{e^{-\mu_a(t-t_0)}-e^{-\eta_n(t-t_0)}\right\}+\Lambda_o\left\{e^{-k_{mo}(t-t_0)}-e^{-\eta_n(t-t_0)}\right\}\\&+\Lambda_d\left\{1-e^{-\eta_n(t-t_0)}\right\}+\Lambda''\left\{e^{-\chi_n(t-t_0)}-e^{-\eta_n(t-t_0)}\right\}\\&+\Lambda_n\left\{e^{-\beta_n(t-t_0)}-e^{-\eta_n(t-t_0)}\right\}+\Lambda_a\left\{e^{-k'_n(t-t_0)}-e^{-\eta_n(t-t_0)}\right\}\\&+\Lambda_r\left\{e^{-k_{mr}(t-t_0)}-e^{-\eta_n(t-t_0)}\right\}+\Lambda_s\left\{e^{-k_{ms}(t-t_0)}-e^{-\eta_n(t-t_0)}\right\}\\&+\Lambda'\left\{1-e^{-\eta_n(t-t_0)}\right\}\end{aligned} \tag{3.134}$$

where,

$$\eta_n=\frac{q^*_v}{\theta_v H_v}+k_{dv} \tag{3.135}$$

$$\lambda_n=\frac{q^*_{lr}}{\theta_v H_v} \tag{3.136}$$

$$\psi_n=\frac{q^*_d}{\theta_v H_v} \tag{3.137}$$

$$\Lambda'''=\frac{\psi_n\Pi'''}{(\eta_n-\mu_n)} \tag{3.138}$$

$$\Lambda=\frac{\psi_n\Pi'''}{(\eta_n-\mu_a)} \tag{3.139}$$

$$\Lambda_o=\frac{\psi_n\Pi_o}{(\eta_n-k_{mo})} \tag{3.140}$$

$$\Lambda_d=\frac{\psi_n\Pi_d}{\eta_n} \tag{3.141}$$

$$\Lambda''=\frac{\psi_n\Pi''}{(\eta_n-\chi_n)} \tag{3.142}$$

$$\Lambda_n = \frac{\psi_n \Pi_n}{(\eta_n - \beta_n)} \tag{3.143}$$

$$\Lambda_a = \frac{\psi_n \Pi_a}{(\eta_n - k'_n)} \tag{3.144}$$

$$\Lambda_r = \frac{\psi_n \Pi_r}{(\eta_n - k_{mr})} \tag{3.145}$$

$$\Lambda_s = \frac{\psi_n \Pi_s}{(\eta_n - k_{ms})} \tag{3.146}$$

$$\Lambda' = \frac{\psi_n \Pi'}{\eta_n} \tag{3.147}$$

Further simplification of equation 3.134 results in

$$\begin{aligned} \overline{C}_n^v(t) &= \Lambda_t e^{-\psi_n (t-t_0)} + \Lambda''' e^{-\mu_n (t-t_0)} + \Lambda e^{-\mu_a (t-t_0)} + \Lambda_o e^{-k_{mo}(t-t_0)} \\ &+ \Lambda_d + \Lambda'' e^{-\chi_n (t-t_0)} + \Lambda_n e^{-\beta_n (t-t_0)} + \Lambda_a e^{-k'_n (t-t_0)} \\ &\Lambda_r e^{-k_{mr}(t-t_0)} + \Lambda_s e^{-k_{ms}(t-t_0)} + \Lambda' \end{aligned} \tag{3.148}$$

where,

$$\Lambda_t = \overline{C}_n^d(t_0) - \Lambda''' - \Lambda - \Lambda_o - \Lambda_d - \Lambda'' - \Lambda_n - \Lambda_a - \Lambda_r - \Lambda_s - \Lambda' \tag{3.149}$$

3.3.7 Governing equations for saturated zone

Nitrate transport in saturated zone

While most nitrogen models consider the bottom of the vadose zone as the lower boundary of the system, the RISK-N model continues to track the movement of nitrate through the aquifer, and to the water-supply wells of concern. The nitrate groundwater transport and fate equation and its solution are based on the development given in Hantush and Marino (1996) for an adsorbing pesticide. Only minor changes are made in order to simulate the movement of the non-adsorbing nitrate. The two-dimensional advection-dispersion of a reactive solute (Bear, 1979) can be described by the following partial differential equation

$$\frac{\partial C_n}{\partial t} = D_{xx} \frac{\partial^2 C_n}{\partial x^2} + D_{yy} \frac{\partial^2 C_n}{\partial y^2} - u \frac{\partial C_n}{\partial x} - k_{ds} C_n \tag{3.150}$$

in which

C_n = the concentration of the contaminant in groundwater (gm/m^3);
D_{xx} = the hydrodynamic dispersion coefficient along the x axis (m^2/yr);
D_{yy} = the hydrodynamic dispersion coefficient along the y axis (m^2/yr);
u = the average linear pore-water velocity along the x axis;
k_{ds} = the rate of dentrification.
The dispersion coefficients, D_{xx} and D_{yy} can be expressed in terms of two components (Freeze and Cherry, 1979) as:

$$D_{xx} = D^* + \alpha_L u \tag{3.151}$$

$$D_{yy} = D^* + \alpha_T u \tag{3.152}$$

in which
D* = the molecular diffusion coefficient multiplied by the tortuosity (m^2/yr);
α_L = the longitudinal dispersivity (m) along the mean flow direction;
α_T = the transverse dispersivity (m).
If the following is defined

$$C_n^*(x,y,t) = e^{k_{ds}t} C_n(x,y,t) \tag{3.153}$$

then the equation 3.150 can be reduced to

$$\frac{\partial C_n^*}{\partial t} = D_{xx}\frac{\partial^2 C_n^*}{\partial x^2} + D_{yy}\frac{\partial^2 C_n^*}{\partial y^2} - u\frac{\partial C_n^*}{\partial x} \tag{3.154}$$

The solution of the above equation 3.154 in an infinite domain for an instantaneous injection of solute mass per depth, M, at time $t = 0$, and with zero initial concentration, $C(x,y,0) = 0$, is given by (Bear, 1979) as

$$C_n^*(x,y,t) = \frac{M}{4\pi\sqrt{D_{xx}D_{yy}t}}\exp\left\{-\left(\frac{(x-ut)^2}{4D_{xx}t} + \frac{y^2}{4D_{yy}t}\right)\right\} \tag{3.155}$$

The solution of 3.150 equation is obtained by substituting the elementary solution (Equation 3.155) in to equation 3.153 and is given by:

$$C_n(x,y,t) = \frac{M}{4\pi\sqrt{D_{xx}D_{yy}t}}\exp\left\{-\left(\frac{(x-ut)^2}{4D_{xx}t} + \frac{y^2}{4D_{yy}t} + k_{ds}t\right)\right\} \tag{3.156}$$

The solute mass is injected at the interface between the unsaturated zone and the water table. The actual model zone located above the water table depends on the application, and could be the lower-root zone, sub-drainfield zone, or the intermediate-vadose zone. In the following equations, $C_u(\tau)$ represents the concentration in which the unsaturated model zone overlies the aquifer. For nitrate applied over an area L_x by L_y (m), and injected per unit depth B (m) of the aquifer, the solution to equation 3.156 is given by:

$$C_n(x,y,t) = (1/B)\int_0^t q_s(\tau)C_u(\tau)e^{-(k_{ds})(t-\tau)}G(\tau;x,t)F(\tau;y,t)d\tau \qquad (3.157)$$

where,

$$G(\tau;x,t) = \frac{1}{2}erf\left(\frac{l_x/2+|(x-u(t-\tau))|}{2\sqrt{D_{xx}(t-\tau)}}\right) - \frac{1}{2}erf\left(\frac{-l_x/2+|(x-u(t-\tau))|}{2\sqrt{D_{xx}(t-\tau)}}\right), \quad if|x-u(t-\tau)| > l_x/2$$

$$= \frac{1}{2}erf\left(\frac{l_x/2-(x-u(t-\tau))}{2\sqrt{D_{xx}(t-\tau)}}\right) + \frac{1}{2}erf\left(\frac{l_x/2+(x-u(t-\tau))}{2\sqrt{D_{xx}(t-\tau)}}\right), \quad if|x-u(t-\tau)| \le l_x/2$$

(3.158)

and

$$F(\tau;y,t) = \frac{1}{2}erf\left(\frac{l_y/2+|y|}{2\sqrt{D_{yy}(t-\tau)}}\right) - \frac{1}{2}erf\left(\frac{-l_y/2+|y|}{2\sqrt{D_{yy}(t-\tau)}}\right), \quad if|y| > l_y/2$$

$$= \frac{1}{2}erf\left(\frac{l_y/2-y}{2\sqrt{D_{yy}(t-\tau)}}\right) + \frac{1}{2}erf\left(\frac{l_y/2+y}{2\sqrt{D_{yy}(t-\tau)}}\right), \quad if|y| \le l_y/2$$

(3.159)

Equations 3.157 to 3.159 analytically describe the movement, spreading, and denitrification characteristics of a nitrate mass in ground water, after leaching through the unsaturated soil. In addition, equation 3.157 may be written on a seasonal basis as

$$C_n(x,y,t) = (1/B)\sum_{s=1}^{N} q_s \int_{t_{s-1}}^{t_s} C_u(\tau)e^{-k_{ds}(t-\tau)}G(\tau;x,t)F(\tau;y,t)d\tau \qquad (3.160)$$

where, $t_N = t$. For complete derivations of equations (3.157 to 3.160) for an adsorbing pesticide instead of nitrate is given by Hantush and Marino (1996). A FORTRAN code was written by Gusmen and Marino (1999) to perform the solutions of above equations (3.39 to 3.160). The inputs required for the model were generated from the field and a few were taken from the literature.

4.0 STUDY AREA

4.1 Location

The approximate length of the East Coast of India is about 3000 km along the Bay of Bengal. The well-known deltas in the East Coast of India are Cauvery, Krishna, Godavari, Mahanadhi and Sundarbans. The study area, Kakinada urban coastal aquifer, is a part of the River Godavari eastern delta system in the East Godavari district of Andhra Pradesh, India. Bobba (2002) conducted numerical modeling of salt-water intrusion in Godavari delta and observed that there was no seawater intrusion at that time in the Kakinada urban coastal aquifer. The study area is about 415 km^2 and lies between the streams of Eleru and Nakkalakhandi, and the Bay of Bengal. The average density of population in the Kakinada Municipal Corporation (KMC) i.e urban area is 9000 per km^2 and in nearby rural areas it is 800 per km^2 as per the census data of 2001. The location of the study area is shown in Figure 4.1. The study area lies between 82^0 10' 00"to 82^0 21' 41" E longitude and 16^0 55' to 17^0 10' N latitude. The saltwater creek is acting as main cargo handling point in the coast. The Kakinada coast has mild slope. There is no planned drainage network in the city and most of the residential buildings allow sewage disposal through soak pits, and make obstructions to the natural drainage on account of construction of the new roads and colonies. The KMC supplies treated water within municipal limits through taps for drinking as well as domestic purposes and the source of this water is the River Godavari. The water is brought by Samalkot branch canal to treatment plant.

4.2 Geology

The main geology of the East Godavari District is shown in Figure 4.1. The coastal plain is occupied by coastal alluvium composed of sand, silt and clay and the northwestern side is underlain by alluvium of Eleru stream. The coastal plain (I) consists of low beach ridges, strandlines, mudflats, marshes and the narrow beach. Beach ridges and strandlines have fresh groundwater while mudflats and marshes contain brackish/saline water from the top zone itself. In the beach ridges and strandlines, groundwater occurs under water table conditions. These areas are suitable for construction of dug wells or filter point wells down to a maximum depth of 8 m below ground level (bgl). The average depth of water table varies between 0.6 m and 3.5 m bgl. The prime source of recharge is rainfall. Groundwater is being used mainly for domestic and drinking purposes only.

Eleru alluvium (II) comprises of alternating layers of sand and clay. Groundwater occurs under water table conditions to confined conditions. Filter point wells and tube wells are suitable for extracting groundwater and depths of these wells range from 20 to 50 m bgl. Groundwater utilization is for drinking and to a limited extent for agriculture. Both the coastal plain and Eleru alluvium rest over Rajahmundry sand stone formation, which is exposed near Rajahmundry, about 60 km from the seacoast. The general dip of Rajahmundry sandstone is towards southeast. The lithology of two wells in the East (Kakinada) –West (Jaggampeta) direction in the study area

is shown in Figure 4.2. The area is underlain by recent alluvium followed by sand stones in the East direction and sand stones are exposed in the West direction. Groundwater in the area occurs under phreatic to semi-confined conditions.

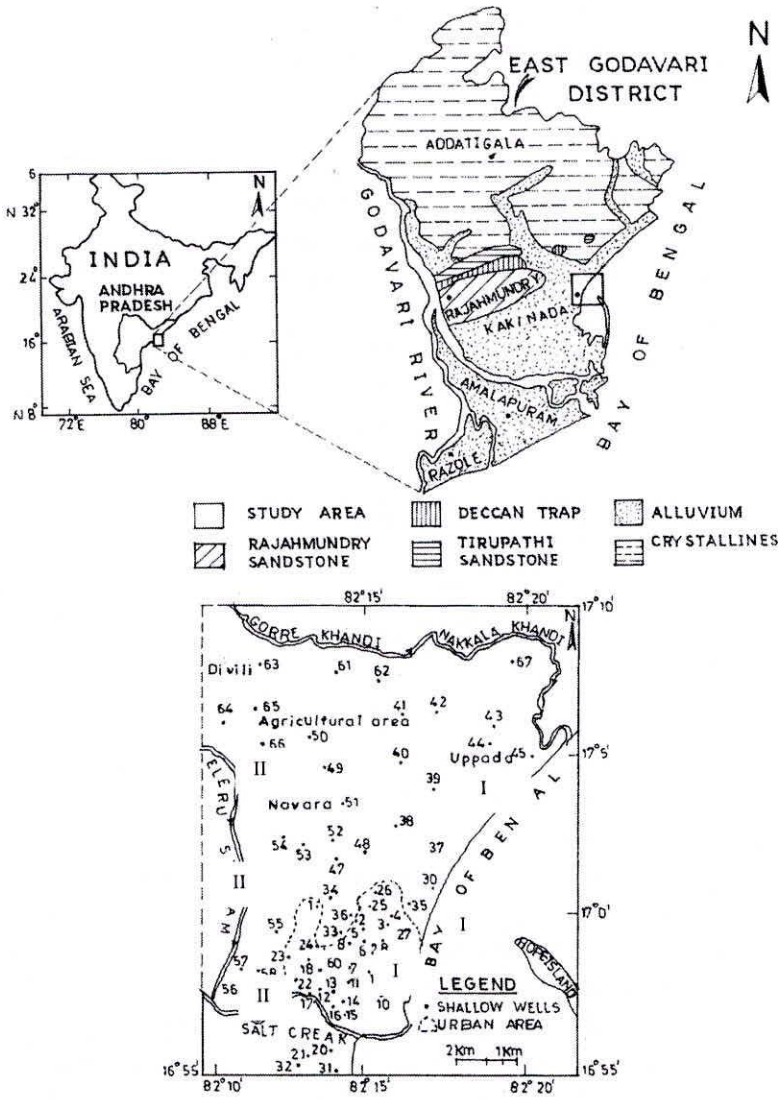

Fig. 4.1 Location of the study area, geology and observation wells

4.3 Climate

The tropical climate is warm from April to June, with a maximum temperature of 40^0 C. The winter months are December and January with the minimum average temperature of 20^0C. The major portion of rainfall falls during the southwest monsoon from July to September. Annual normal rainfall in Kakinada town is 1095 mm. The Kakinada coast is also affected by cyclonic storms and depressions in the Bay of Bengal. The average evaporation rate varies from 2.5 to 9 mm/day.

4.4 Groundwater quality

The preliminary evaluation of shallow groundwater quality (less than 6 m bgl) in the year 1994 has been carried out by Jain et al. (1997) within the Kakinada Municipal Corporation (KMC) by monitoring 29 wells in coastal plain within the area of 30 km^2. The quality evaluation is limited to major ions (Ca^{2+}, Mg^{2+}, Na^{+}, K^{+} and HCO_3^-, Cl^-, SO_4^-, PO_4^- and NO_3^-) only. The study revealed the highest nitrate concentrations up to 298 mg/l within the KMC in the year 1994, and 20 wells out off 29 wells exceeded the permissible limit of 45 mg/l. Jain et al. (2004) evaluated trace metals (Cu, Fe, Mn, Co, Ni, Cr, Pb and Cd) concentrations in and around KMC in the year 2000 and concluded that iron and manganese were up to 0.910 and 1.022 mg/l respectively, which are above desirable limits. This affects taste, appearance of water and has adverse effect on domestic uses and water supply structures. The other trace elements are within the limits of drinking water. At present, no sewerage lines are available for the disposal of septic effluents in the study area. Every house has septic tank with soak pit, which acts as source of pollution to the shallow groundwater.

4.5 Data used

Field sampling was conducted in and around KMC during the month of May 2000, August 2000 and November 2000. A total number of 63 samples were collected during each survey and they were analyzed for a number of physical and chemical parameters at Water Quality Laboratory of National Institute of Hydrology, Kakinada. These test results were utilized in making groundwater quality data sets for three periods, and have been used for characterization of shallow groundwater quality. To estimate nitrogen load from septic system in each village, the village map was digitized using GIS from atlas of the East Godavari district and topographical features were digitized using GIS from Survey of India (SOI) topographical maps on 1:50,000 scale. These thematic layers were projected to common coordinate system, and a base map was prepared to carryout further analysis. GIS computed geographical area of each polygon is in good agreement with statistical records of areas. Total number of polygons in the study area is found to be 83. Area of each polygon varies between 1 to 21 km^2. The attribute data of population and number of houses are obtained from census data of the years 1991 and 2001.

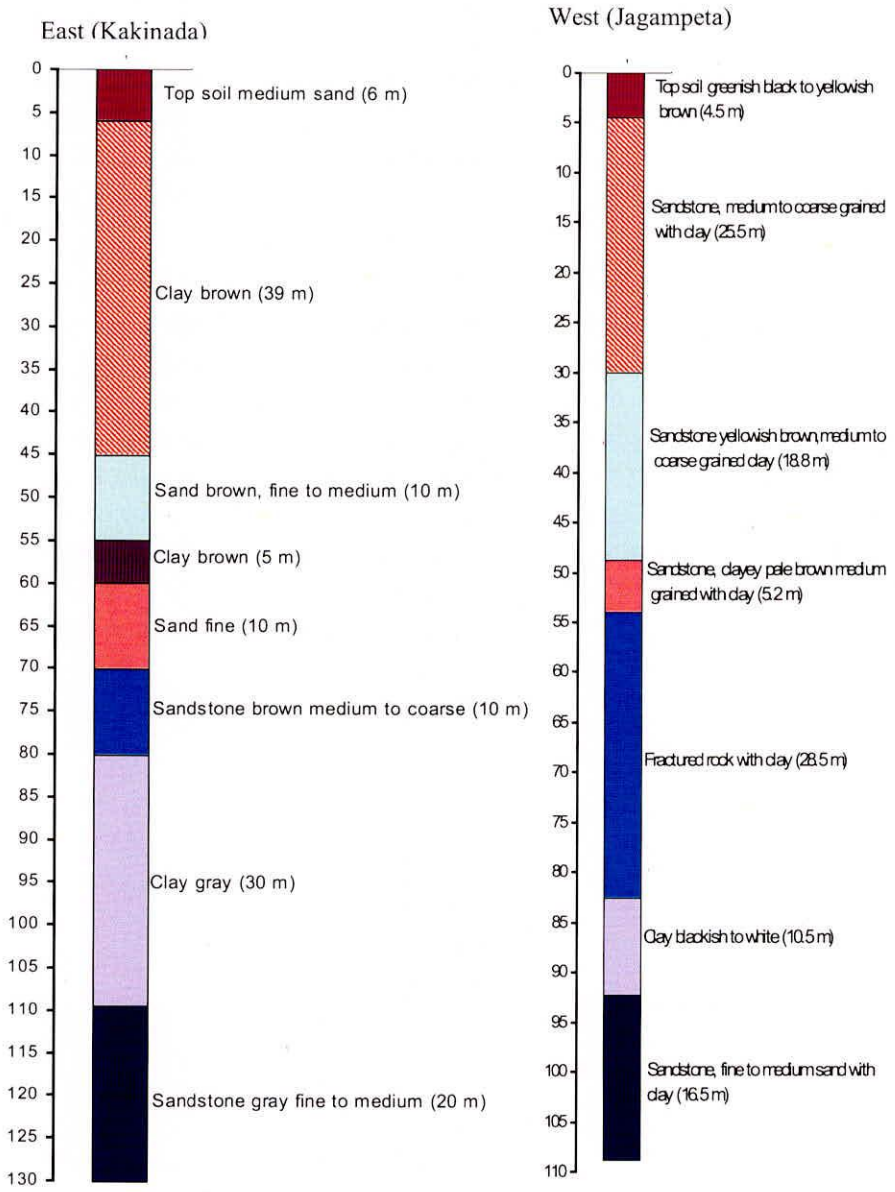

Fig. 4.2. Lithology of wells in the East and West direction in the study area

The average soil type of each polygon was obtained from Andhra Pradesh State Agricultural Department, Kakinada after analyzing 10 to 40 samples in each polygon. The percentage of malfunctioning of septic system in each soil type was obtained from literature. The average total nitrogen in septic effluent and the average quantity of water generated by each person in the study was obtained from literature. Field surveys were conducted to find out the average groundwater quality of each village particularly EC, NO_3^-, PO_4^- and K^+ concentrations in the month of July 2004, December 2004, February 2005 and May 2005. The chemical analysis was carried out in the same laboratory as mentioned earlier.

The Kakinada Municipal Corporation (KMC) was selected for further detailed analysis including the modeling of nitrate leaching into water table aquifer. Three observation wells were selected in Lal Bahadur Nagar (Lb nagar), Madavnagar and Sureshnagar. These locations represent different population densities/plot areas within KMC. The ground levels in these areas are +5.5 m, +4 m and +5 m above mean sea level. These three observation wells were monitored monthly for a period of 12 months (July 2002 to June 2003) for groundwater levels, EC and Nitrate. The chemical analysis was carried out in the same laboratory as mentioned earlier. The average climatic information like rainfall, pan evaporation, air temperature was obtained from a hydrometrological observatory located within the premises of NIH, Kakinada which falls within the KMC. The soil properties considered in the study area are based on the field investigations and reported in the literature.

5.0 RESULTS AND DISCUSSIONS

5.1 Statistical analysis of groundwater quality data

The measured concentrations of water quality parameters for various observation wells monitored during pre-monsoon (May 2000), monsoon (August 2000) and post-monsoon (November 2000) seasons are shown in Figure 5.1. The spatial locations of these observation wells are shown in Figure 3.2. The chemical ion balance error for each sample was within $\pm 10\%$. The desirable and permissible drinking water limits of important chemical parameters are as per the Indian standards (BIS, 1991) are also marked in Figure 5.1. Results revealed that most groundwater samples exceed the desirable drinking water limits for Ca^{2+}, HCO_3^-, Cl^-, SO_4^{2-} and NO_3^-. The percentage exceedence values of these parameters are 7, 31, 9, 7 and 43, respectively. These percentages were computed using water quality data sets (201 samples) generated from three field surveys conducted in the year 2000.

The ion concentrations are in the order of $HCO_3^->Cl^->SO_4^{2-}>NO_3^-$ (anions) and $Na^+>Ca^{2+}>K^+>Mg^{2+}$ (cations) in the study area. High concentration of nitrate up to 421 mg/l was observed in well No. 49 which is in the intensive agricultural area (paddy). A preliminary analysis based on examination of water quality parameters (major cations and anions) of individual wells in the study area (Figure 5.1) suggest significant temporal variations in chemical concentrations in some of the observation wells. These variations are mainly due to land use, proximity to seacoast, evapotranspiration from shallow water table, rainfall recharge and backwater effect in salt creeks. The detailed water quality of each well (Temp., pH, EC, Ca^{2+}, Mg^{2+}, Na^+, K^+, HCO_3^-, Cl^-, SO_4^{2-}, NO_3^-) with location, well number and Piper's classification during pre monsoon period is shown in Table 5.1. The range of pH was 7.0 to 7.9, thus indicating that there is no significant acid or base property in the shallow groundwater in the study area (Table 5.1) and there is no significant spatial variation in groundwater temperature within the study area (Table 5.1). High values of electrical conductivity up to 9693 ($\mu S\ cm^{-1}$) is observed in well No. 30, which is very close to the sea coast. Most of the wells indicate Na^+-HCO_3^- type of groundwater in the study area. However few groundwater samples quality has been plotted on Pipers diagram and for few samples Stiff and Pie diagrams have been prepared. These three diagrams are shown in Figures 5.1(a), 5.1(b) and 5.1(c) respectively. These diagrams indicate few wells (4, 23, 38) are Na-Cl type, few wells (5, 13, 58, 62) are Na-HCO_3 type and few wells (26, 63) are Ca-Cl type in the study area. Minimum, maximum, mean, standard deviation and skewness coefficient of groundwater quality data of the aerobic zone (< 8 m below ground level) in each season and pooling of three seasons data in the year 2000 are summarized in Table 5.2. All cations and anions are positively skewed, except pH and temperature (Table 5.2). Hoyle (1989) and Bjerg and Christensen (1992) have also reported similar results for different study areas. The mean value of Ca^{2+}, HCO_3^-, SO_4^{2-} and NO_3^- concentrations in the study area are 105, 482, 186 and 95 mg/l, respectively during monsoon periods. These concentrations are less in pre and post monsoon periods (Table 5.2). Unlike other water quality parameters, the

mean concentration of Cl^- is 403 mg/l during pre monsoon period and decreased during monsoon and post monsoon period. These changes are mainly due to shallow groundwater table conditions in the study area and contaminants leaching through rainfall recharge into shallow groundwater table. The changes in maximum, mean and minimum ion concentrations could be seen on Schoeller diagram (Figure 5.2). Montgomery et al. (1987) concluded similar findings in their study of statistical characteristics of groundwater quality variables.

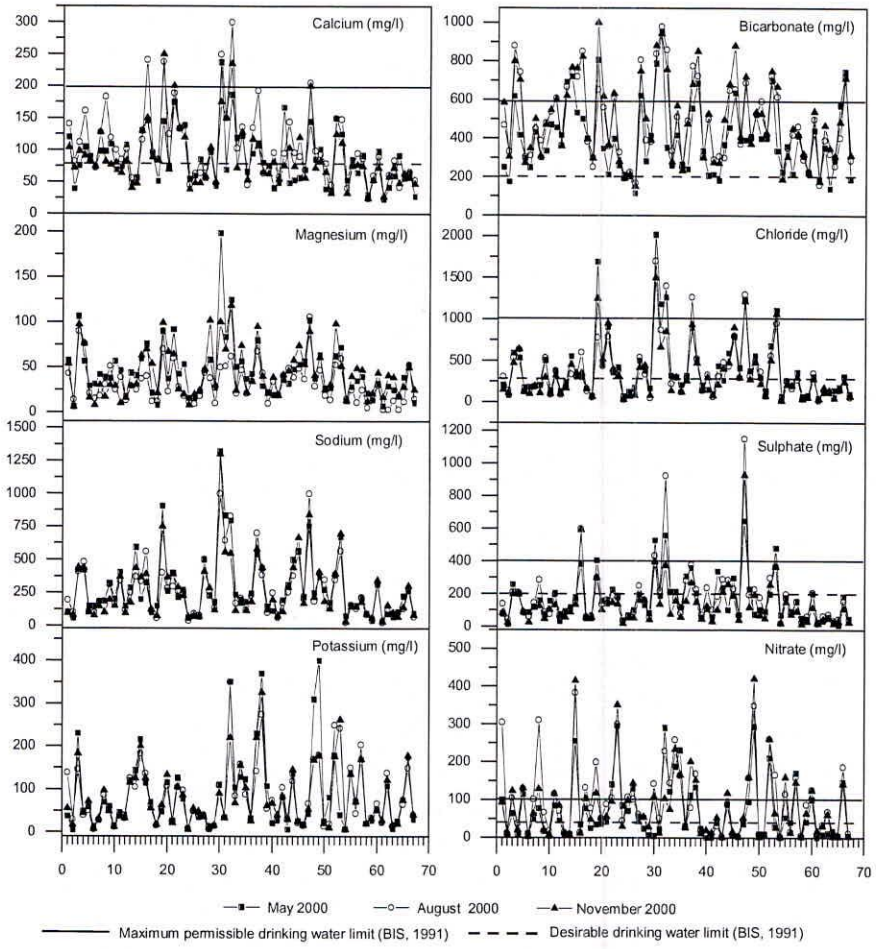

Fig. 5.1 Ion concentrations in each observation well in the study area

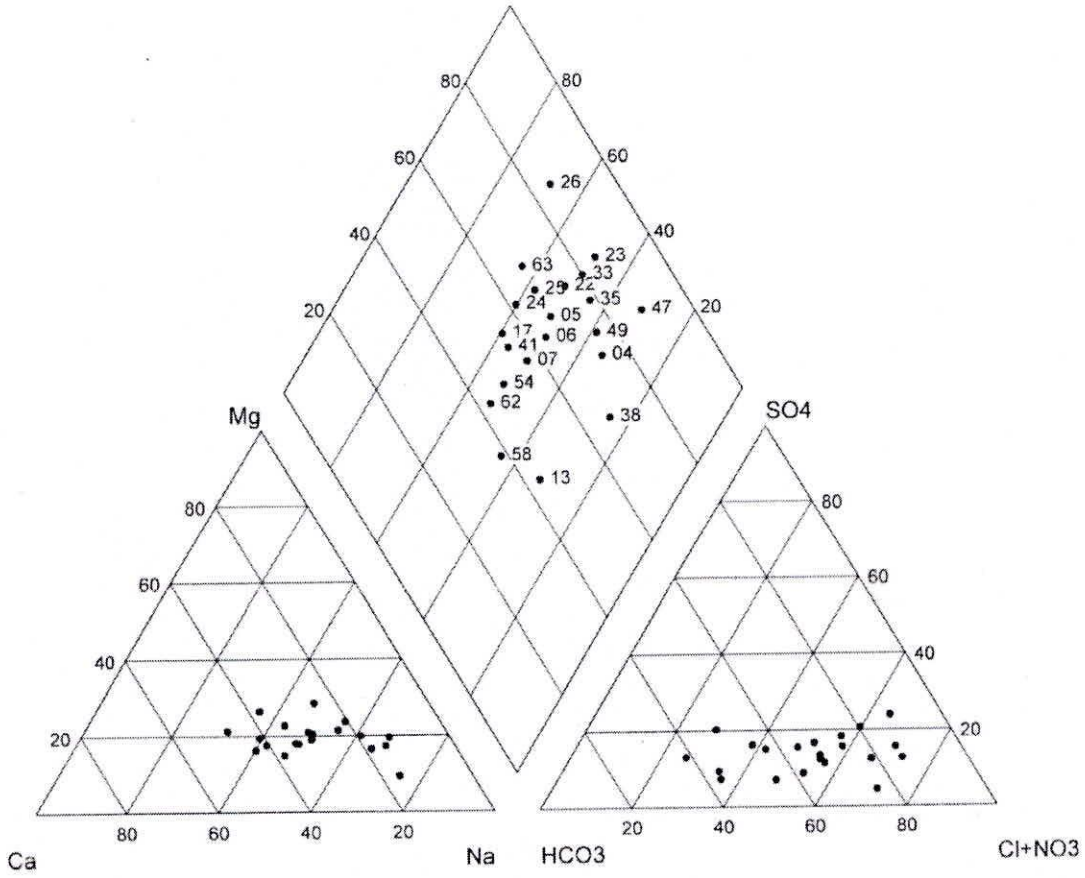

Fig. 5.1 (a). Pipers classification of few groundwater samples during May 2000

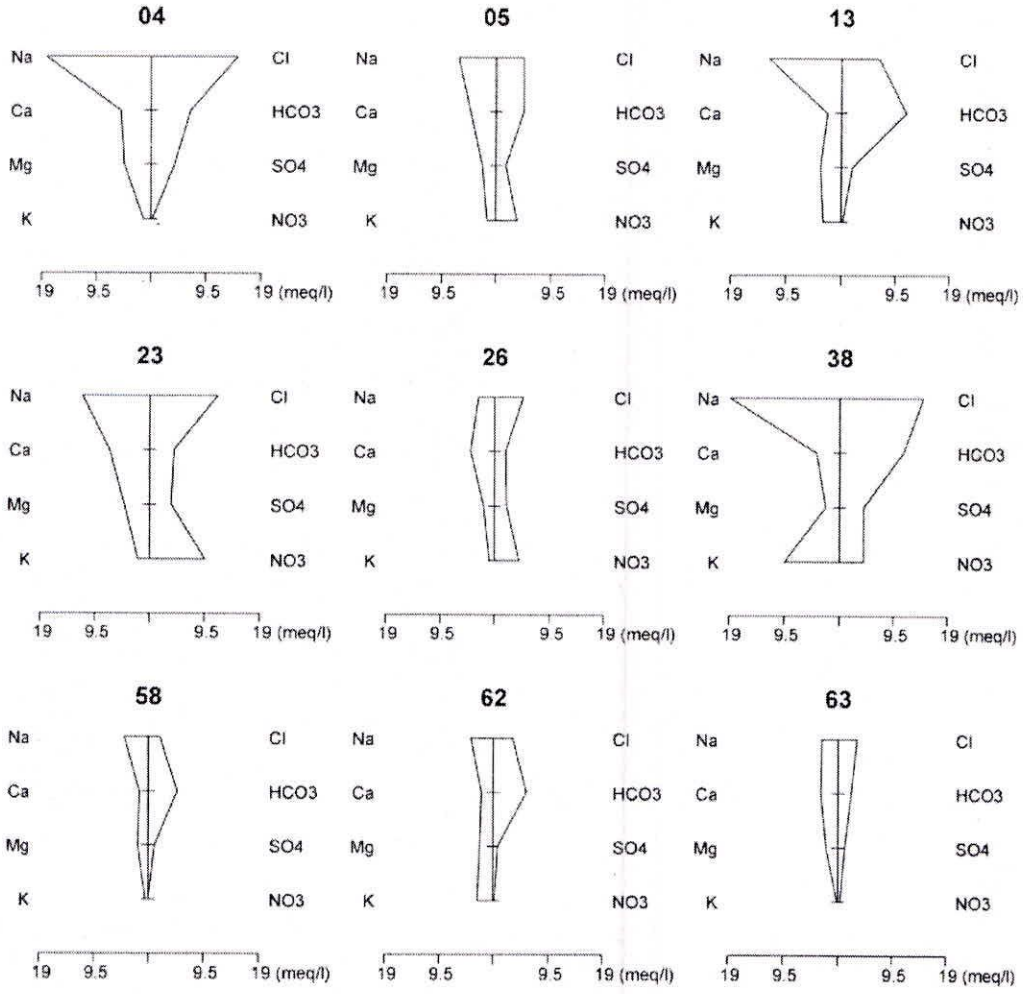

Fig. 5.1 (b) Stiff diagrams of few groundwater samples during May 2000

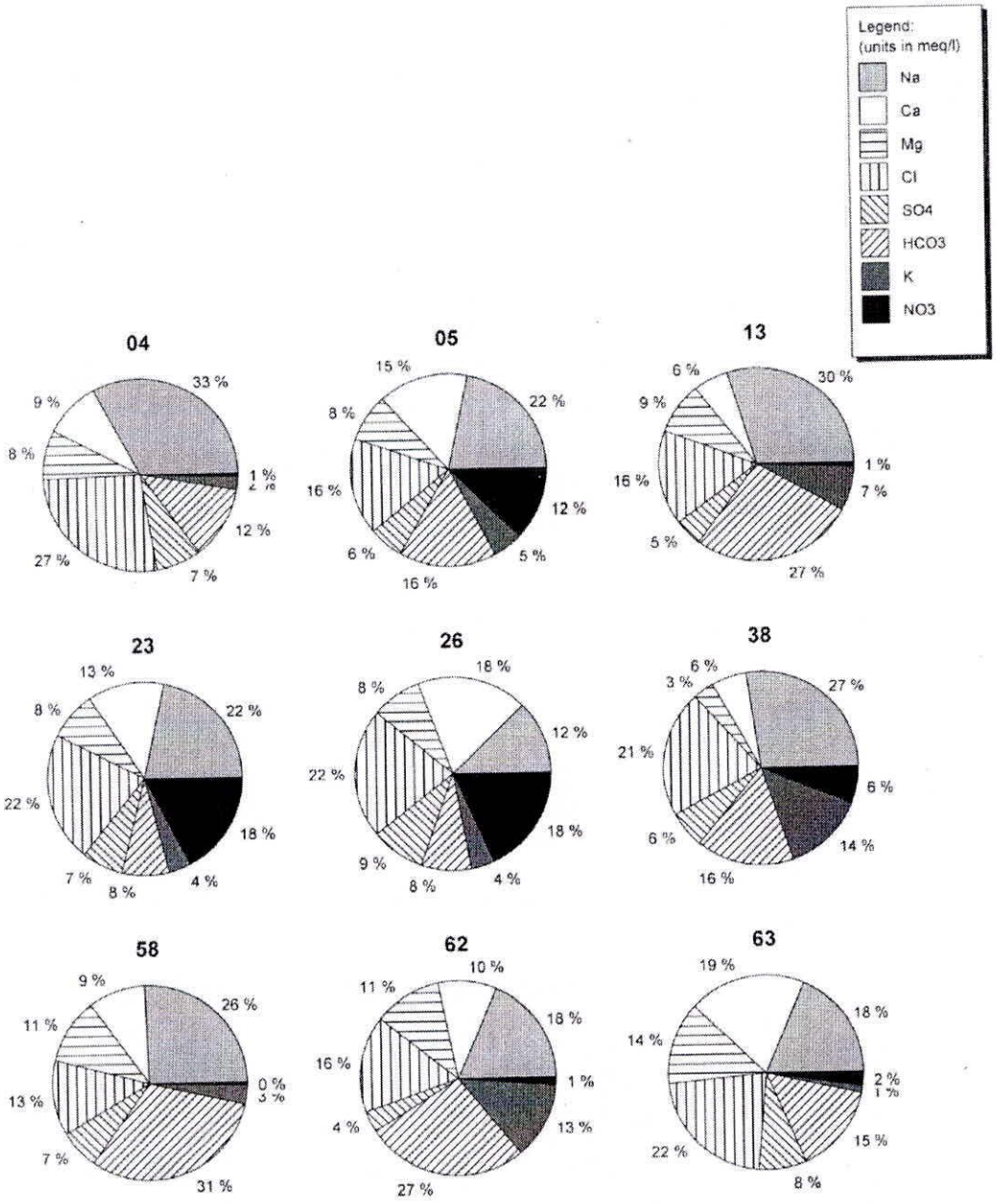

Fig. 5.1(c) Pie diagrams of few groundwater samples during May 2000

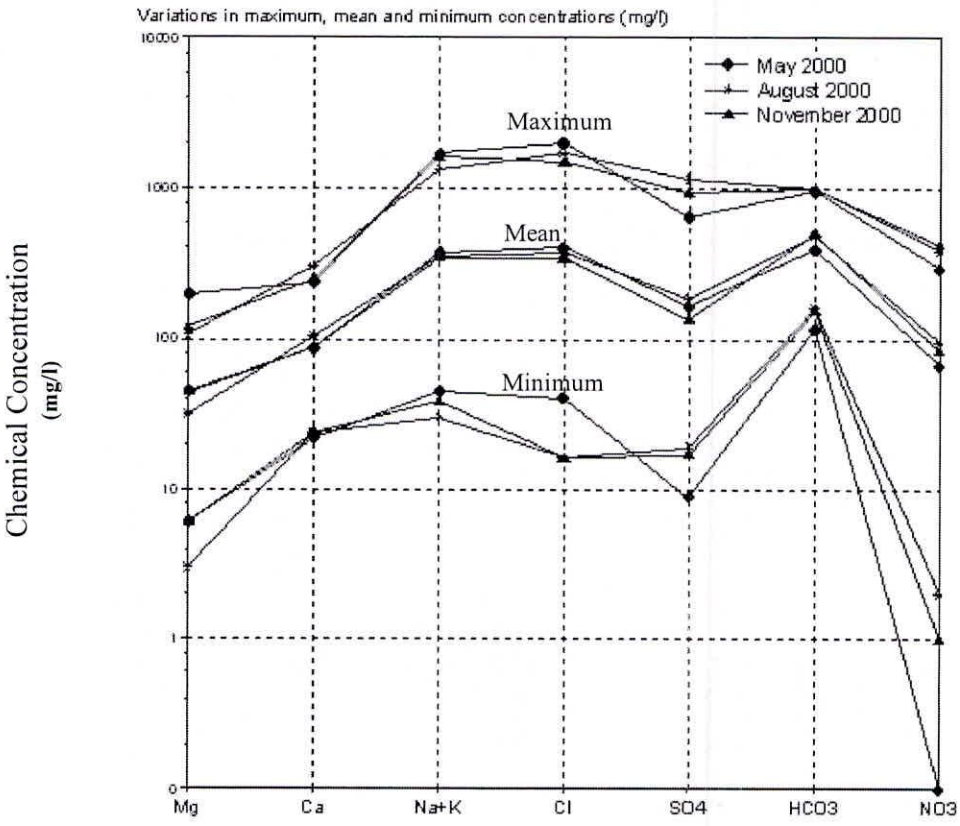

Fig. 5.2 Scholler diagram of maximum, mean and minimum groundwater quality in the study area

5.2 Principal Component Analysis (PCA) of groundwater quality data

The correlations between water quality parameters in each season and pooled data of three seasons are shown in Table 5.3. Significant correlation (>0.80) between EC and Na^+, Cl^-, SO_4^{2-}, Mg^{2+} were observed consistently during three seasons in the study area. These correlations are indicative of salinity process in a typical coastal aquifer. Similarly, nitrate is correlated only with potassium (>0.60) among all other water quality parameters. It may be due to high nutrients in shallow groundwater. The changes in correlation coefficients especially between EC and Ca^{2+}, HCO_3^-, Cl^- indicate that there was a significant seasonal change in the

shallow groundwater quality. The PCA was used to establish the dominant associations between physico-chemical variables. In PCA factors, eigen values >1 explain more than 75% of the variance in all three seasons (Table 5.4). The cumulative percent of variance in first three/four eigen values is 74, 75 and 80% during pre-monsoon, monsoon and post-monsoon periods, respectively. These components are used to explain the background hydrochemical processes without loosing much of the groundwater quality characteristics. However, by observing the principal axis matrix (Table 5.4), two main factors were identified for contamination assessment in the study area.

The first factor (F1) reveals strong association of Na^+, EC, Cl^-, Mg^{2+} (> 0.80) and less for NO_3^-, pH, temperature and HCO_3^-. This factor may be related to historical marine formation (salinity), which is common in coastal areas. The second factor (F2) reveals a strong association of NO_3^-, K^+ (>0.78), and less for other parameters. Factor 2 may be related to nutrient contamination due to the unsewered urban environment and nearby agriculture (paddy) practices. This also supports the interpretations made from correlations between water quality parameters (Table 5.3). Further, the contributions of water quality parameters in Factor 1 and Factor 2 are also plotted on 2-D plot (Figure 5.3) and it indicates two predominant clusters (salinity and nutrients), and significant seasonal change especially in Ca^{2+} and HCO_3^- concentrations.

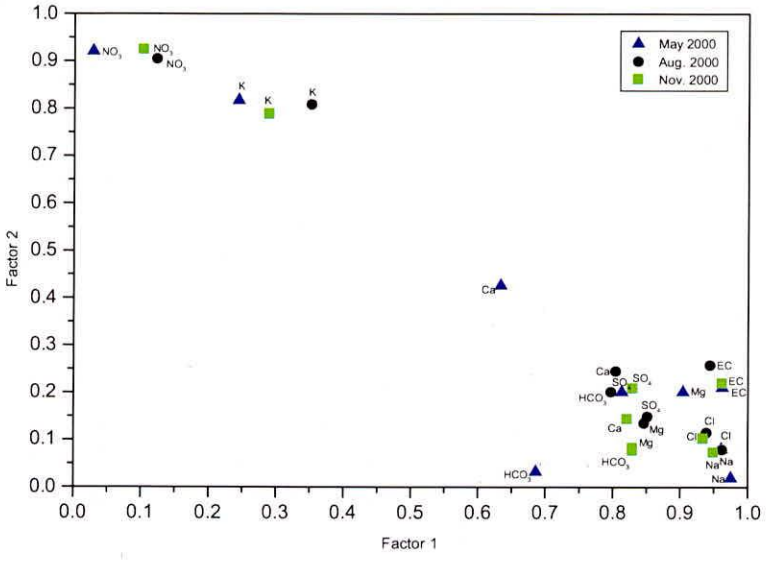

Fig. 5.3 2-D plot between Factors 1 and 2

These seasonal changes were also observed from statistical analysis of groundwater quality data (Table 5.2). The third factor (F3) reveals no significant association of water quality parameters, even though these change with seasons. Therefore, this factor is not considered further. The geological and hydrogeological conditions in the study area confirm that salinity and nutrients are major contaminants in the shallow groundwater. Based on these two Factors 1 and 2, principal component scores are projected on 67 observation wells using varimax rotation method in respective seasons of data. Results of principal component scores of each well during pre monsoon period are shown in Table 5.1. These new scores for each season are used for geostatistical analysis to map the salinity and nutrients contamination in the urban coastal aquifer.

5.3 Mapping of salinity (F1) and nutrients (F2) contamination

Geostatistical techniques were utilized to analyze the spatial continuity of the two factors F1 (salinity) and F2 (nutrients) reported in Table 5.1 by calculating experimental and modeled variograms. The experimental and modeled variograms of Factors 1 and 2 during pre-monsoon, monsoon and post-monsoon periods are shown in Figure 5.4. Factor 1 modeled variogram (spherical model) indicated that the range (spatial correlation) of salinity is about 10 km consistently in all three seasons. The fitted spherical model parameters of Factor 1 are also shown in Figure 5.4 and the same parameters were used in block Kriging for mapping salinity over the study area. The ratio of nugget to sill for Factor 1 during pre monsoon, monsoon and post monsoon seasons are 0.05, 0.18 and 0.18, respectively, in the study area. The ratio close to 0.1 indicates strong strength of modeled spatial structure of observation wells (Kravchenko, 2003). Mapping of salinity (F1) during pre-monsoon, monsoon and post -monsoon periods are shown in Figure 5.5. High salinity zones (due to historic marine formation) were identified along the Bay of Bengal and nearby salt creek with lower concentration along the Gorre Khandi stream. The pattern of spatial distribution during monsoon was different from pre-monsoon and post-monsoon seasons, thus indicating seasonal change in shallow groundwater quality. The maximum mean Cl^-/HCO_3^- ratio (Table 5.1) during pre monsoon (7.37) is more than in monsoon (3.79) and post monsoon periods (4.48). These changes are assumed to be due to monsoon rainfall, which occurs in July/August. The range of Cl^-/HCO_3^- ratio is limited to 0.15 to 7.53, thus indicates that there is no sub surface sea water intrusion in the study area.

Factor 2 (nutrients) modeled variogram indicated the pure nugget effect (Figure 5.4). This indicates that there was no spatial correlation of nutrients over the study area. This is mainly due to the in-situ field conditions of nearby well which causes contamination of groundwater. This type of contamination may be attributed to septic systems unlike in agricultural areas where some spatial correlation in nutrients may be observed in the shallow groundwater. Bjerg and Christensen (1992) reported pure nugget effect of nitrate in their study of spatial and temporal small-scale variation in groundwater quality of a shallow sandy aquifer, Denmark. The inverse distance weighted method was used for mapping Factor 2 during pre monsoon, monsoon and

post monsoon seasons and its spatial distributions are shown in Figure 5.5. Factor 2 demonstrates high values consistently in localized areas especially in KMC and adjacent agricultural areas, and low values near Salt Creek, Eleru Stream, Gorre Khandi stream and along the Bay of Bengal. Influent effect of these two streams on nutrient concentration is clearly indicated. The steep gradient of salinity and nutrient concentrations in NW direction indicates the effects of groundwater flow and influent of Gorre Khandi stream at the upstream side. The high concentrations of nutrients are an indication of new dimension of groundwater contamination problem in coastal aquifers. The ratio of SO_4^{2-}/Cl^- more than 0.25 in groundwater indicate the impact of agricultural activity (Hirschberg and Appleyard, 1996). The high value of SO_4^{2-}/Cl^- ratio (0.63) during post-monsoon (Table 5.2) indicated that there is impact of agriculture activity on groundwater quality. This impact may also depend on other factors namely type of crop, timing of fertilizers, plant uptake, soil type, groundwater table and paddling.

5.4 Assessment of nitrogen load from septic systems

The extended study area between two streams namely Gorre Khandi and Eleru has been demarcated with village boundaries and the same is shown in Figure 5.6. The study area comprises 83 polygons (390 km^2), which includes villages and towns. Each polygon was assigned index numbers from 1 to 83 (Figure 5.6) and details are given in Annexure I. The geographical area of polygons varies between 1 to 21 km^2. The highest elevation of the study area is about + 28 m at polygon 64 and + 0.5 m along the coast of Bay of Bengal. The largest area (21 km^2) is of the polygon Kakinada Municipal Corporation (KMC, index 12) is shown in Figure 5.6. The main soil types in these polygons are sandy loam, sandy clay loam, sandy clay and clay.

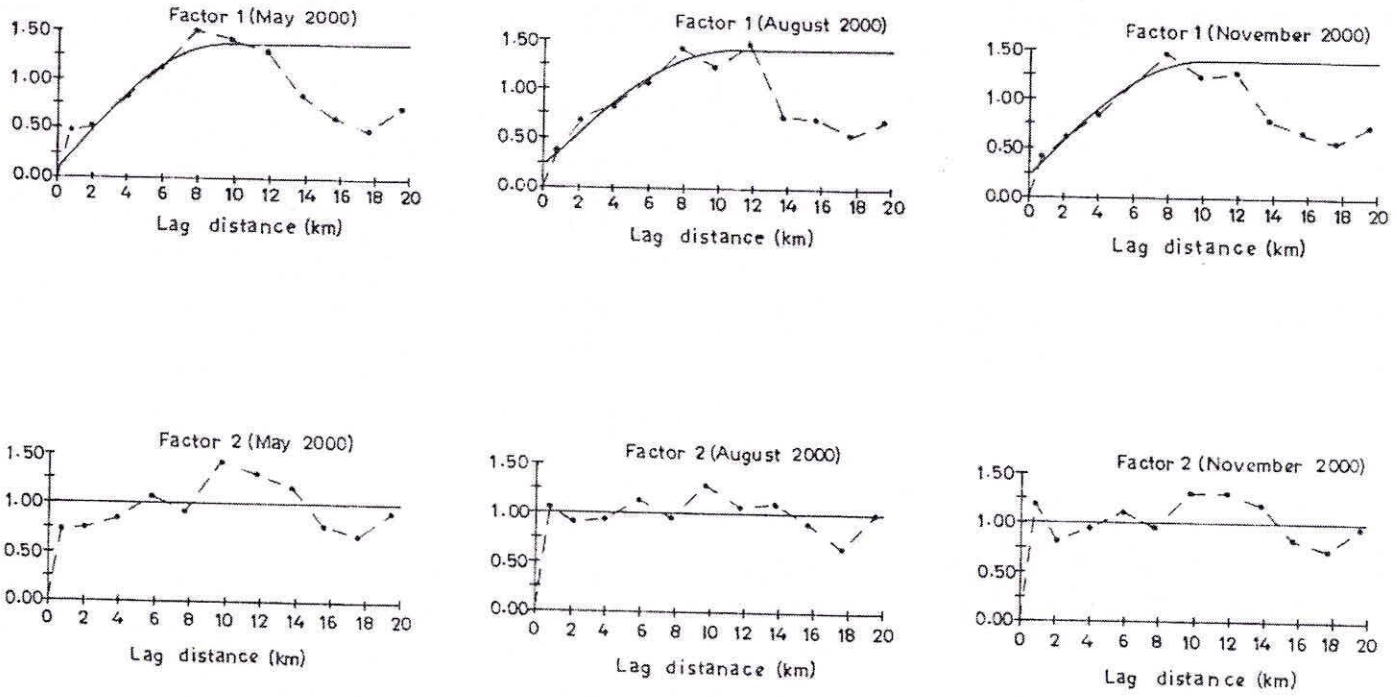

Variable	Range (a)			Sill (c)			Nugget (n)		
	May	Aug.	Nov.	May	Aug.	Nov.	May	Aug.	Nov.
Factor 1	9.407	10.607	9.796	1.307	1.200	1.183	0.060	0.219	0.219

Fig. 5.4 Experimental (dashed line) and modeled (thick line) variograms of Factors 1 and 2

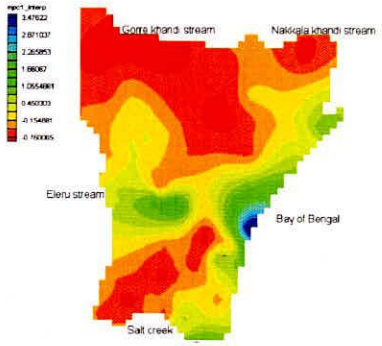

F1 May 2000

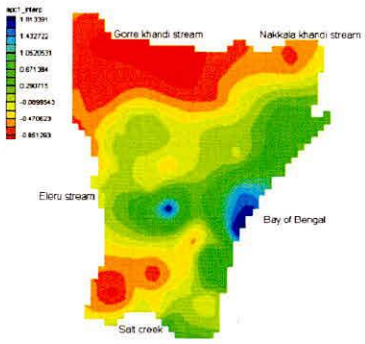

F1 August 2000

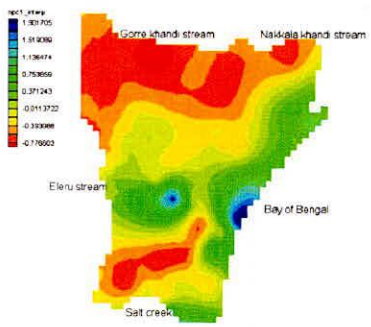

F1 November 2000

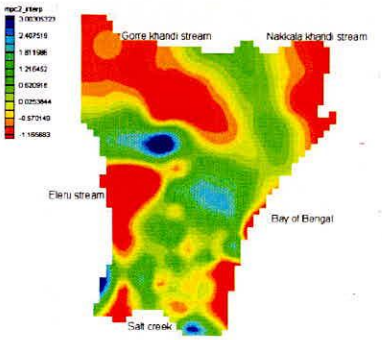

F2 May 2000

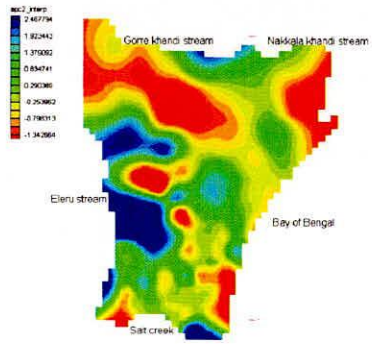

F2 August 2000

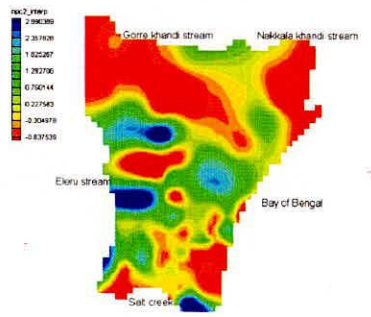

F2 November 2000

Fig. 5.5 Spatial distributions of salinity (Factor 1) and nutrients (Factor 2)

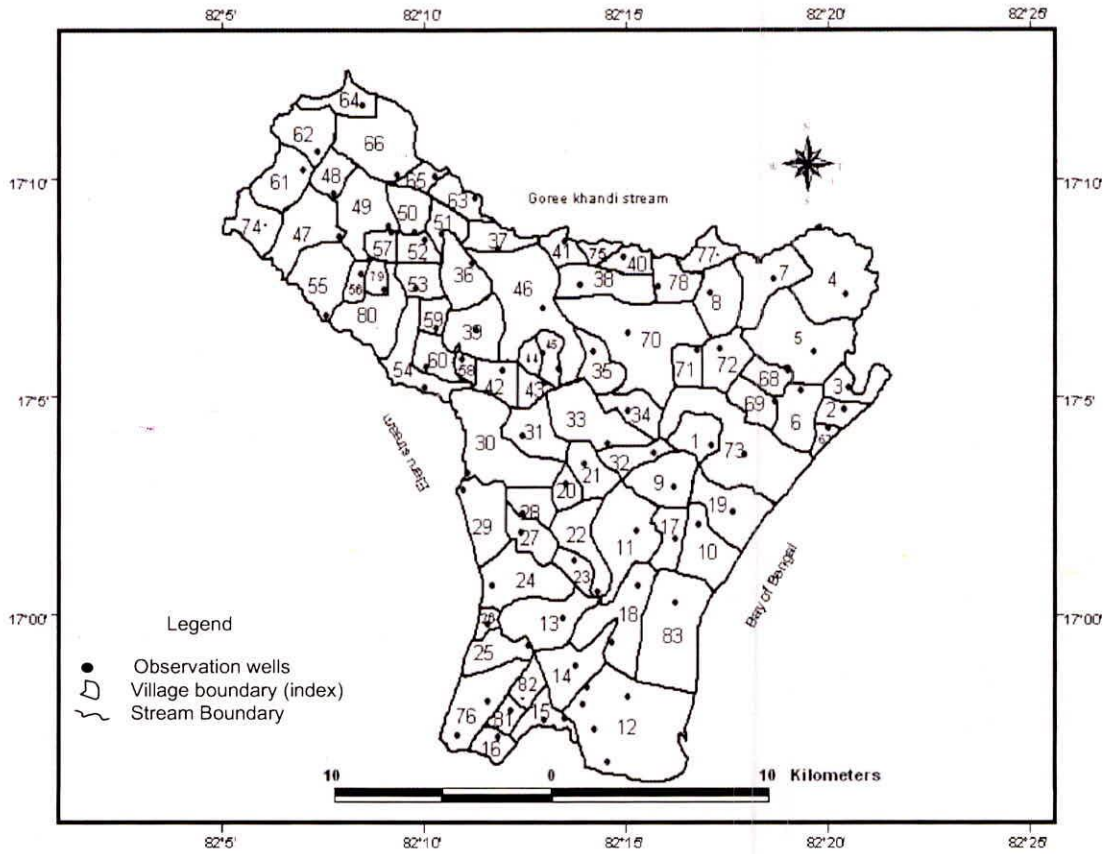

Fig. 5.6 Study area showing village boundaries with index numbers and location of groundwater sampling points

The groundwater table contours and flow direction in the study area during the month of November 2005 is shown in Figure 5.7. The major direction of groundwater flow is towards the Bay of Bengal and also follows the topographical gradient of the study area. To assess nitrogen load in each village, it is assumed that the wastewater generated to septic systems by each person per day in India is around 100 L (Bhargava, 1984) where continuous water supply is available and the average total nitrogen concentration in septic effluent is around 95 mg/L (Rajasekhar et al., 1994) in the study area. Therefore, the total nitrogen (N) produced by each person comes out to be 3.5 kg person^{-1} yr^{-1} (95 x 10 $^{-6}$ N L^{-1} x 100 L d^{-1} x 365 d yr^{-1}). Many authors (Whelan and Titamnis, 1982; Alhajjar et al., 1989; Naranjo and Larsen 1998; Schouw et al., 2002) reported similar values irrespective of age and sex. The septic systems density per sq.km in each polygon is shown in Figure 5.8.

The amount of nitrogen (kg yr^{-1}) produced by each polygon (village/town) is estimated by multiplying 3.5 kg person^{-1} yr^{-1} by the number of people using septic systems and by

considering the % of malfunction of septic system in each soil type given by Matelski (1975) and Hoover et al. (1981). The class of soil limitation and percentage of malfunctioning of septic systems for various soil types for the computation of nitrogen load due to septic systems are given in Table 5.5.

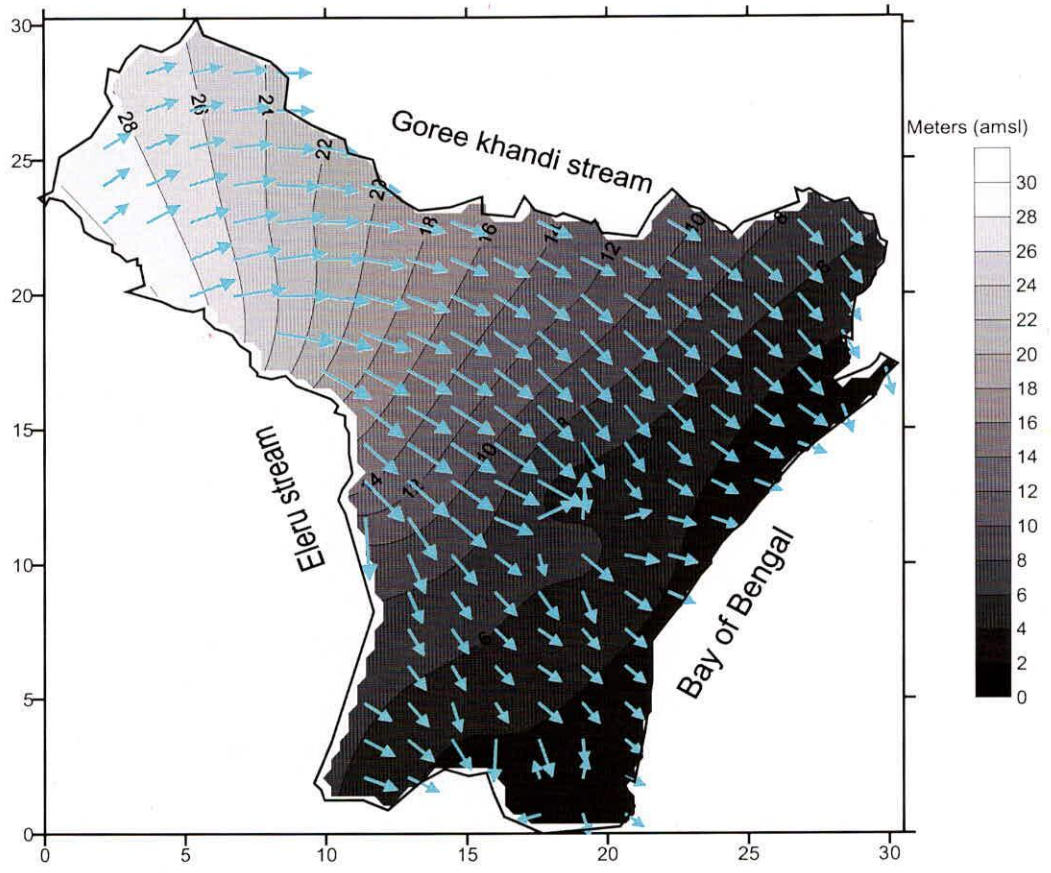

Fig. 5.7 Groundwater table contours and flow direction during Nov., 2005

It is assumed that all nitrogen released as a result of septic system failure reach groundwater without loss due to various biogeochemical processes. Costas-Carlos and Gomez-Gomez (1998) also advocated this assumption. The Indian guidelines for proper septic tank construction (BIS, 1996) also recognize the fact that the septic tank treatment is not efficient in coastal regions where groundwater table is very shallow. The conceptual plan of housing plots and cross section of septic tank and soak pit systems are shown in Figures 5.9 and 5.10, respectively. The field conditions indicate that, the assumption of nitrogen released from septic systems reaches the groundwater holds good in the present coastal aquifer.

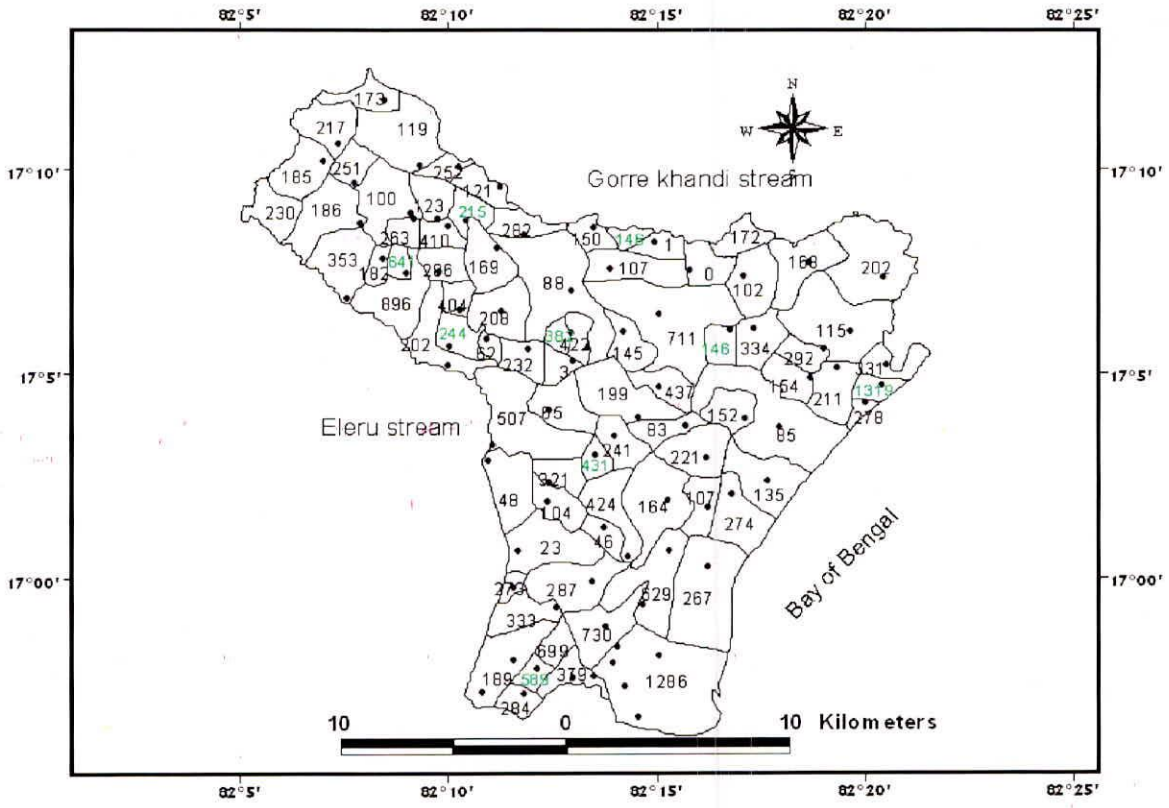

Fig. 5.8 Density of septic systems per sq. km in each polygon

The nitrogen loadings from septic systems for the years 1991 and 2004 were computed for each polygon (village/town) of the study area by performing map calculation in GIS environment as explained in the methodology. The highest density of septic tanks per sq.km (1286) is observed in the KMC (Index 12). The nitrogen loading (kg/year) from septic systems for each village for the years 1991 and 2004 except KMC (index 12), which is having very high average nitrogen load of 2,39,313 kg/year is shown in Figure 5.11. It is evident from Figure 5.11 that the nitrogen loading increased in most of the polygons (towns) from the year 1991 to 2004 except in village indices 4, 55 and 57 (Rural areas). The maximum percentage increase of nitrogen loading is in towns and peripherals of KMC (12). These changes are mainly due to population growth in towns and migration of people from rural areas to towns. The nitrogen loading of each polygon from septic systems for the years 1991 and 2004 were used to classify the study area into low, medium and high zones using 2-D FCM clustering technique. The 2-D FCM clustering of nitrogen loads and the classification of the study area into low, medium and high zones are shown in Figures 5.12(a) and 5.12(b), respectively.

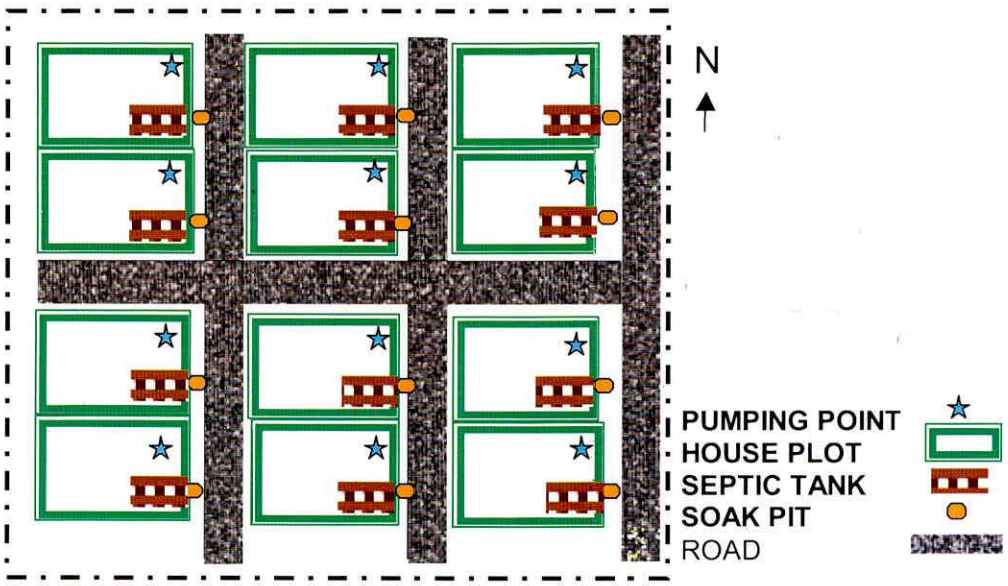

Figure 5.9 Plan showing house plots in a town with septic tank-soak pit

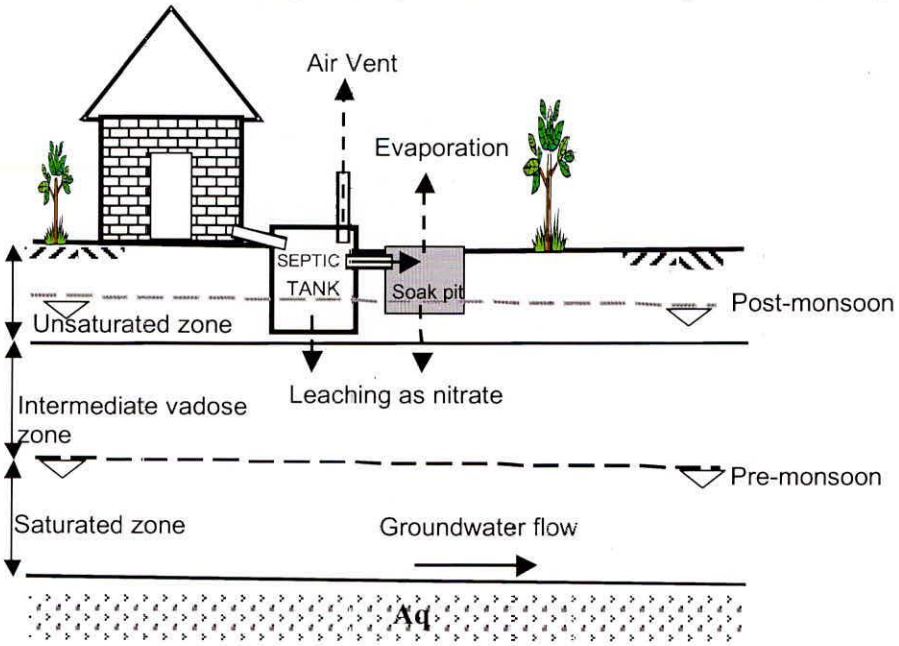

Fig. 5.10 Conceptual cross section of septic tank-soak pit systems in the study area

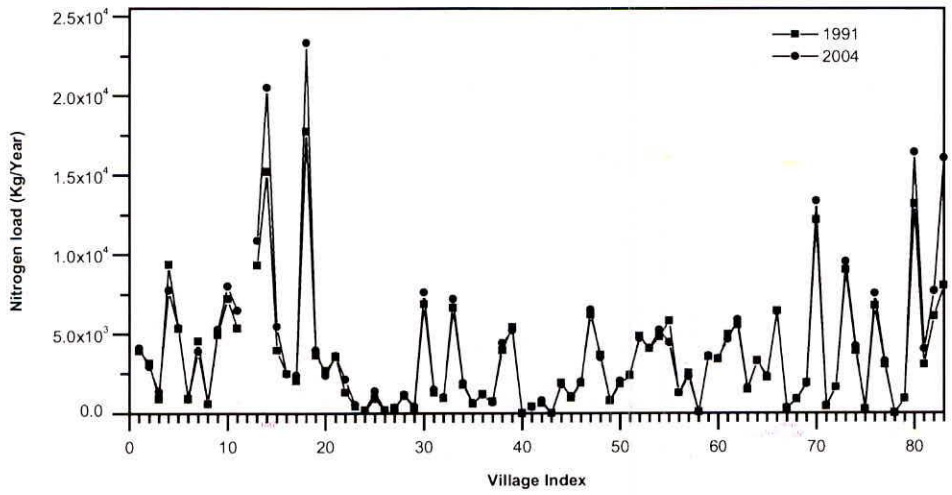

Fig. 5.11 Nitrogen load (kg/yr) in each village during the years 1991 and 2004

The ranges of nitrogen loadings (kg/year) in low, medium and high zones as obtained by using FCM technique are 1 to 3255, 3434 to 10, 883 and 13,357 to 2,39,313 respectively. It may be noted from Figure 5.12(a) that the high nitrogen load of KMC (index 12) is not considered in cluster analysis for obtaining better clustering groups, therefore only five points are marked (high zone) in the graph shown in Figure 5.12(a). However, categorization of KMC is shown in nitrogen loading zonation map as shown in Figure 5.12(b). It appears from Figure 5.12(b), that the spatial distribution of nitrogen loads is mainly a reflection of septic tank density and to some extent on soil types. The nitrogen load in each village (Index) under high, medium and low zones are shown in Figure 5.13.

The high, medium and low nitrogen zones obtained by using 2-D FCM classification is compared with respective zones average groundwater quality (nitrate, phosphate, EC, potassium) in the months of July 2004, Dec., 2004, Feb., 2005 and May 2005. The locations of groundwater sampling sites in each polygon are shown in Figure 5.8. The variations of NO_3^-, PO_4^{3-}, EC and K^+ in each village are shown in Figures 5.14, 5.15, 5.16 and 5.17, respectively. The analysis of samples collected during four surveys revealed that 28% of the villages exceeded the maximum allowable drinking water limits of nitrate (100 mg/l) and 47% of villages exceeded the allowable limit (45 mg/l) of drinking water standards (BIS, 1991). Table 5.6 shows the comparison between classified average nitrogen loading zones (low, medium and high), number of villages, total geographical area, average nitrate and phosphate concentrations in the study area. Similarly, the comparison between nitrogen loading zones and average EC and K^+ concentrations in each zone are shown in Table 5.7.

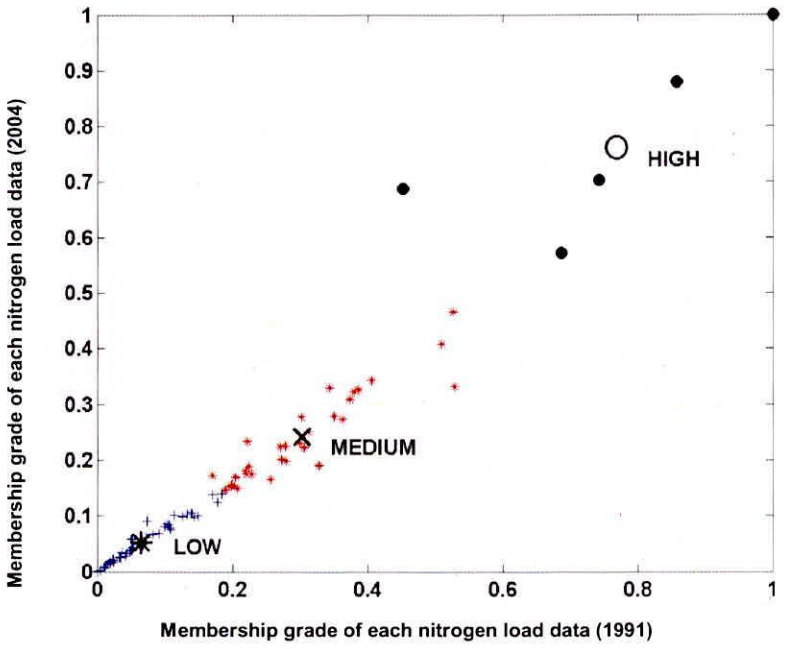

Fig. 5.12 (a) 2-D FCM clustering of nitrogen load

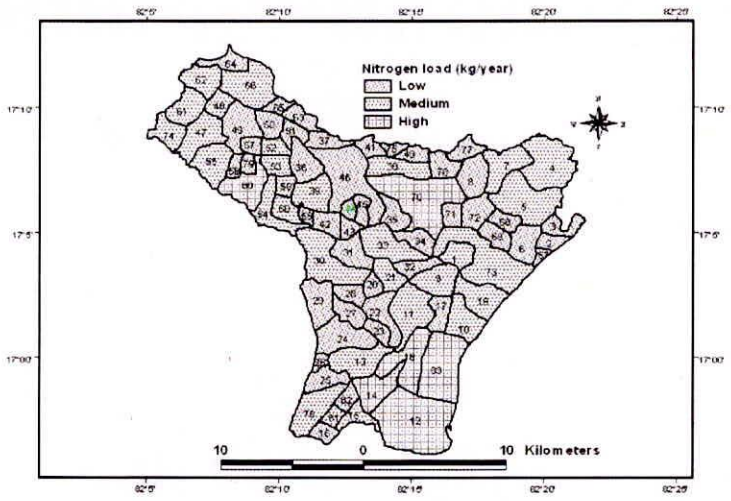

Fig. 5.12 (b) Classification of study area into low, medium and high nitrogen zones

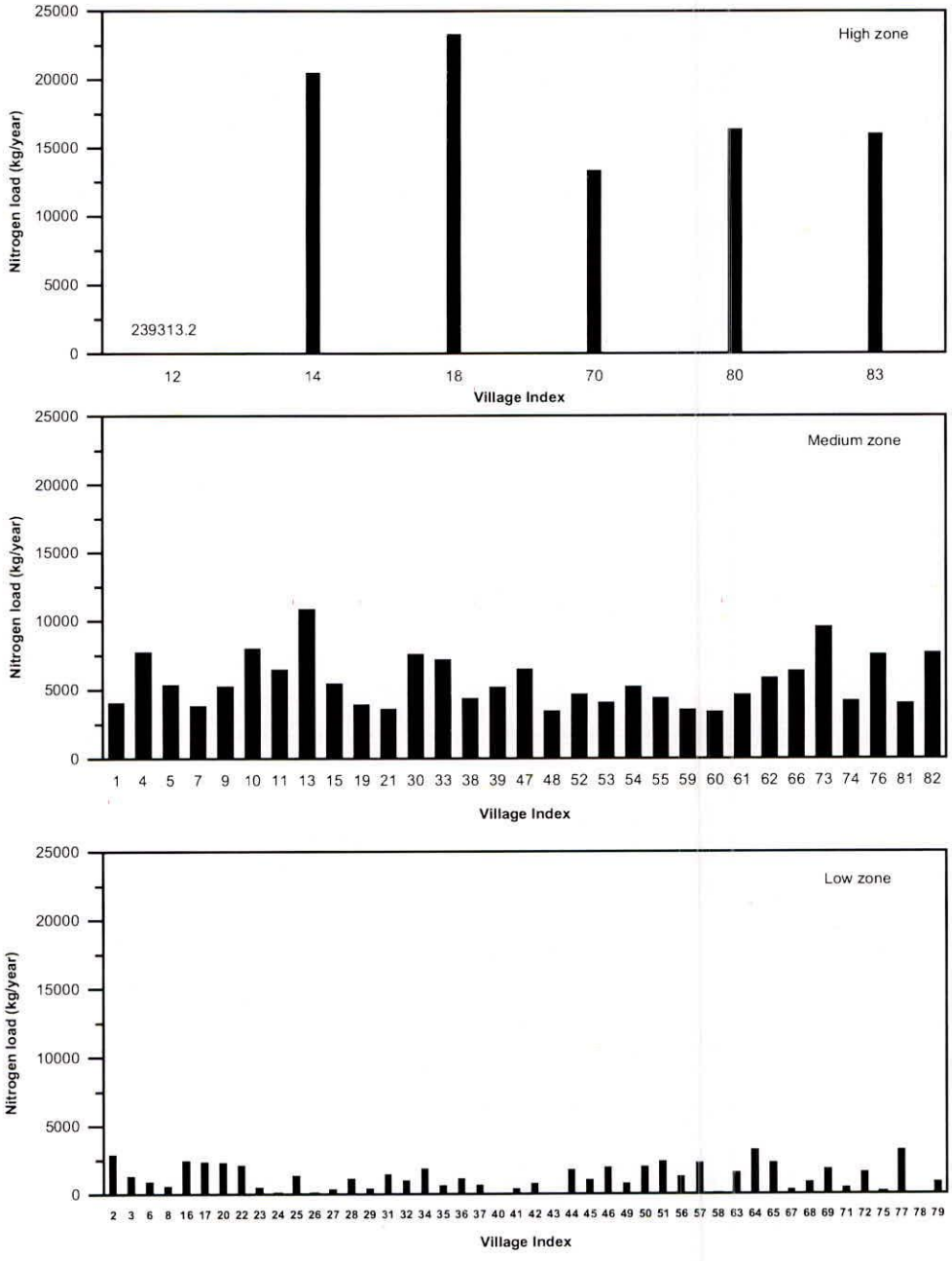

Fig. 5.13 Nitrogen load variations under high, medium and low zones

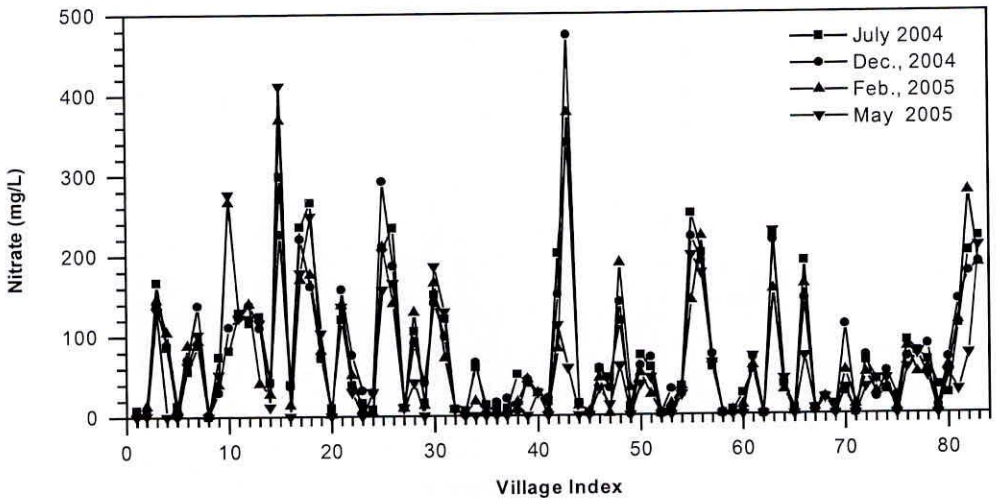

Fig. 5.14 Nitrate variations in each village in the study area

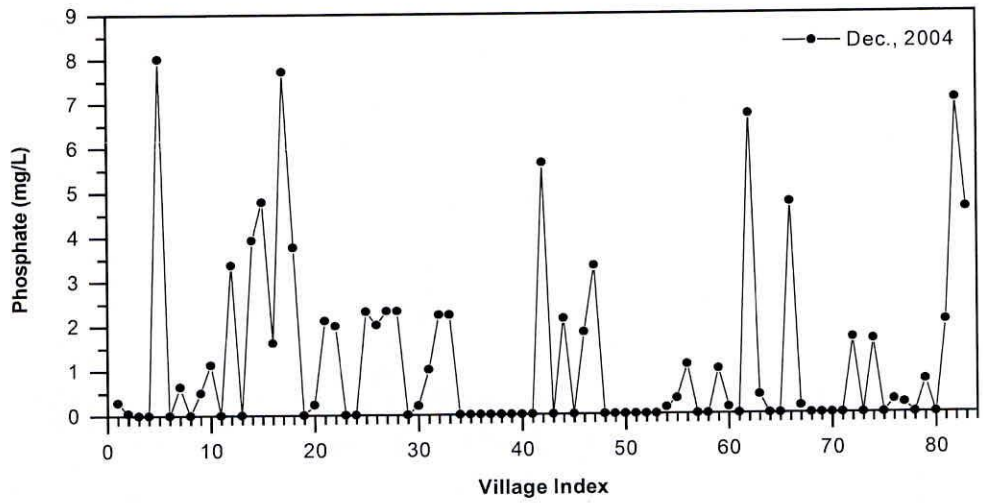

Fig. 5.15 Phosphate variations in each village in the study area

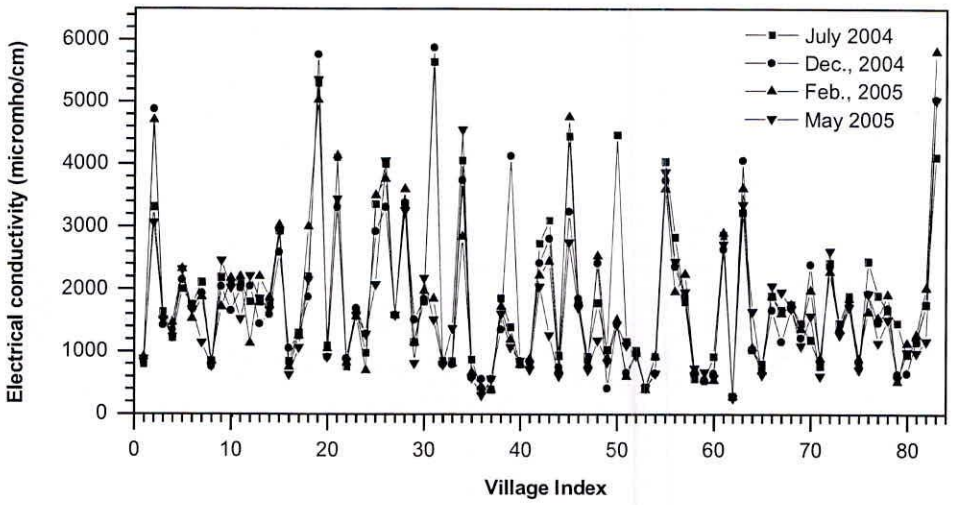

Fig. 5.16 Electrical conductivity variations in each village in the study area

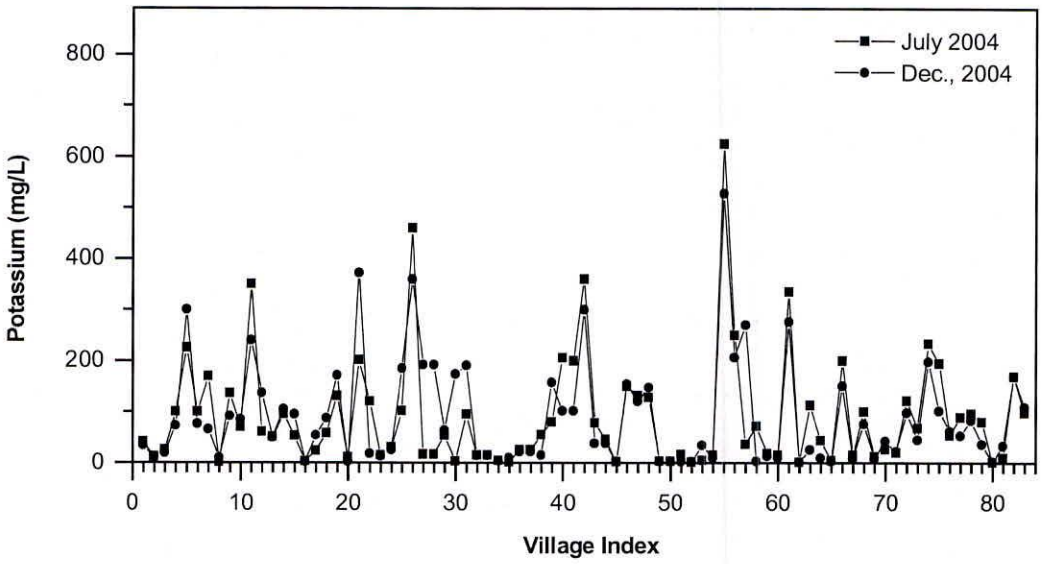

Fig. 5.17 Potassium concentrations in each village in the study area

Further, Figure 5.11 indicates estimated nitrogen load (kg/yr) from septic system alone in each polygon in the study area. Figures 5.14 and 5.17 indicate groundwater nitrate (mg/l) and

phosphate (mg/l) concentrations from multiple sources including septic systems and agricultural runoff over a period of time. These concentrations vary with respect to groundwater table, landuse/cover conditions and anthropogenic activities in the study area. The high nitrogen load (kg/yr) in some of the villages (in Figure 5.11) is mainly due to high density of septic systems. The measured groundwater nitrate and phosphate concentrations in various polygons in particular time period are indicative of contribution from septic systems up to some extent. Therefore, the average nitrogen load in each zone and its corresponding average groundwater quality is compared. This is also due to the dominant groundwater flow direction in the study area (Figure 5.7). The average NO_3^-, PO_4^{3-} and EC are following the pattern of nitrogen loading zones except potassium. The source of potassium concentration in groundwater is due to agricultural activities in rural areas. The comparison reveals that the present methodology adopted to estimate nitrogen load from septic system along with 2-D FCM clustering technique is suitable for assessment of nitrogen loading from septic system to coastal aquifers. It may also be concluded that there is a significant contribution of nitrate from septic systems and phosphate and EC are also following the trends of nitrate. It is evident from the above discussion that nitrate is the major groundwater contaminant in coastal towns and nearby areas in addition to the salinity.

5.5 Estimation of NO_3^--N leaching from septic system

Based on the septic system nitrogen load map (Figure 5.12(b)) and groundwater gradient map (Figure 5.7), a polygon of KMC (index 12) is considered to estimate nitrate leaching into shallow groundwater table using RISK-N model. Three representative locations at Lalbahadoor nagar (Lb nagar), Madav nagar, and Suresh nagar have been selected as per the density of population in high, medium and low zones, respectively. The locations of observation wells (RL of ground level) within KMC (from Figure 5.12(b)) are shown in the Figure 5.18. The existing average plot size in Lb nagar, Madav nagar and Suresh nagar areas are 0.0167, 0.0251, and 0.0376 Ha, respectively in the study area. The average total persons living in each plot computed in these three areas are 14, 6, and 6, respectively. Due to multistoried buildings in the Lb nagar area, the average total number of persons living in each plot is computed as 14. In each representative area, one observation well was established and monitored for monthly groundwater nitrate-nitrogen, EC and groundwater levels during the period of July 2002 to June 2003.

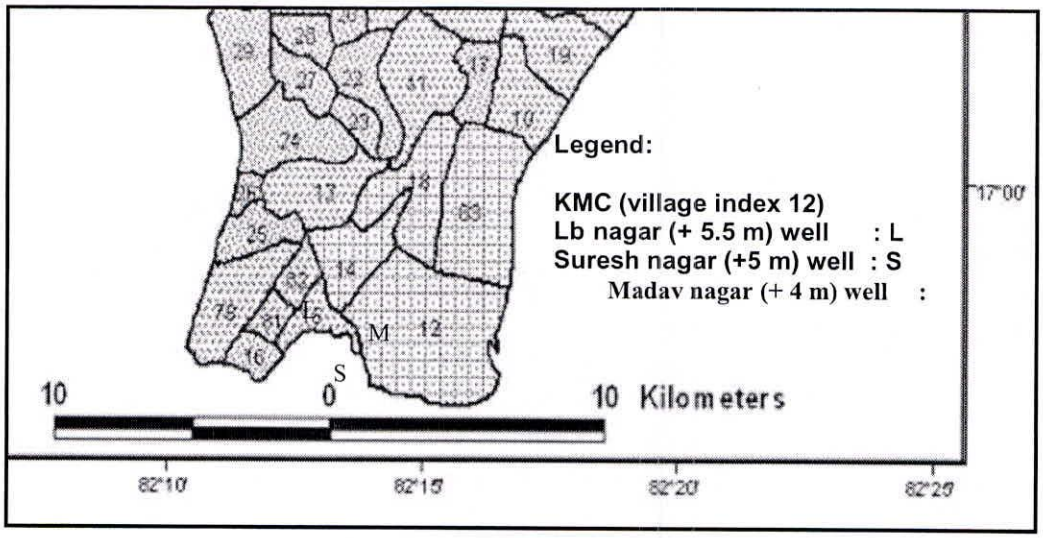

Fig. 5.18 Location of representative observation wells with reference to the MSL

The monthly variations of measured groundwater NO_3^--N, electrical conductivity, rainfall and groundwater levels within the KMC (polygon index 12) are shown in Figures 5.19, 5.20 and 5.21, respectively. The groundwater NO_3^--N concentration in Figure 5.19 indicates that high population density in Lb nagar shows high concentrations of groundwater NO_3^--N and low population density in Suresh nagar shows low concentrations of groundwater NO_3^--N. The EC also followed the similar trend of NO_3^--N. Figures 5.19 to 5.21 indicate that NO_3^--N and EC values have gone down due to high rainfall in the month of October 2002. It is also observed from Figure 5.19 that the groundwater NO_3^--N concentrations are rising during Jan., 2003 to April 2003 in Lb nagar well unlike in other two wells. This may be attributed to the use of more fertilizers applied in the paddy fields during *rabi* period (Jan 2003 to April 2003) in the upstream areas.

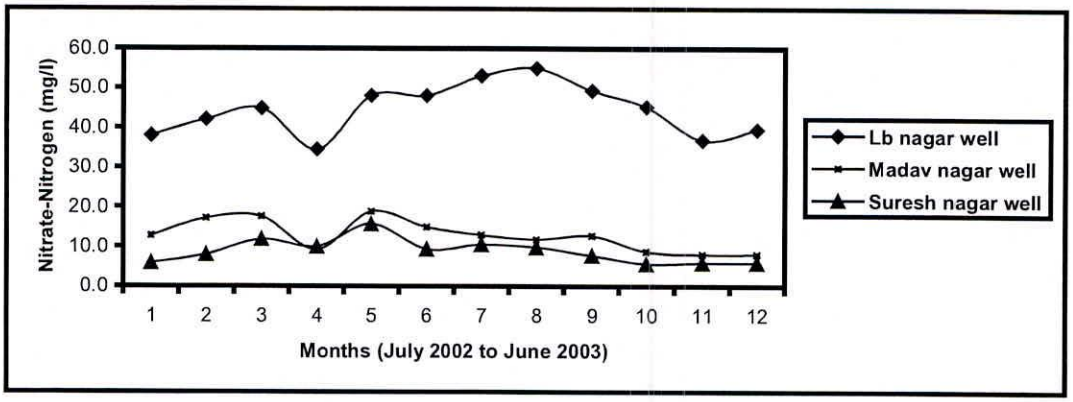

Fig. 5.19 Variation of groundwater NO_3^--N (mg/l) concentration

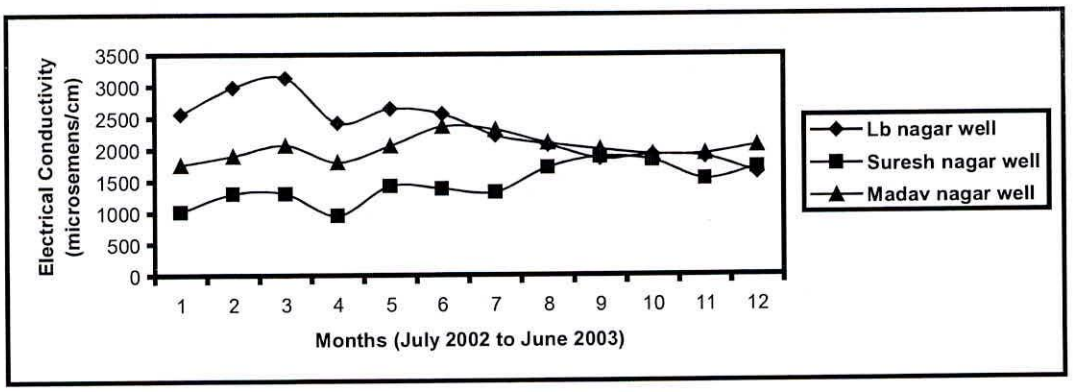

Fig. 5.20 Variation of groundwater electrical conductivity

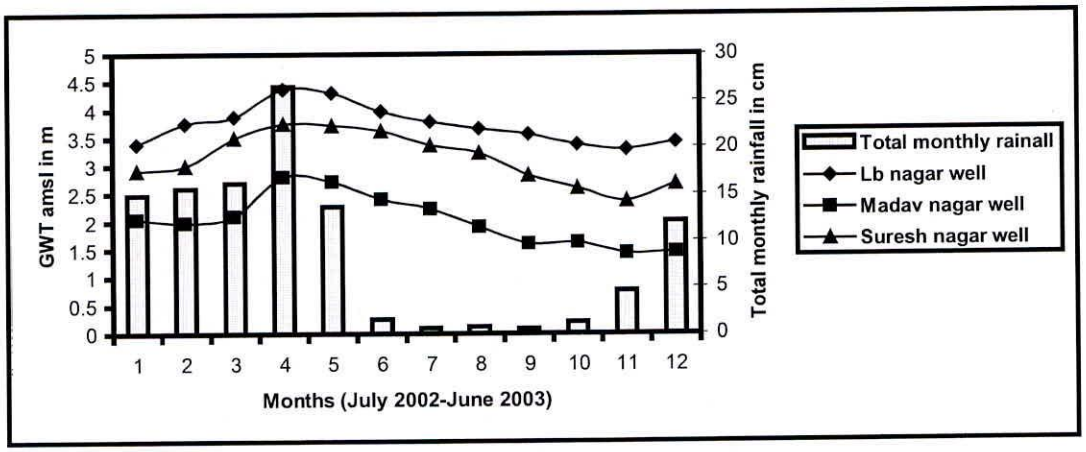

Fig. 5.21 Comparison of rainfall and groundwater table fluctuations

The RISK-N model was applied to these three representative locations independently to estimate monthly nitrate-nitrogen contribution from septic systems. The conceptualization of RISK-N model application in the field is shown in Figures 5.22 (a) and 5.22 (b).

The lot size (500 x 500 m) considered in Lb nagar, Madav nagar and Suresh nagar areas, the location of observation well at W_1 (250, 250) and imaginary well at W_2 (500, 250) and groundwater flow direction are shown in Figure 5.22(a). The distance of 250 m was selected based on the optimum radius of influence of well suggested by Lee et al. (2003). Based on the field conditions, the depth of upper zone, lower zone, drain field zone and intermediate vadose zone are fixed as 0.5, 0.5, 1.0, 0.5 m, respectively, in these three representative areas and the same depths were used in the RISK-N model. However, the saturated zone depths or mixing depths (amsl) at Lb nagar, Suresh nagar and Madav nagar are 3.0, 2.5, and 1.5 m, respectively. The septic effluent total nitrogen concentration is taken as 95 mg/l (Rajashekar et al. 1994) and the seepage from septic tank/soak pit system per person is taken as 10 l/day (estimated during

non monsoon period in the study area). The monthly climatic variables and soil temperatures are kept same for all three representative areas as these areas are close to hydrometeriological observatory and the values of climatic variables are given in Table 5.8. Similarly, the soil properties (porosity, field capacity, bulk density, NH_4^+ adsorption coefficient) are similar at three representative areas as these areas fall in the similar soil type. The unsaturated zone parameters considered for the RISK-N model are given in Table 5.9. The monthly septic coefficient for evaporation (k_{septic}) is taken as 0.15.

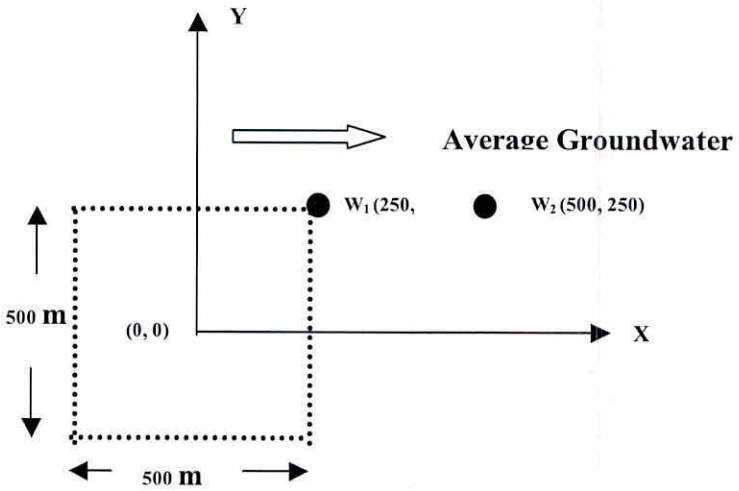

Fig.5.22 (a) Representation of lot size (500 x 500 m) and location of observation well (W_1) and imaginary well (W_2)

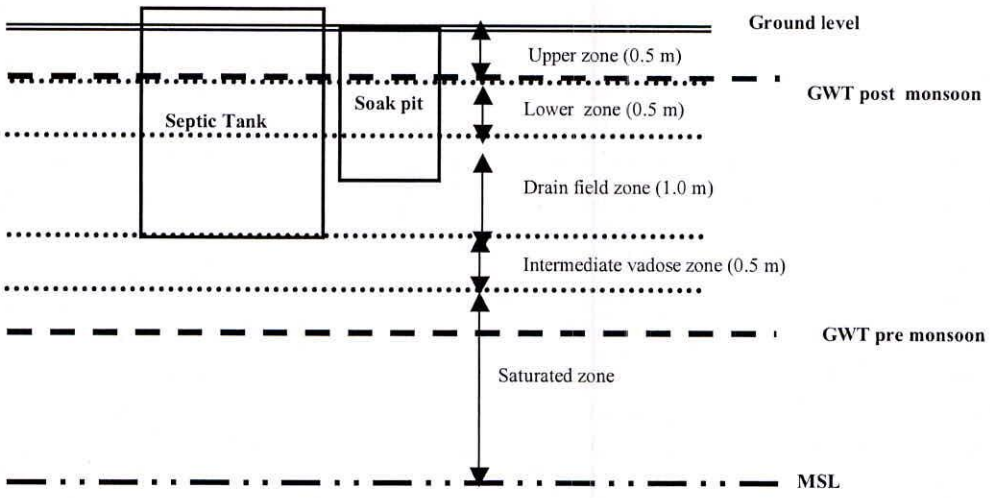

Fig. 5.22 (b) Conceptualization of subsurface zone depths

The runoff coefficients obtained from Ponce (1989) have been modified to incorporate antecedent conditions and land use. The monthly average runoff coefficient during June to November is 0.65 (range is 0.48 to 0.89) and December to May is 0.11 (range is 0.07 to 0.19). The monthly water flux in each zone is computed from Equations 3.39 to 3.46, and the annual water balances (July 2002 to June 2003) at three representative areas are given in the Table 5.10. As there is a uniform rainfall and similar soil properties in Lb nagar, Madav nagar and Suresh nagar, rows 2, 3, 4 and 5 in Table 5.10 is similar, and due to shallow groundwater table, the percolation from intermediate vadose zone is directly joining to the saturated zone without significant losses. Therefore, rows 7 and 8 in Table 5.10 are similar. In areas where spatial variability of rainfall and soil properties is more and groundwater table is not shallow, values in rows 2, 3, 4, 7 and 8 would be significantly different. The average runoff coefficient and the rainfall recharge coefficient obtained from annual water balance are 0.640 and 0.180, respectively. The computed rainfall recharge coefficient of 0.180 agreement with the results obtained by Tyagi et al. (1997) who estimated it value to be 0.17-0.20 after conducting detailed groundwater balance study in the Godavari delta.

The computed average mineralization rates (using equations 3.47 and 3.48) and denitrification rates (using equation 3.50) using RISK-N model for upper, lower, drain field and vadose zones along with average soil moisture are given in Table 5.11. The average volumetric soil moisture content is calculated using bulk density of soil, water content by weight and unit weight of water. It is noted from Table 5.11 that the average net mineralization rate in upper zone and drain field zone are 0.0157 (1/day) and 0.0336 (1/day), respectively, in the study area (polygon index 12). The more mineralization rate in drain field zone is mainly due to soil temperature/soil moisture and the availability of high organic nitrogen in the septic effluent. Similarly, it is also observed that the average denitrification rate in upper zone and drain field zone are 0.00453 (1/day) and 0.00186 (1/day), respectively. Further, the denitrification rate is decreasing with the increase of sub surface depth. This may be mainly due to the decrease of soil temperature. The high mineralization rate and less denitrification rates in the drain field zones cause significant leaching of nitrate into groundwater. The leaching concentration further depends on the groundwater table and soil types in the sub surface profiles.

The ammonia mass balance in the upper and drain field zones were computed using Equations 3.62 to 3.67 and 3.75 to 3.89, respectively at three representative areas. The nitrate-nitrogen flux (gm/m^2) from upper zone, lower zone, drain field zone and intermediate zone were computed for all three well locations. As the major input of nitrogen mass is at the drain field zone, the monthly average nitrate-nitrogen flux (gm/m^2) during July 2002 to June 2003 from the drain field zone and the vadose zone at three representative areas are shown in Figures 5.23, 5.24, and 5.25, respectively. It may be noted from these figures that the nitrate flux in the drain field zone is always greater than the nitrate flux from the intermediate zone. It is mainly due to the contribution of septic effluent directly joining into the drain field zone. The average nitrate fluxes from the drain field zone at Lb nagar, Madav nagar and Suresh nagar are 2.09, 0.394 and

0.345 (gm/m^2), respectively. These fluxes are in direct correspondence with the population densities at respective places.

Using the flux coming from the intermediate zone and saturated zone properties, the monthly NO_3^--N concentration in the wells (W_1 and W_2) were computed by solving 2-D groundwater transport equations (3.150 to 3.160), and results are shown Figure 5.22(a). The RISK-N model parameters of saturated zone in Lb nagar, Madav nagar and Suresh nagar areas are given in Table 5.12. With reference to the mean sea level, the average thickness of the mixing zone or the saturated zone is fixed as + 3.0, +1.5, and +2.5 m at Lb nagar, Madav nagar and Suresh nagar, respectively. The porosity of soil is measured in the field and the average Darcy's velocity is estimated from groundwater gradient and hydraulic conductivity of the soil. The longitudinal and transverse dispersivities of porous medium for nitrate are taken from field-scale dispersion in aquifers. Since the septic system eliminates organic carbon, it is reasonable to assume that denitrification is insignificant below the septic tank. However, in the present study the denitrification rate has been varied between 0.001 and 0.0 to compare the results obtained from the RISK-N model with the measured groundwater nitrate concentrations. Results obtained from the RISK-N model are applicable only when the groundwater table is above the mean sea level.

The monthly estimated groundwater NO_3^--N concentrations from septic systems using RISK-N model were compared with measured groundwater NO_3^--N concentrations at W1 (250,250), and the percentage of septic system contribution to groundwater is obtained. The monthly percentages of septic systems contributions to the groundwater at well (W_1 (250, 250)) in the area of Lb nagar, Madav nagar and Suresh nagar are shown in Figures 5.26, 5.27 and 5.28, respectively. The ranges of contribution of septic system nitrate-nitrogen (mg/l) concentration (in percentage) at well W_1(250, 250) in the area of Lb nagar, Madav nagr and Suresh nagar are 51 to 65, 61 to 98, and 64 to 90, respectively. The average % of septic system nitrate-nitrogen (mg/l) contribution at these three locations is 61, 72 and 71%, respectively.

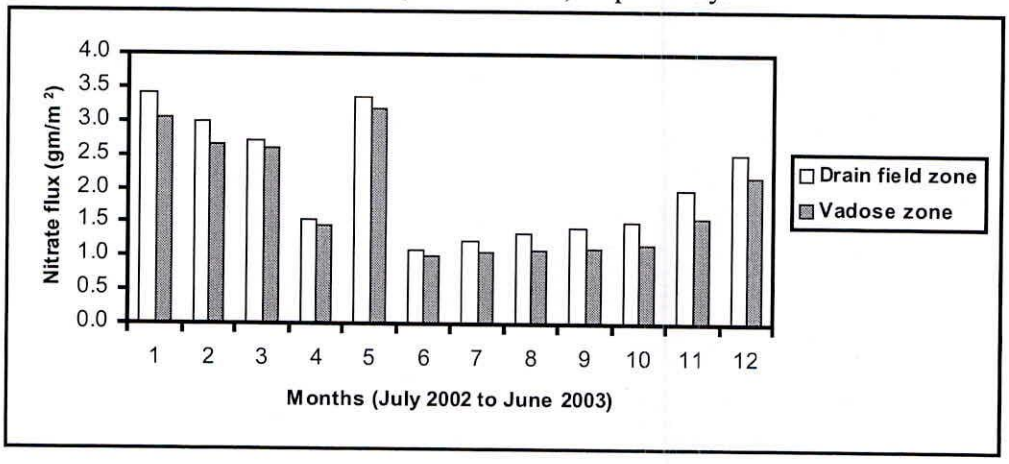

Fig. 5.23 Nitrate flux (gm/m^2) from Lb nagar area

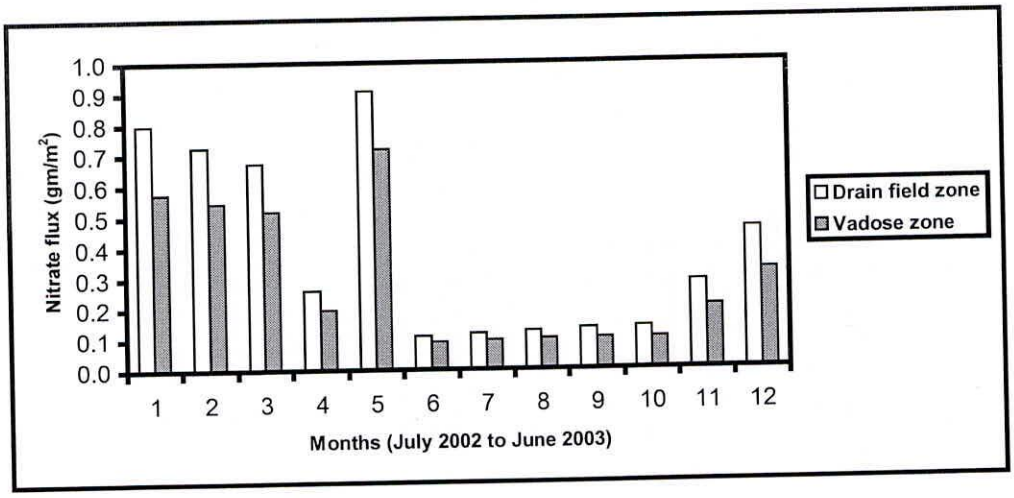

Fig. 5.24 Nitrate flux (gm/m^2) from Madav nagar area

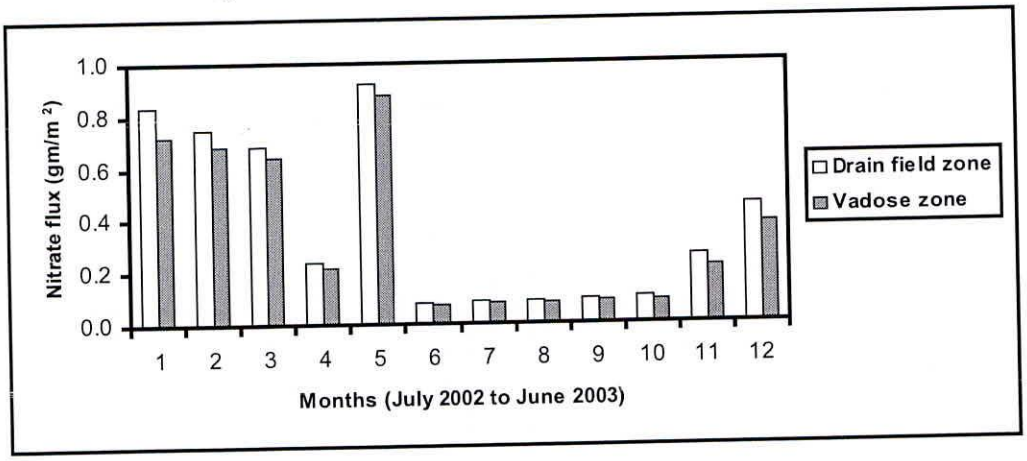

Fig. 5.25 Nitrate flux (gm/m^2) from Suresh nagar area

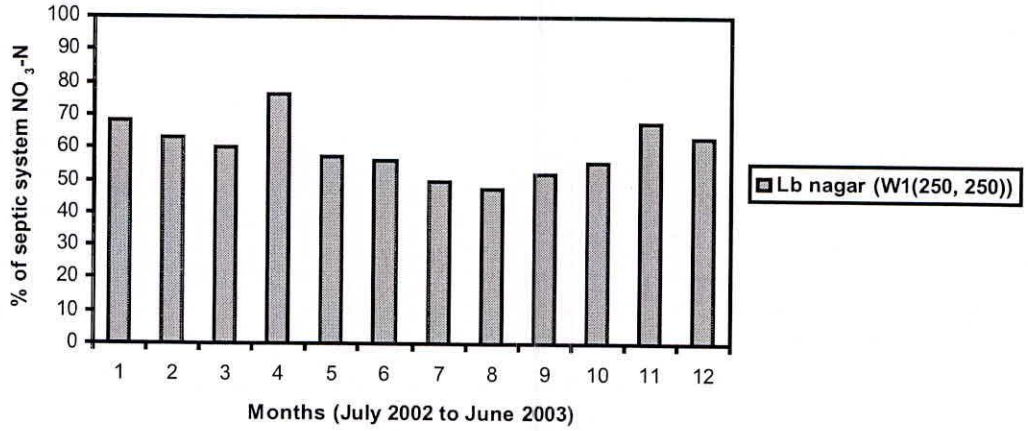

Fig. 5.26 RISK-N model estimated % of NO_3^--N from septic systems at LB Nagar

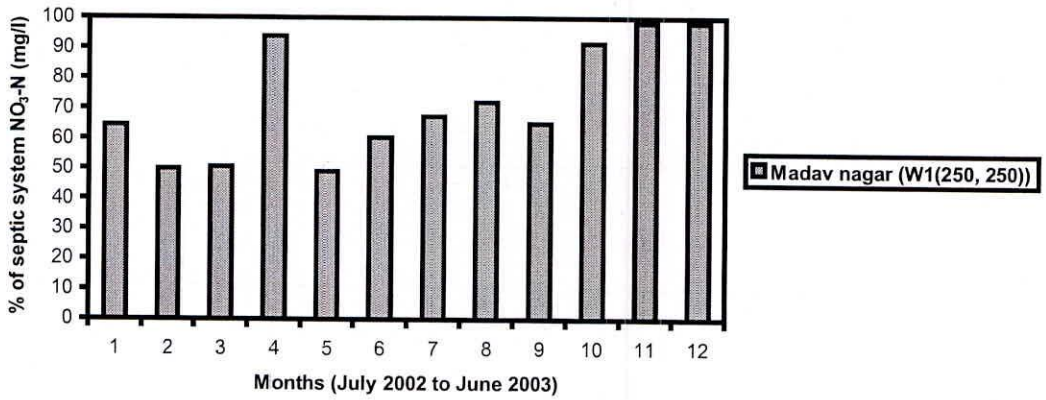

Fig. 5.27 RISK-N model estimated % of NO_3^--N from septic systems at Madav Nagar

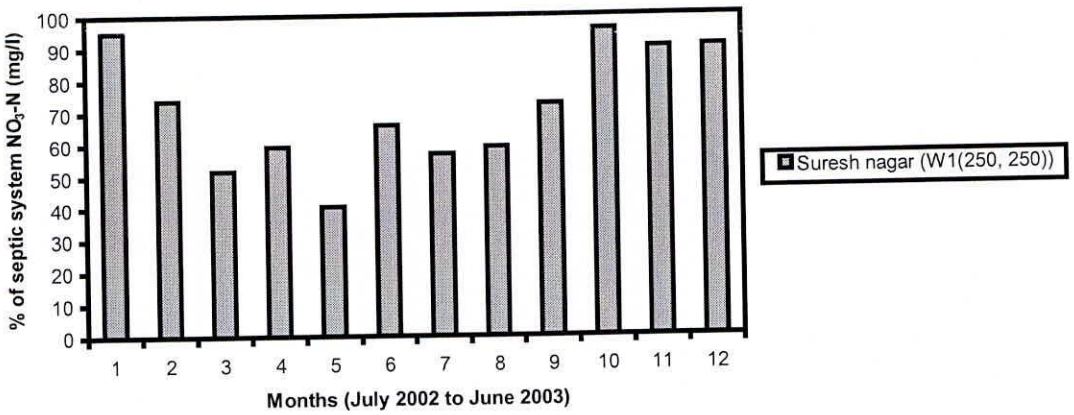

Fig. 5.28 RISK-N model estimated % of NO_3^--N from septic systems at Suresh Nagar

It is observed that the % of septic system NO_3^--N into groundwater mainly depends on the groundwater table condition, the mixing zone depth and the population density. Further, the correlation coefficients between estimated (from RISK-N model) and measured groundwater NO_3^--N at well W_1(250, 250) during non-monsoon period (Jan., 2003 to June 2003) in the area of LB Nagar, Madav Nagar, and Suresh Nagar areas are 0.83, 0.81 and 0.95, respectively. These results are shown in Figures 5.29, 5.30 and 5.31, respectively. The estimated average percentage of NO_3^--N contribution from septic systems during non monsoon period is 72% in the study area (polygon index 12).

This high contribution is due to the average groundwater table (+ 2.68 m) which is just below the septic tank bed level (+2.83 m). During the monsoon period (July 2002 to December 2002), the impact of rainfall recharge is more in the shallow groundwater and the entry of lateral contribution of nitrates from upstream areas (agricultural areas) is also more in the coastal areas. Therefore, there is poor correlation coefficient between measured groundwater NO_3^--N and estimated NO_3^--N from septic systems during monsoon period. The estimated average percentage of NO_3^--N contribution from septic systems during monsoon period is 63% in the study area (polygon index 12). This low contribution is due to the average groundwater table (+3.23m) being above the bed level of septic tank system (+2.83 m).

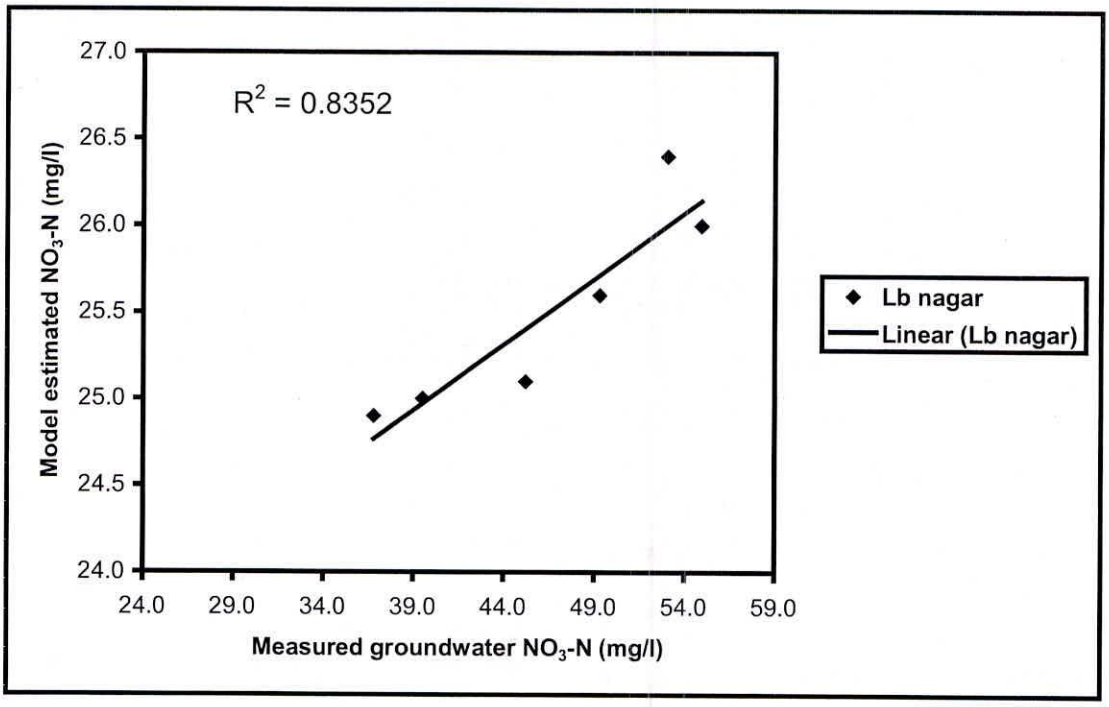

Fig. 5.29 Correlation between monthly observed and model estimated NO_3^--N (mg/l) at well (W_1(250, 250)) during non-monsoon period

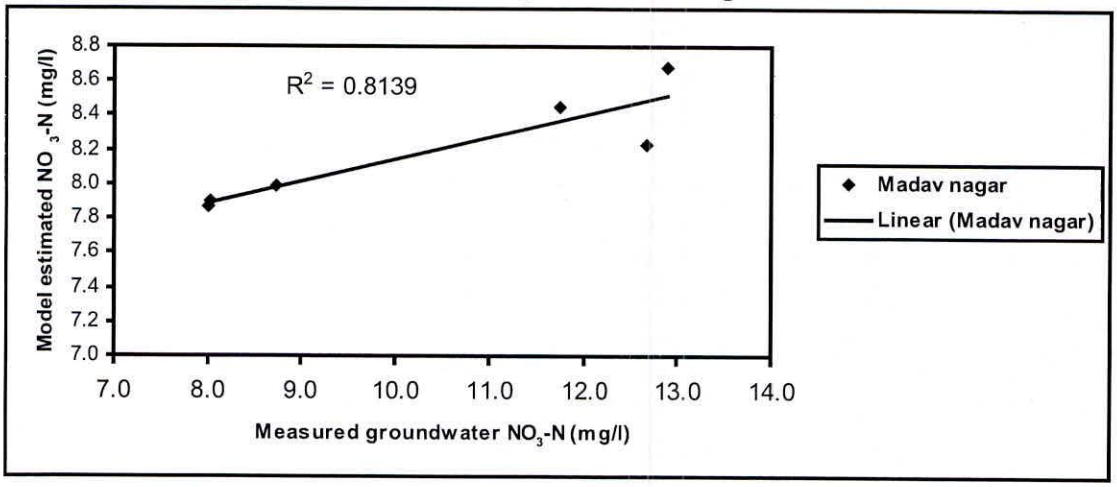

Fig. 5.30 Correlation between monthly observed and model estimated NO_3^--N (mg/l) at well (W_1(250, 250)) during non-monsoon period

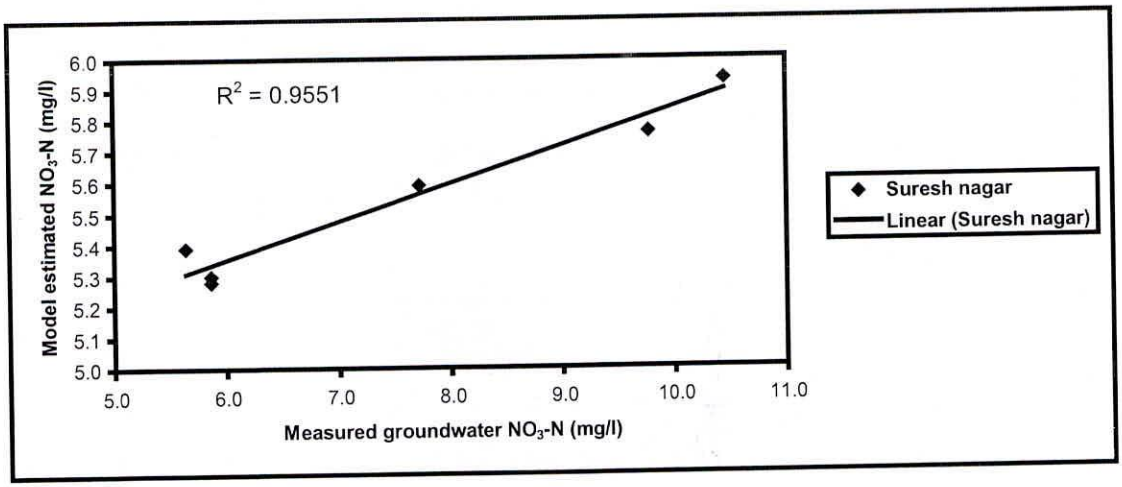

Fig. 5.31 Correlation between monthly observed and model estimated NO_3^--N (mg/l) at well (W_1(250, 250)) during non-monsoon period

The high correlation coefficient up to 0.95 is observed in Suresh nagar, which is in middle of the polygon index 12 and away from the agricultural and sea coast environments. The long term annual average NO_3^--N concentrations (mg/l) in wells located at W_1(250, 250) and W_2(500, 250) in the areas of Lb nagar, Madav nagar and Suresh nagar are shown in Figures 5.32, 5.33, and 5.34 respectively. Results reveal that concentrations of NO_3^--N at well W_2(500, 250) in the areas of Lb nagar, Madav nagar, and Suresh nagar are 30% less than that of at well W_1(250, 250). The NO_3^--N concentrations at well W_1(250, 250) located in Madav nagar and Suresh nagar are not exceeding the drinking water limit (10 mg/l). It should be noted that the initial NO_3^--N well concentrations were set to zero in these three representative areas. Generally, the initial values of groundwater NO_3^--N (mg/l) may be in the order of 0 to 1 mg/l, where there is no influence of agricultural activity.

Further, the impact of seasonal variations in groundwater NO_3^--N on other groundwater quality parameters especially on HCO_3^- were studied and results obtained are shown in Table 5.13. The monthly values of HCO_3^- are obtained using multiple regression equations (HCO_3 = 99.821 + 0.355EC - 0.989Cl - 0.702NO_3 (R^2 = 0.806); Cl = - 122.716 + 0.241EC - 0.498NO_3 (R^2 = 0.947)) developed by Satyaji Rao et al. (2003) for the present study area using the network of observation wells as shown in Figure 4.1.

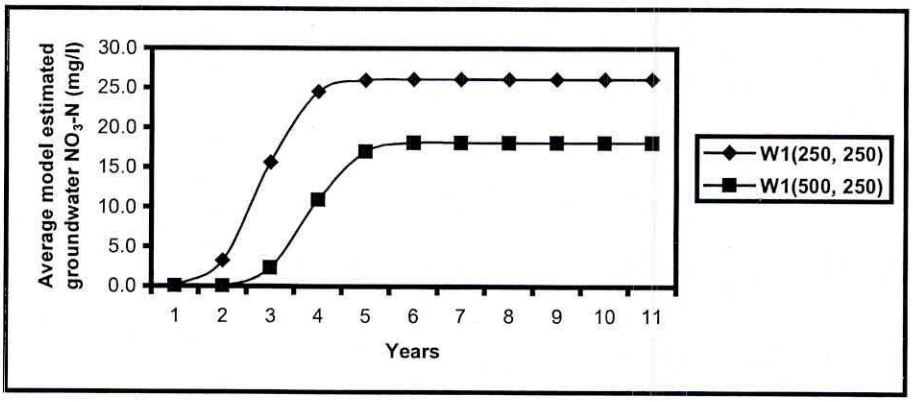

Fig. 5.32 Average annual groundwater NO_3^--N concentrations in the Lb nagar area

As discussed earlier, groundwater quality in the Lb nagar area is influenced by agricultural activities, therefore the average concentration of NO_3^--N is more in non-monsoon period where high dose of fertilizers are applied for the paddy crop (rabi season). In other two areas, groundwater NO_3^--N concentrations are reduced from monsoon to non monsoon period as the groundwater goes down. The decrease of nitrate concentrations and corresponding increase of HCO_3^- concentration (especially in Madav nagar and Suresh nagar areas) indicates the heterotrophic denitrification process in shallow groundwater in the urban coastal aquifer. This phenomenon was established by Trudell et al. (1996) in their experimental studies and stated that one gram of nitrate denitrification produces 2.459 grams of HCO_3^- in the calcareous soils and 1.23 grams in general groundwater where the groundwater pH lies in between 6.53 to 8.3.

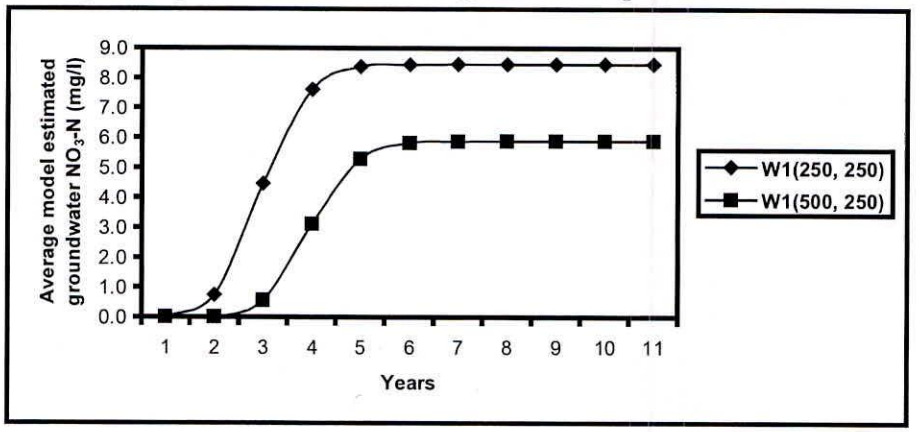

Fig. 5.33 Average annual groundwater NO_3^--N concentrations in the Madav Nagar area

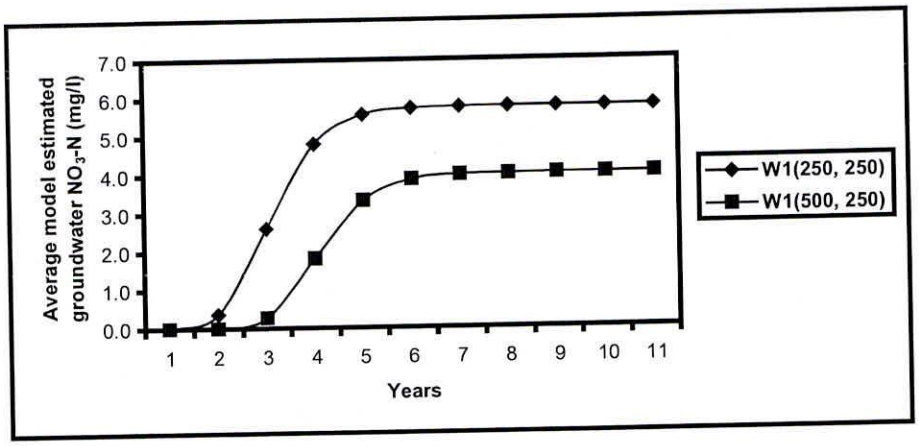

Fig. 5.34 Average annual groundwater NO_3^--N concentrations in the Suresh Nagar area

For two different values of denitrification rate (per day) as 0.0 and 0.001 the monthly groundwater NO_3^--N was estimated at three locations by using the RISK-N model and its average values during July 2002-June 2003 are given in Table 5.14. Results reveals that with zero denitrification rate, the estimated NO_3^--N concentrations are in agreement with average measured groundwater NO_3^--N. Similarly, with the 0.001 denitrification rate the estimated NO_3^--N concentrations are in agreement with minimum measured groundwater NO_3^--N. Since the present study is limited to the extent of nitrate contamination resulting from septic tanks, the results obtained from RISK-N model are not expected to match with maximum nitrate concentrations. It opens ups new directions of research for future study to modify RISK-N model for heterogeneous area having combination from septic systems and agricultural runoff and also lateral contributions resulting from various sources. It may be concluded from Table 5.14 that the application of RISK-N model provides more useful information to understand groundwater NO_3^--N characteristics from septic systems.

5.5.1 Sensitivity analysis of RISK-N model variables

Apart from denitrification rate and plot size, the sensitivity analysis was performed at Madav nagar area (using existing plot area and zero denitrification rate) by varying intermediate vadose zone thickness, seepage from septic/soak pits systems and saturated zone soil porosity. The average groundwater NO_3^--N (mg/l) concentration at Madav nagar area computed using RISK-N model was 12 mg/l (Table 5.14). The RISK-N model computed NO_3^--N concentrations at well W_1(250, 250) due to variations of vadose zone thickness, seepage and saturated zone soil porosity are shown in Figures 5.35, 5.36 and 5.37, respectively.

To investigate the sensitivity of vadose zone thickness, the vadose zone thickness was increased and decreased by 25% from 1.5 m actually considered in the RISK-N model. It is evident from Figure 5.35 that the increase of vadose zone (by 25%) shows that the average

groundwater NO_3^--N decreased by 20% (9.58 mg/l). Similarly, that decrease of vadose zone (by 25%) shows that the average groundwater NO_3^--N increased by up to 33 % (16 mg/l).

To investigate the sensitivity of seepage from septic tank/soak pit system, seepage was increased and decreased by 25% from 10 lt/day/person actually considered in the RISK-N model. It is evident from Figure 5.34 that the increase of seepage (by 25%) shows that increase of average groundwater NO_3^--N by 30 % (15.5 mg/l) and decrease of seepage (by 25%) shows that the decrease of average groundwater NO_3^--N by 25% (9 mg/l). It may be stated that, if the present seepage is reduced by 25% (by improving the quality of construction of septic system, avoiding penetrating tree roots into septic tank and frequent empting of septic tank), the present average groundwater NO_3^--N concentration may reach below the drinking water limit (10 mg/l) in the Madav nagar and Suresh nagar areas. To investigate the sensitivity of porosity in saturated zone, porosity was increased and decreased by 25% from 0.40 considered in the RISK-N model. It is evident from Figure 5.35 that there was no significant change in average groundwater NO_3^--N concentration with the variability of porosity.

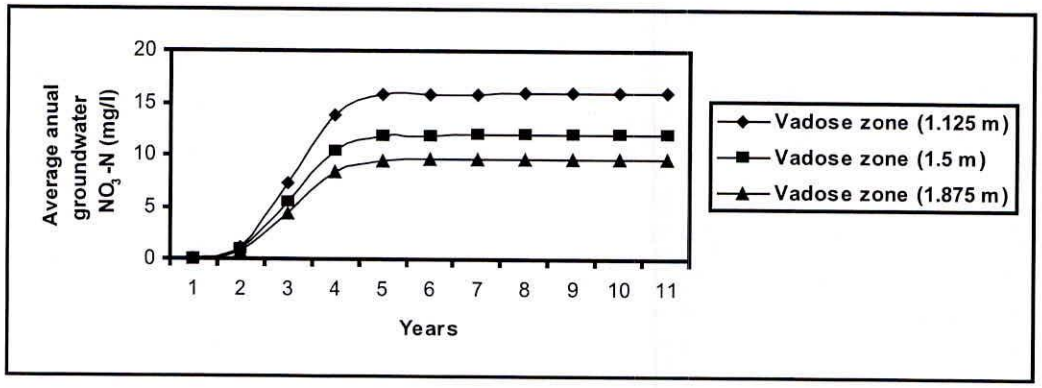

Fig. 5.35 Sensitivity analysis of Intermediate vadose zone in RISK-N model

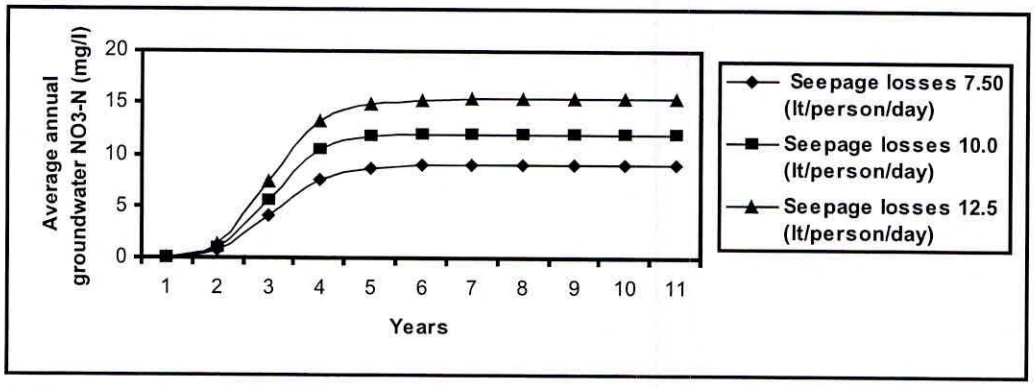

Fig. 5.36 Sensitivity analysis of seepage from septic tank/soak pit system in RISK-N model

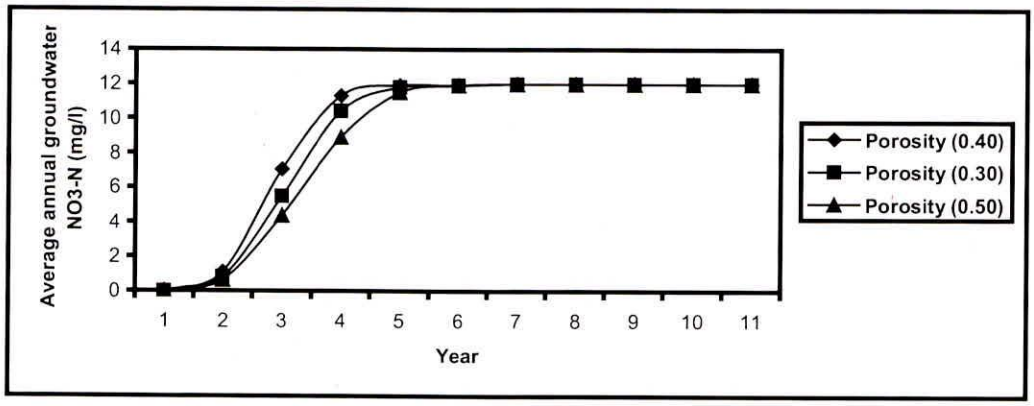

Fig. 5.37 Sensitivity analysis of saturated zone soil porosity in RISK-N model

5.6 Source of salinity using isotope techniques

The characterization of groundwater chemistry in and around Kakinada town indicated that salinity and nutrients are major contaminants in the shallow aquifer. Further, an attempt has been made to find out the source of salinity by analyzing δD‰ and $\delta^{18}O$ ‰ isotope values of groundwater samples collected from salinity zones where the Electrical Conductivity (EC) is more than 2000 micromho/cm. The details of groundwater samples collected in the month of January 2007 is shown in the Table 5.15 and the location of samples with polygon numbers are shown in Figure 5.6. The plot between $\delta^{18}O$‰ and δD‰, and the plot between $\delta^{18}O$‰ and EC are shown in Figures 5.38 and 5.39 respectively. The Local Meteoric Water Line (LMWL) of Kakinada is also marked in the Figure 5.37. The points (well locations) which are falling on precipitation line indicates that the recharge to shallow groundwater is mainly due to local precipitation even though groundwater EC is more than 2000 micromho/cm, as the relation between δO18‰ and δD‰ is deviated from precipitation line it indicates that the groundwater is getting recharged from precipitation but due to evaporation effect it is deviating from LMWL. The increase EC may be due to geological environment. Also sources of salinity may be from seawater, but this is mainly due to diffusion of effect of seawater where in the aquaculture and salt water creeks were present. Further, the scatter plot between EC and **δO18‰** (Figure 5.39) indicates no significant linear relation. It may be due to fact that recharge is from precipitation. Moreover the groundwater table is above mean sea level as indicated in Figure 5.7. Therefore, it may be concluded that the source of salinity is mainly due to diffusion effect of seawater but not directly connected to the seawater. The salinity of groundwater may further deteriorate when the groundwater table is below mean sea level due to urbanization and over exploitation.

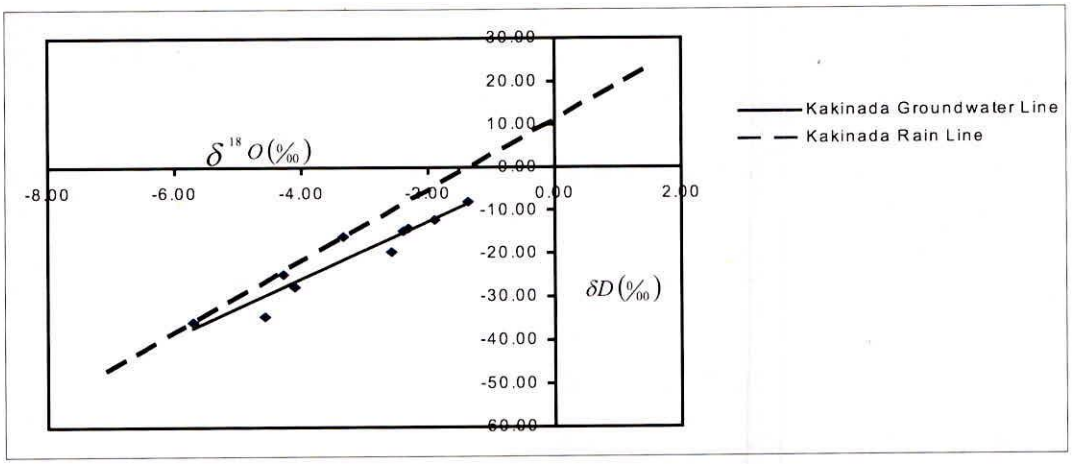

$\delta D(‰) = 6.5742\,\delta^{18}O(‰) + 0.5912$ (Groundwater Line)

$\delta D(‰) = 8.2516\,\delta^{18}O(‰) + 11.541$ (LMWL of Kakinada)

Fig. 5.38 Plot between δ^{18}O‰ and δD‰ values of groundwater samples

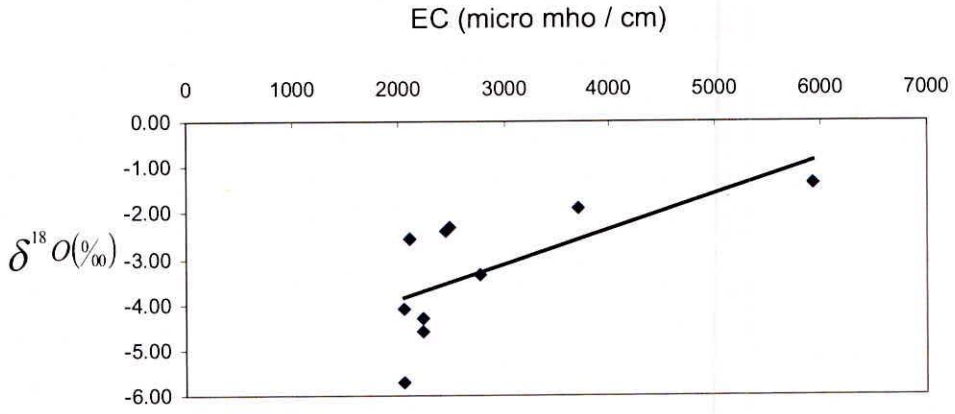

Fig. 5.39 Scattered plot between EC and δ^{18}O‰ values of groundwater samples

6.0 CONCLUSIONS

A methodology utilizing Principal Component Analysis (PCA), GIS, fuzzy clustering technique and a RISK-N model is presented systematically to quantitatively analyze nitrate contamination from septic systems. The study reveals that the methodology presented can be used effectively to carryout modeling studies pertaining to nitrate contamination in urban coastal aquifers. The methodology can help in addressing groundwater quality problems and in decision making for better groundwater quality management and to address health related issues. The sensitivity analysis of RISK-N model parameters is carried out by identifying most influential parameters in order to take appropriate measures to reduce the impact of septic tanks on groundwater NO_3^--N contamination. The major findings of the study are enumerated below:

The measured concentrations of water quality parameters exceeded the permissible drinking water limits for Ca^{2+}, HCO_3^-, Cl^-, SO_4^{2-} and NO_3^-. The ion concentrations are in the order of $HCO_3^->Cl^->SO_4^{2-}>NO_3^-$ (anions) and $Na^+>Ca^{2+}>K^+>Mg^{2+}$ (cations) in the study area. The Piper classification indicated that most of the groundwater samples collected from the study area are Na^+- HCO_3 type. Characterization of groundwater quality using PCA in the study area indicated that salinity and nutrients are major contaminants in the shallow groundwater. Among the nutrients, nitrates are dominant (up to 421 mg/l) in the shallow groundwater. The Cl^-/HCO_3^- ratio in the groundwater is limited to 7.37, indicating no sea water intrusion, resulting from the historical marine coastal environment and present land use practices. The isotope values of groundwater samples collected in salinity zones indicated that there is no direct connection between seawater and shallow groundwater and the present salinity is mainly due to diffusion effect of seawater (aquaculture practices and salt water creeks).

Geostatistical analysis of salinity and nutrients contaminants over the aquifer during different seasons revealed that high salinity zones were along the Bay of Bengal and nearby salt creek, and low zones along the streams. High concentrations of nutrients are observed in the urban and agricultural areas. Nitrogen loading in each polygon (village/town) from septic systems is estimated for the years 1991 and 2004. The comparison between nitrogen load zones and corresponding average groundwater quality (especially EC, nitrate and phosphate) indicates that the shallow groundwater nitrate contamination is significantly influenced by high density of septic systems and unsewered conditions in the study area. The percentage ranges of monthly septic system NO_3^--N contributions to groundwater obtained by using RISK-N model during July 2002 to June 2003 in Lb nagar, Madav nagar, and Suresh nagar areas are 51 to 65, 61 to 98, and 64 to 90, respectively. The RISK-N model application revealed that the average septic system NO_3^--N contribution to groundwater significantly depends up on the prevailing groundwater table conditions and nitrogen load. Results obtained from the RISK-N model for Lb nagar, Madav nagar and Suresh nagar locations indicate that the less denitrification rate (0.0014 per day) and high mineralization rate (0.0382 per day) in the drain field zone allows leaching of nitrate into groundwater without significant losses.

The seasonal decrease in groundwater NO_3^--N and its corresponding increase of HCO_3^- concentration indicates heterotrophic denitrification processes in the subsurface. The sensitivity analysis of RISK-N model parameters reveals that intermediate vadose zone thickness, seepage from septic-soak pit system, saturated zone denitrification rate and average plot size are the most sensitive parameters. Results obtained from the RISK-N model are valid only when the groundwater table is above the mean sea level.

REFERENCES

Agrawal, G.D., Lunkad, S.K., Malkhed, T., 1999. Diffuse agriculture nitrate pollution of groundwater in India. Wat. Sci. Tech., 39(3): 67-75.

Alhajjar, B.J., Harkin, J.M., Chesters, G., 1989. Detergent formula and characteristics of waste water in septic tanks. Journal of Water Pollution Control, 61:605-613.

Almasri, M.N., Kaluarachchi, J.J., 2004. Implications of on-ground nitrogen loading and soil transormations on groundwater qualtiy managment. Journal of the American Water Resources Association, 03113:165-186.

Anderson, D.L., Rice, J.N., Voorhees, M.L., Kirkner, R.A., Sherman, K.M., 1987. Groundwater modeling with uncertainty to assess the contamination potential from onsite sewage disposal systems (OSDS) in Florida. In: Proceedings of the fifth National Symposium on individual and small community sewage systems. Published by ASAE 10-87, USA.

ASCE., 1990 a. Review of geostatistics in geohydrology I: Basic concepts. Journal of Hydraulic Engineering, 116(5):612-632.

ASCE., 1990 b. Review of geostatistics in geohydrology II: Applications. Journal of Hydraulic Engineering, 116(5):633-658.

Babiker, S.I., Mohamed, A.A., Terao, H., Kato, K., Ohta, K., 2004. Assessment of groundwater contamination by nitrate leaching from intensive vegetable cultivation using geographical information system. Environment International, 29(8):1009-1017.

Babuska, R., 1998. Fuzzy Modeling for Control. International series in Intelligent Technologies, Kluwer Academic Publications, The Netherlands, pp.51-57.

Bear, J., 1979. Hydraulics of Groundwater. Mc Graw-Hill, New York.

Bezdek, J.C., 1981. Pattern Recognition with Fuzzy Objective Function Algorithms, Plenum, NY.

BGS., 1996. Identification and quantification of groundwater nitrate pollution from non-agricultural sources. British Geological Survey, R & D technical report, P33.

Bhargava, D.S., 1984. Monographs for Septic Tank Design. Institute of Engineers (India) Journal, 64:59-60.

BIS., 1991. Bureau of Indian Standards. Specifications for Drinking Water, IS:10500:1991, New Delhi, India.

Bjerg, P.L., Christensen, T.H., 1992. Spatial and temporal small-scale variation in ground water quality of a shallow sandy aquifer. Journal of Hydrology, 131:133-149

Bobba, A.G., Singh, V.P., Bengtsson, L., 1997. Sustainable development on water resources in India. Environmental Management, 21(3):367-393.

Butler, D., Payne, J., 1995. Septic Tanks: Problems and Practice. Building and Environment, 30(3):419-425.

Canter, L.W., 1997. Nitrates in Groundwater, CRC, Boca Raton, Florida.

Ceron, J.C., Espinosa, R.J., Bosch, A.P., 2000. Numerical analysis of hydrogeochemical data: a case study (Alto Guadalentin, southeast Sapin). Applied Geochemistry, 15:1053-1067.

Costas-Carlos, C., Gomez-Gomez, F., 1998. Nitrate contamination of the upper aquifer in the Manati-Vegabaja area, Puerto Rico. In: Proc., of AWRA Third International Symposium on Tropical Hydrology, San Juan, Puerto Rico.

Davis, C.J., 1986. Statistics and Data Analysis in Geology. Second Edition, John Wiley & Sons, Inc.

Flipo, N., Jeannee, N., Poulin, M., Even, S., Ledoux, E., 2007. Assessment of nitrate pollution in the Grand Morin Aquifers (France): Combined use of geostatistics and physically based modeling. Environmental Pollution, 146: 241-256.

Freeze, R.A., Cherry, J.A., 1979. Groundwater. Prentice-Hall, Inc.

Gogu, R.C., Carabin, C., Hallet, V., Peters, V., Dassargues, A., 2001. GIS-based hydrogeological databases and groundwater modeling. Hydrogeology Journal, 9:555-569 .

Grande, J.A., González, A., Beltran, R., Sanchez-Rodas, D., 1996. Application of factor analysis to study the contamination in the aquifer system of Ayamonte-Huelva (Spain). Ground Water, 34(1):155-161.

Guler, C., Thyne, D.G., McCray, J.E., Turner, A.K., 2002. Evaluation of graphical and multivariate statistical methods for classification of water chemistry data. Hydrogeology Journal, 10:455-474.

Gupta, S.K., Gupta, R.C., Seth, A.K., Gupta, A.B., Bassin, J.K., Gupta, D.K., Sharma, S., 1999. Epidemiological evaluation of recurrent stomatitis, nitrates in drinking water and Cytochrome B Reductase activity. The American Journal of Gastroenterology, 94(7):1808-1812.

Gusman, A.J., Marino, M.A., 1999. Analytical modeling of nitrogen dynamics in soils and groundwater. Journal of Irrigation and Drainage Engineering, ASCE, 125(6):330-337.

Hansen, S., Jensen, H.E., Nielsen, N.E., Svendsen, H., 1991. Simulation of nitrogen dynamics and bio mass production in winter wheat using the Danish simulation model DAISY. Fertlizer Research, 27:245-259.

Hantush, M.M., Marino, A.M., 1996. An analytical model for the assessment of pesticide exposure levels in soils and groundwater. Environmental Modeling and Assessment, 1:263-276.

Hantzsche, N.N., Finnemore, E.J., 1992. Predicting groundwater nitrate-nitrogen impacts. Ground Water, 30(4):490-499.

Helena, B., Rafael, P., Marisol, V., Enrique, B., Manuel, F.J., Luis, F., 2000. Temporal evolution of groundwater composition in an alluvial aquifer (Pisuerga River, Spain) by principal component analysis. Water Research, 34(3):807-816.

Hession, W.C., 2000. Statewide Non-Point source pollution assessment methodology. Journal of Water Resources Planning and Management, 126(3):146-155.

Hirschberg, K-J.B., Appleyard, S.J., 1996. A baseline survey of non point source groundwater contamination in the Perth basin, Western Australia. Geological Survey of Western Australia, Department of Minerals and Energy, Record 1996/2, ISBN 0 7309 6524 4.

Hoover, T.M., Petersen, G.W., Fritton, D.D., 1981. Utilization of mound systems for sewage disposal in Pennsylvania, N.I., Mc Clelland and J.L., Evans (ed.), In: Proc. 7th National Conference on Individual On-Site Wastewater Systems, National Sanitation Foundation, Ann Arbor, MI. 41-60.

Hoyle, B.L., 1989. Groundwater quality variations in a silty alluvial soil aquifer, Oklahoma. Ground Water, 27:540-549.

Isaaks, E.H., Srivstava, R.M., 1989. Applied Geostatistics. Oxford University Press, New York, USA.

Istok, D.J., Rautman, A.C., 1996. Probabilistic assessment of groundwater contamination: 2: Results of case study. Ground Water, 34(6):1050-1064.

Jain, C.K., Bhatia, K.K.S., Vijay, T., 1997. Groundwater quality in a coastal region of Andhra Pradesh. Indian Journal of Environment and Health, 39(3): 182-192.

Jain, C.K., Kumar, S., Rao, Y.R.S., 2004. Trace elements contamination in a coastal aquifer of Andhra Pradesh. Pollution Research, 23:13-23.

Journel, A.G., Huijbregts, C.J., 1978. Mining Geostatistics. Academic Press, London, England.

Kaplan, B.O., 1987. Septic systems hand book. LEWIS publishers, INC, Michigan, USA.

Kapoor, A., Viraraghavan, T., 1997. Nitrate removal from drinking water – review. Journal of Environmental Engineering (ASCE), 123(4):371-380.

Kravchenko, A.N., 2003. Influence of spatial structure on accuracy of interpolation methods. Soil Science Society of America Journal, 67:1564-1571.

Lee, S.M., Min, K.D., Woo, N.C., Kim, Y.J., Ahn, C.H., 2003. Statistical models for the assessment of nitrate contamination in urban groundwater using GIS. Environmental Geology, 44:210-221.

Liu, C.W., Lin, K.H., Kuo, Y.M., 2003. Application of factor analysis in the assessment of groundwater quality in a blackfoot disease area in Tiawan. The Science of the Total Environment, 313:77-89.

Majumdar, D., Gupta, N., 2000. Nitrate pollution of groundwater and associated human health disorders. Indian Journal of Environmental and Health, 42(1):28-39.

Mani, M., Reddy, B.V.V., Avvannavar, S.M., 2007. Design of a modified compact septic-tank to suit coastal (island) habitations with high-water table. In: Proceedings of World Toilet Summit 2007, 31st Oct., to 3rd Nov., 2007, New Delhi, India, pp.73-77.

Mara, D.D., Feachem, R.G.A., 1999. Water-and excreta-related diseases: unitary environmental classification. Journal of Environmental Engineering, ASCE, 125(4):334-339.

Martos, F.S., Espinosa, R.J., Bosch, A.P., 2001. Mapping groundwater quality variables using PCA and geostatistics: A case study of Bajo Andarax, Southeastern Spain. Hydrologic Sciences Journal, 46(2):227-242.

Matelski, R.P., 1975. The field percolation rate of Pennsylvania State Univ., Agric. Exp. Stn., University Park, PA.

Melloul, A., Collin, M., 1992. The principal components statistical method as a complementary approach to geochemical methods in water quality factor identification: application to the coastal plain aquifer of Israel. Journal of Hydrology, 140:49-73

Mercado, A., 1976. Nitrate and Chloride pollution of aquifers: A regional study with the aid of a single-cell model. Water Resources Research, 12(4):731-747.

Mohan, S., Kananan, K., 1998. GIS based decision support system for pollution assessment. In: Proc., of Eighth user's interaction workshop on Remote Sensing, NRSA, Hyderabad, March 17-18, pp.56-60.

Montangero, A., Belevi, H., 2007. Assessing nutrient flows in septic tanks by eliciting expert judgment: A promising method in the context of developing countries. Water Research, 41(5):1052-1064.

MoWR. 2000. Ministry of Water Resources, Problems facing water/irrigation sector-water quality issues, Web site information, www.wrmin.nic.in. (Feb. 5, 2004).

Naranjo, E., Larsen, H., 1998. An integrated model to assess pollution loads with use of GIS and Numerical methods. In: Hydroinformatics'98, Babovic and Larsen (eds), Balkema, Rotterdam, ISBN 9054109831, pp.409-416.

Navarro, A., Carbonell, M., 2007. Evaluation of groundwater contamination beneath an urban environment: The Besos river basin (Barcelona, Spain). Journal of Environmental Management, 85(2):259-269.

Nizeyimana, E., Petersen, G.W., Anderson, M.C., Evans, B.M., Hamlett, J.M., Baumer, G.M., 1996. Statewide GIS/Census data assessment of nitrogen loadings from septic systems in Pennsylvania. Journal of Environmental Quality, 25:346-354.

Novichikhin, E.P., Tarko, A.M., 1984. Modeling of global biogeochemical carbon and nitrogen cycles in the atmosphere-plant-soil-system. Biol. Bull. Acad. Sci. USSR, 11(2):190-198.

Ojha, C.S.P., Rai, A. K., 1996. A non linear root water extraction model. Journal of Irrigation and Drainage Engg., 122 (4):198-202.

Oyarzun, R., Arumi, J., Salgado, L., Marino, M., 2007. Sensitivity analysis and field-testing of the RISK-N model in the Central Valley of Chile. Agricultural Water Management, 87(3):251-260.

Paz, J.M.D., Ramos, C., 2002. Linkage of geographical information system with the GLEAMS model to assess nitrate leaching in agricultural areas. Environmental Pollution, 118:249-258.

Piper, A.M., 1944. A graphic procedure in the geochemical interpretation of water analysis: American Geophysical Union Transactions, 25:914-923.

Ponce, V.M., 1989. Engineering Hydrology, Principles and Practices. Prentice Hall.

Rajasekhar, C.H., Reddy, V.C., Kotaiah, B., 1994. Groundwater pollution from unsewered sanitation – A case study in Tirupati. Indian Journal of Environmental Protection, 14(11):845-847.

Rao, N.S., Rao, J.P., Devadas, J.D., Rao, K.S., Krishna, C., 2001. Multivariate analysis for identifying the governing factors of groundwater quality. Journal of Environmental Hydrology, 9(16):1-9.

Reay, W.G., 2004. Septic tank impacts on groundwater quality and nearshore sediment nutrient flux. Ground Water, 42(7):1079-1089.

Rengaraj, S., Murugesan, V., Elango, L., Elampooranan, T., 1996. Nitrate in ground waters of suburban regions of Madras city. Indian J. Environmental Protection, 16(8):573-576.

Robinson, K., Ragan, M.R., 1993. Geographic Information System based nonpoint pollution modeling. Water Resources Bulletin, American Water Resources Association, 29(6):1003-1008.

Schouw, N.L., Danteravanich, S., Mosbaek, H., Tjell, J.C., 2002. Composition of human excreta – a case study from Southern Thailand. The Science of the Total Environment, 286:155-166.

Shaffer, M.J., Halvorson, A.D., Peirce, F.J., 1991. Nitrate leaching and economic analysis package (NLEAP): Model description and application. In R.F Follett et al., Eds., Managing N for Groundwater Quality and Farm Profitability. Madison, WI:SSSA, 285-322.

Shaffer, M.J., Wylie, B. K., Hall, M.D., 1995. Identification and migration of nitrate leaching hot spots using NLEAP-GIS technology. Journal of Contaminant Hydrology, 20:253-263.

Sikora, L.J., Corey, R.B., 1976. Fate of nitrogen and phosphorus in soils under septic tank waste disposal fields. Transactions of the ASAE, 866-875.

Simone, A.L., Howes, L.B., 1998. Nitrogen transport and transformations in a shallow aquifer receiving waste water discharge: A mass balance approach. Water Resources Research, 34(2):271-285.

Srinivasan, R., Ramanarayanan, T.S., Arnold, J.G., Bednarz, S.T., 1998. Large area hydrologic modeling and assessment: part II- model application. Journal of American Water Resources Association, 34(1):91-102.

Swamy, N.K., Rao, M.V.V., 1989. Nitrate ion as an indicator of the extent of pollution of urban ground water from domestic wastes- A case study. Indian Journal of Environmental Protection, 9(11):840-844.

Tabachow, R.M., Peirce, J.J., Richter, D.D., 2001. Biogeochemical models relating soil nitrogen losses to plant-Available nitrogen. Environmental Engineering Science, 18(2):81-89.

Trauth, R., Xanthopoulos, C., 1997. Non point pollution of groundwater in urban areas. Water Research, 31(11):2711-2718.

Trudell, M.R., Gillham, R.W., Cherry, J.A., 1996. An in-situ of the occurrence and rate of denitrification in a shallow unconfined sand aquifers. Journal of Hydrology, 83:251-268.

Tsihrintzis, V.A., Hamid, R., Fuentes, H.R., 1996. Use of geographic information systems (GIS) in water resources: a review. Water Resources Management, 10:251-257.

Tyagi, J.V., Rao, Y.R.S., Seethapathi, P.V., 1997. Rainfall recharge coefficient variability in the deltas of the east coast of India. In: Proceedings of 8th National Symposium on Hydrology (Theme: Coastal Hydrology) held at Calcutta during 11-12 April, pp.27-32.

Ventura, S.J., Kim, K., 1993. Modeling urban non point source pollution with a geographic information system. Water Resources Bulletin, AWRA, 29(2):189-198.

Voudouris, K., Panagopoulos, A., Koumantakis, I., 2004. Nitrate pollution in the coastal aquifer system of the Korinthos Prefecture (Greece). Global Nest: the International Journal, 6(1):31-38.

Wackernagel, H., 1995. Multivariate Geostatistics: An introduction with Applications. Springer-Verlag, Berlin, Germany.

Wakida, F.T., Lerner, D.N., 2005. Non-agricultural sources of groundwater nitrate: a review and case study. Water Research, 39(1):3-16.

Ward, M.H., Mark, S.D., Cantor, K.P., Weisenburger, D.D., Correa-Villasenor, A., Zahm, S.H., 1996. Drinking-water nitrate and the risk of non-Hodgkin's lymphoma. Epidemiology, 7:465-471.

Whelan, B.R., Titamnis, Z.V., 1982. Daily chemical variability of domestic septic tank effluent. Water, Air, and Soil Pollution, 17:131-139.

WHO., 1984. Guidelines for drinking water quality, Vol-I, Recommendations, World Health Organization, Geneva, 1-130.

Wilhelm, S.R., Schiff, S.L., Cherry, J.A., 1994. Biogeochemical Evolution of domestic waste water in septic systems: 1. Conceptual Model. Ground Water, 32(6):905-916.

Annexure I

Polygon number	Polygon name (Village Name)	Area(km^2)
1	Gorasa	3
2	Uppada	1
3	Amenabad	2
4	Nagulapalli	10
5	Yandlapalli	10
6	Kothapalli	4
7	Isukapalli	6
8	Madavapuram	4
9	Panduru	7
10	Tammavaram	5
11	Timmapuram	10
12	Kakinada	20
13	Sarpavaram	9
14	Suryarao peta	3
15	Cheediga	2
16	Repuru	3
17	Penumarthi	2
18	Ramanayapeta	10
19	Nemam	7
20	P Vemavaram	2
21	Navara	4
22	Panasapadu	7
23	Koppavaram	2
24	Mamilladoddi	3
25	Madavapatnam	4
26	Boyanapudi	3
27	Valluru	3
28	Unduru	2
29	Bhimaram part	11
30	Samalkot M part	6
31	Kapavaram	4
32	Pandravada	2
33	Pavara	10
34	Chitrada	4
35	Kumarapuram	3
36	Virava	4
37	Mengaturthi	3
38	Agraharam	5
39	Mallam	6
40	Veeraraghavapuram	3

Polygon number	Polygon name (Village Name)	Area (km^2)
41	Jammalapalli	2
42	Jalluru	3
43	Somavaram	2
44	F K Palem	2
45	Khandarada	2
46	Viravada	7
47	Kandrakota	5
48	Marlava	2
49	Tirupathi	5
50	Chandrampalli	1
51	Tatiparthi	1
52	Divili	2
53	Pulimeru	3
54	G Ragampeta	3
55	Kattamuru	10
56	Sirivada	2
57	Chadalada	2
58	Govindarajupalem	1
59	Gorinta	2
60	Vadlamuru	3
61	Goneda	5
62	Tamarada	4
63	Mukkollu	5
64	Srungarayanipalem	3
65	Rajupalem	3
66	Veeravaram	7
67	Subbampeta	1
68	Vakatippa	2
69	kuthukudumilli	3
70	Pithapuram	19
71	Navakandarada	1
72	Kodevaram	6
73	Komaragiri	17
74	k1	4
75	p1	1
76	s1	7
77	p2	3
78	Illandrada	1
79	Gudivada	1
80	Peddapuram(part)	14
81	Kovvada	2
82	Ganganapalli	3
83	Vakalapudi	9

Table 5.1 Groundwater quality analysis, Piper's classification and varimax rotated factor scores (F1 and F2) during pre monsoon period (May 2000)

Well No.	Location	Temp	pH	EC	Ca	Mg	Na	K	HCO_3	Cl	SO_4	NO_3	Piper's classification	F1	F2
1	Sarpavaram	31.0	7.5	1391	120	58	100	37	250	200	77	100	Ca-Mg-Na-Cl-HCO_3-NO_3	-0.536	0.367
2	Balaji Nagar	31.0	7.2	606	38	6	60	5	176	80	14	9	Na-Ca-HCO_3-Cl	-1.082	-0.614
3	Valasapakalu	32.0	7.3	3730	75	106	425	230	616	588	258	64	Na-Mg-Cl-HCO_3	0.934	0.698
4	Vakalapudi	31.0	7.1	3200	104	56	420	49	416	532	198	9	Na-Cl-HCO_3	0.537	-0.491
5	Ramanayya Peta	31.0	7.2	937	90	29	150	59	296	172	83	115	Na-Ca-HCO_3-Cl-NO_3	-0.729	0.513
6	R.R. Nagar	32.0	7.3	1410	74	31	145	13	248	184	85	10	Na-Ca-Mg-Cl-HCO_3	-0.533	-0.360
7	Madhav Nagar	30.0	7.4	1520	98	42	185	28	432	188	120	49	Na-Ca-Mg-HCO_3-Cl	-0.261	-0.435
8	Lal Bahadur Nagar	31.0	7.6	1743	98	39	185	70	300	204	160	78	Na-Ca-Cl-HCO_3	-0.396	0.179
9	Godarigunta	31.0	7.8	2540	109	38	320	60	336	508	75	16	Na-Ca-Cl-HCO_3	0.032	-0.507
10	Sambamurthy Nagar	31.0	7.3	1689	69	56	205	16	472	144	157	4	Na-Mg-Ca-HCO_3-Cl-SO_4	-0.042	-0.737
11	Bhanugudi	32.0	7.8	2670	74	47	405	46	456	372	204	85	Na-Cl-HCO_3	0.207	-0.113
12	Ramarao Peta	30.0	7.2	1320	107	17	150	40	416	128	30	46	Na-Ca-HCO_3-Cl	-0.570	-0.253
13	Surya Rao Peta	30.0	7.3	2050	48	44	285	121	692	236	92	9	Na-HCO_3-Cl	0.102	-0.642
14	S.N.Puram	31.0	7.6	3480	56	41	590	143	720	556	121	9	Na-Cl-HCO_3	0.750	-0.666
15	Budam Peta	31.0	7.5	3140	130	59	200	215	532	316	178	256	Na-Ca-Cl-HCO_3-NO_3	-0.135	2.204
16	Temple Street	31.0	7.8	2670	146	76	325	114	500	304	383	36	Na-Ca-Mg-Cl-HCO_3-SO_4	0.626	0.051
17	Frazer Peta	31.0	7.4	1480	95	21	100	70	400	160	50	77	Ca-Na-HCO_3-Cl	-0.636	0.223
18	Pratap Nagar	30.0	7.2	611	51	8	150	17	300	80	50	25	Na-Ca-HCO_3-Cl	-0.849	-0.688
19	Gogudanayya Peta	32.0	7.3	6612	144	90	905	48	808	1692	405	35	Na-Cl-HCO_3	2.757	-0.740
20	M.S.N. Charties	32.0	7.5	2440	74	37	260	115	348	452	159	36	Na-Cl-HCO_3	-0.066	0.103
21	Ravindra Nagar	31.0	7.6	3940	175	91	400	25	212	908	137	44	Na-Ca-Mg-Cl	0.761	-0.201
22	Indra Palem	31.0	7.8	2680	133	43	215	126	396	360	229	141	Na-Ca-Cl-HCO_3	-0.084	0.902
23	Chidiga	31.0	7.9	2830	140	53	270	77	260	420	180	296	Na-Ca-Cl-NO_3	-0.336	1.782
24	Madhura Nagar	31.0	7.8	830	55	16	60	6	212	75	39	85	Ca-Na-HCO3-NO_3-Cl	-1.058	-0.217
25	Rayudu Palem	31.0	7.6	981	59	16	70	50	204	120	67	72	Na-Ca-Cl-HCO_3-NO_3	-0.978	-0.009
26	Penumarthy	31.0	7.6	1150	85	23	65	35	116	176	99	132	Ca-Na-Cl-NO_3	-1.002	0.498
27	V.Pakalu-NFCL	30.0	7.8	3230	56	47	500	37	620	504	197	57	Na-Cl-HCO_3	0.591	-0.995

28	Suresh Nagar	30.0	7.5	2250	96	58	230	6	280	380	134	24	$Na-Ca-Mg-Cl-HCO_3$	-0.039	-0.758
29	Sita Ram Nagar	30.0	7.7	1390	43	27	180	14	412	164	83	7	$Na-HCO_3-Cl$	-0.433	-1.131
30	Chinna VPudi	31.0	7.8	9693	237	198	1320	110	788	2016	529	5	Na-Cl	4.462	-0.891
31	Raghavendra P	31.0	7.6	5740	69	84	835	34	956	1180	191	23	$Na-Cl-HCO_3$	2.129	-1.464
32	V.Turangi	32.0	7.7	7200	186	124	795	350	352	1260	558	290	Na-Cl	1.870	3.082
33	Rajendra Nagar	31.0	7.3	2320	119	51	235	103	260	320	217	122	$Na-Ca-Cl-SO_4$	-0.200	0.826
34	Panasa Padu	31.0	7.5	2500	122	56	200	128	416	308	215	187	$Na-Ca-Cl-HCO_3-NO_3$	-0.154	1.305
35	Vakalapudi	30.0	7.4	1929	66	37	180	123	264	212	122	231	$Na-NO_3-Cl-HCO_3$	-0.789	1.298
36	Anjaneya Na	30.0	7.6	2060	95	43	245	33	240	320	310	33	$Na-Ca-Cl-SO_4$	-0.046	-0.550
37	Elwyn Peta	31.0	7.7	4517	111	80	540	230	556	900	362	113	$Na-Cl-HCO_3$	1.153	0.782
38	Panduru	31.0	7.8	3840	80	29	435	370	684	520	206	134	$Na-K-Cl-HCO_3$	0.330	1.535
39	Gorasa	32.0	7.8	830	75	22	145	108	336	200	55	24	$Na-Ca-Cl-HCO_3$	-0.654	0.003
40	Nagam Peta	31.0	7.8	1037	40	19	110	21	208	156	110	0	$Na-Ca-Cl-HCO_3-SO_4$	-0.744	-0.849
41	N. Kandarada	31.0	7.4	841	48	19	70	27	212	104	60	0	$Na-Ca-Mg-HCO_3-Cl$	-0.864	-0.620
42	Kondevaram	31.0	7.5	2308	167	36	195	82	180	440	338	39	$Na-Ca-Cl-SO_4$	0.004	0.319
43	Endapalli	32.0	7.2	1961	48	32	310	6	368	260	236	0	$Na-Cl-HCO3-SO_4$	-0.013	-0.702
44	U.Kothapally	32.0	7.3	1853	53	48	500	136	456	588	102	90	$Na-Cl-HCO_3$	0.140	0.353
45	Uppada	31.0	7.4	4050	56	53	565	25	636	792	298	9	$Na-Cl-HCO_3$	1.144	-1.167
46	Subbam Peta	32.0	7.7	2105	69	57	220	19	388	420	71	2	$Na-Mg-Cl-HCO_3$	-0.005	-0.717
47	Atcham Peta	32.0	7.2	5200	144	102	755	43	392	1240	646	37	$Na-Cl-SO_4$	2.139	-0.280
48	Timma Puram	32.0	7.0	2080	85	38	250	310	408	380	231	96	$Na-K-Cl-HCO_3$	-0.186	1.735
49	Chandram	31.0	7.0	3210	101	64	370	400	524	564	77	294	$Na-K-Cl-NO_3-HCO_3$	-0.119	3.301
50	Kandarada	30.0	7.8	1688	38	27	275	26	400	296	105	10	$Na-Cl-HCO_3$	-0.253	-1.176
51	Navara	30.0	7.6	1200	37	27	175	81	400	136	94	11	$Na-HCO_3-Cl$	-0.520	-0.742
52	Gonchala	30.0	7.2	3960	150	62	385	179	700	684	200	211	$Na-Cl-HCO_3$	0.637	1.423
53	Brahmananda	30.0	7.3	4220	125	72	675	40	336	1112	479	29	$Na-Cl-SO_4$	1.472	-0.763
54	Unduru	30.0	7.8	640	53	13	75	7	228	72	71	1	$Na-Ca-HCO_3-Cl-SO_4$	-0.905	-1.021
55	Madhav Pat	30.0	7.2	1943	85	28	155	137	360	260	179	54	$Na-Ca-Cl-HCO_3-SO_4$	-0.365	0.209
56	A. Trayam	31.0	7.4	1660	64	35	155	72	216	200	94	41	$Na-Ca-Mg-Cl-HCO_3$	-0.592	-0.098
57	Rameswaram	31.0	7.1	2460	91	40	210	169	412	360	155	170	$Na-Cl-HCO_3-NO_3$	-0.307	1.376
58	Karakuduru	30.0	7.8	771	30	21	95	20	308	72	52	2	$Na-Mg-HCO_3-Cl$	-0.806	-1.104
59	Kowada	31.0	7.5	777	53	14	40	27	224	88	47	42	$Ca-Na-HCO_3-Cl$	-1.004	-0.317
60	Kodayapalem	31.0	7.2	2370	98	32	315	52	440	312	201	101	$Na-Ca-Cl-HCO_3$	-0.030	0.223
61	Virava	30.0	7.1	255	22	7	40	23	188	40	29	1	$Na-Ca-HCO_3-Cl$	-1.150	-0.790
62	Viravada	30.0	7.2	1032	42	29	90	108	352	120	36	8	$Na-K-Mg-HCO_3-Cl$	-0.719	-0.397

63	Divili	30.0	7.3	833	59	25	65	7	140	120	58	11	Ca-Na-Mg-Cl-HCO_3	-0.902	-0.712
64	Goranta	31.0	7.9	1043	91	17	105	25	288	148	31	18	Na-Ca-HCO_3-Cl	-0.728	-0.556
65	Mallam	31.0	7.4	1530	56	39	225	75	572	180	9	5	Na-HCO_3-Cl	-0.223	-0.610
66	Jelleru	30.0	7.5	3432	64	53	265	175	744	312	186	147	Na-HCO_3-Cl	0.243	0.589
67	Eskapalli	31.0	7.8	789	27	11	95	30	188	100	49	5	Na-HCO_3-Cl	-0.976	-0.795

Temp.- Temperature ^{0}C, EC- Electrical Conductivity ($\mu S\ cm^{-1}$), all other units (mg/l), F1 and F2 = Factor1 and Factor 2.

Table 5.2 Descriptive statistics of water quality parameters (67 samples) in each season and pooling together (201 samples) in the year 2000.

Variables	*May 2000 (Pre monsoon)*					*August 2000 (Monsoon)*					*November 2000 (Post monsoon)*					*All three seasons*				
	Min.	*Max.*	*Mean*	*STD*	*Skew*	*Min.*	*Max.*	*Mean*	*STD*	*Skew*	*Min.*	*Max.*	*Mean*	*STD*	*Skew*	*Min.*	*Max.*	*Mean*	*STD*	*Skew*
Temp	30	32	30.9	0.69	0.16	29	31	30.31	0.63	-0.44	29	30	29.54	0.50	-0.15	29	32	30.24	0.82	0.17
pH	7	7.9	7.48	0.25	-0.04	6.6	7.6	7.22	0.23	-0.05	6.9	7.6	7.24	0.15	0.65	6.6	7.9	7.31	0.25	0.34
EC	255	9693	2394	1705	1.87	354	6660	2229	1470	1.27	390	6440	2224	1417	1.11	255	9693	2282	1530	1.51
Ca^{2+}	22	237	87	42	1.07	24	300	105	57	1.33	24	250	88	47	1.56	22	300	93	49	1.42
Mg^{2+}	6	198	45	31	2.20	3	106	32	21	1.06	6	118	44	28	0.87	3	198	40	28	1.65
Na^{+}	40	1320	288	239	1.96	24	1000	269	215	1.64	32	1300	264	229	1.97	24	1320	273	227	1.85
K^{+}	5	400	86	90	1.85	6	350	82	73	1.44	6	325	81	70	1.27	5	400	83	78	1.63
HCO_3^-	116	956	396	182	0.93	160	980	482	204	0.50	152	1000	497	214	0.41	116	1000	458	205	0.60
Cl^-	40	2016	403	388	2.17	16	1704	368	350	1.84	16	1496	339	324	1.72	16	2016	370	354	1.96
SO_4^{2-}	9	646	165	135	1.61	19	1151	186	187	3.21	17	928	136	144	3.23	9	1151	162	158	2.95
NO_3^-	0	296	67	78	1.57	2	384	95	95	1.26	1	421	83	93	1.93	0	421	82	89	1.60
Cl^-/HCO_3^-	0.37	7.37	1.73	1.42	2.14	0.17	3.79	1.17	0.82	1.38	0.15	4.48	1.05	0.76	2.08	0.15	7.37	1.35	1.15	2.64
SO_4^{2-}/Cl^-	0.02	0.47	0.18	0.09	0.74	0.06	0.56	0.23	0.11	0.85	0.05	0.63	0.18	0.99	2.14	0.02	0.63	0.19	0.11	1.52

Temp.- Temperature ^{0}C, EC- Electrical Conductivity ($\mu S\ cm^{-1}$), STD - Standard Deviation, Skew – Skewness Coefficient , all other units (mg/l).

Table 5.3 Matrix of Correlation between water quality parameters (67 samples) during different seasons and all seasons (201 samples) in the year 2000

Variable	Temperature				pH				EC				Ca^{2+}				Mg^{2+}			
	PRM	M	PSM	Year	PRM	M	PSM	Year	PRM	M	PSM	Year	PRM	M	PSM	Year	PRM	M	PSM	Year
pH	0.006	0.166	-0.060	0.289																
EC	0.271	-0.325	0.127	0.057	0.078	-0.133	-0.040	0.007												
Ca^{2+}	0.223	-0.241	0.023	-0.010	0.065	-0.076	-0.144	-0.087	0.699	0.813	0.773	0.735								
Mg^{2+}	0.286	-0.291	0.234	0.080	0.055	-0.036	0	0.078	0.909	0.827	0.815	0.839	0.738	0.667	0.704	0.619				
Na^{+}	0.279	-0.302	0.125	0.062	0.054	-0.083	-0.034	0.009	0.947	0.966	0.951	0.952	0.557	0.732	0.665	0.635	0.852	0.782	0.733	0.774
K^{+}	0.220	-0.132	0.296	0.113	-0.136	-0.171	-0.122	-0.110	0.398	0.550	0.477	0.466	0.296	0.389	0.204	0.291	0.329	0.385	0.417	0.362
HCO_3^{-}	0.065	-0.185	0.096	-0.140	-0.027	-0.075	0.059	-0.123	0.657	0.801	0.818	0.719	0.188	0.570	0.576	0.466	0.525	0.695	0.719	0.581
Cl^{-}	0.309	-0.311	0.121	0.087	0.034	-0.117	-0.086	-0.008	0.954	0.965	0.964	0.960	0.663	0.804	0.767	0.724	0.869	0.784	0.771	0.791
SO_4^{2-}	0.278	-0.358	0.079	0.031	0.015	-0.096	-0.108	-0.050	0.805	0.842	0.804	0.796	0.679	0.759	0.693	0.720	0.762	0.704	0.647	0.634
NO_3^{-}	0.098	-0.104	-0.020	-0.050	-0.048	-0.059	0.046	-0.081	0.250	0.350	0.293	0.286	0.408	0.367	0.234	0.343	0.211	0.274	0.268	0.213

Variable	Na^{+}				K^{+}				HCO_3^{-}				Cl^{-}				SO_4^{2-}			
	PRM	M	PSM	Year	PRM	M	PSM	Year	PRM	M	PSM	Year	PRM	M	PSM	Year	PRM	M	PSM	Year
K^{+}	0.274	0.417	0.377	0.347																
HCO_3^{-}	0.682	0.822	0.800	0.737	0.388	0.494	0.447	0.417												
Cl^{-}	0.957	0.954	0.951	0.952	0.264	0.432	0.348	0.340	0.565	0.714	0.719	0.626								
SO_4^{2-}	0.768	0.826	0.737	0.761	0.289	0.457	0.324	0.352	0.347	0.567	0.576	0.484	0.786	0.785	0.734	0.755				
NO_3^{-}	0.067	0.184	0.187	0.142	0.651	0.612	0.569	0.592	0.083	0.207	0.136	0.166	0.114	0.219	0.166	0.159	0.185	0.214	0.153	0.189

Temperature - ^{0}C, EC- Electrical Conductivity ($\mu S\ cm^{-1}$), PRM- pre-monsoon, M-monsoon, PSM-post monsoon, Year-three seasons data sets together

Table 5.4 Results obtained from PCA: weights of the principal components together with the percentage of explained variance

Variables	Pre-monsoon			Monsoon			Post-monsoon			
	F1	F2	F3	F1	F2	F3	F1	F2	F3	F4
Temp. (°C)	0.268	0.258	0.314	-0.299	0.069	0.649	0.064	0.040	0.961	-0.038
PH	0.052	-0.169	0.672	0.053	-0.154	0.840	-0.035	-0.011	-0.043	0.985
EC ($\mu S\ cm^{-1}$)	0.962	0.211	0.031	0.944	0.258	-0.144	0.962	0.220	0.062	0.000
Ca^{2+}	0.633	0.426	0.393	0.804	0.245	-0.073	0.829	0.083	-0.131	-0.169
Mg^{2+}	0.904	0.201	0.126	0.851	0.149	-0.054	0.829	0.209	0.191	0.055
Na^{+}	0.975	0.019	-0.037	0.962	0.079	-0.104	0.934	0.103	0.079	0.024
K^{+}	0.244	0.817	-0.279	0.352	0.808	-0.111	0.289	0.788	0.346	-0.089
HCO_3^{-}	0.686	0.032	-0.513	0.797	0.201	-0.015	0.821	0.144	0.122	0.161
Cl^{-}	0.961	0.080	0.069	0.939	0.115	-0.139	0.949	0.073	0.052	-0.053
SO_4^{2-}	0.813	0.201	0.205	0.846	0.135	-0.183	0.829	0.077	-0.007	-0.133
NO_3^{-}	0.028	0.920	0.034	0.123	0.904	-0.006	0.103	0.924	-0.145	0.047
Eigen values	5.284	1.924	1.112	5.652	1.725	1.232	5.531	1.618	1.148	1.060
% Variance	48.041	17.493	10.110	51.380	15.685	11.204	50.286	14.713	10.435	9.632

Table 5.5 Soil limitation class and malfunctioning of septic systems

Soil type	Soil limitation class	% Malfunctions of septic systems
Sandy loam	Severe	65
Sandy clay loam	Moderate	40
Sandy clay and Clay	Slight	10

Table 5.6 Annual average nitrogen-loading zones and corresponding average groundwater quality (NO_3^- and PO_4^{3-})

Nitrogen Class (Number of polygons)	Total geographical area (km^2)	Average nitrogen load (kg/yr)		Average NO_3^- (mg/L)				Average PO_4^{3-} (mg/L)
		1991	2004	July 2004	Dec. 2004	Feb. 2005	May 2005	Dec. 2004
Low (46)	152.80	1194	1248	42	65	68	54	0.82
Medium (31)	189.40	5357	5633	71	82	77	86	1.5
High (6)	72.71	51385	54828	112	115	118	107	2.6

Table 5.7 Annual average nitrogen-loading zones and corresponding average groundwater quality (EC and K^+)

Nitrogen Class (Number of polygons)	Electrical Conductivity (micromho/cm)				K^+ (mg/L)	
	July 2004	Dec. 2004	Feb. 2005	May 2005	July 2004	Dec. 2004
Low (46)	1850	1707	1629	1506	75	70
Medium (31)	1830	1805	1812	1691	119	121
High (6)	1998	2264	2485	2269	56	81

Table 5.8 Monthly measured variables during the year July 2002 to June 2003.

Variables	Jul	Aug	Sep	Oct	Nov	Dec	Jan	Feb	Mar	Apr	May	June
Total monthly Rainfall (cm)	14.90	15.61	16.18	26.58	13.65	1.55	0.57	0.74	0.54	1.25	4.62	12.07
Pan evaporation (cm)	14.18	11.70	12.49	11.32	11.12	9.46	9.45	11.09	14.13	16.74	19.60	16.78
Upper zone soil Temp., (^{0}C)	34.5	33.6	34.1	33.0	31.2	29.1	29.0	31.0	33.2	35.3	37.4	36.1
Lower zone soil Temp., (^{0}C)	32.5	31.6	32.1	31.0	29.2	27.1	27.0	29.0	31.2	33.3	35.4	34.1
Drain field and vadose zones soil Temp., (^{0}C)	28.5	27.6	28.1	27	25.2	23.1	23.0	25.0	27.2	29.3	31.4	30.1

Source: Hydrometeriological Observatory, NIH, Kakinada

Table 5.9 Unsaturated zone parameters

Parameter	Upper zone	Lower zone	Drain field zone	Intermediate vadose zone
Average thickness (m)	0.50	0.50	1.00	0.50
Porosity (cm^3/cm^3)	0.35	0.35	0.35	0.40
Field capacity (cm^3/cm^3)	0.20	-	0.20	-
Bulk density (g/cm^3)	1.40	-	1.40	-
NH_4^+ adsorption Coeff. (cm^3/g)	2.00	-	2.00	-

Table 5.10 Annual water balances in the subsurface zones

Parameter	Lb nagar	Madav nagar	Suresh nagar
Rainfall (m/yr) p	1.083	1.083	1.083
Percolation from surface to upper zone (m/yr) q_{ur}	0.388	0.388	0.388
Percolation added by drain field zone (m/yr) q^*_d	0.306	0.087	0.058
Percolation from drain field zone to intermediate vadose zone (m/yr) q^*_v	0.505	0.286	0.257

Table 5.11 RISK-N model computed average mineralization and denitrification rates

Location	Parameters	Average values			
		Upper zone	Lower zone	Drain field zone	Vadose zone
Lb nagar	*Rapid mineralization rate (1/day)	0.0247	-	0.0344	-
	*Slow minneralization rate (1/day)	0.0017	-	-	-
	*Denitrification rate (1/day)	0.0032	0.0028	0.0014	0.0017
Madav nagar	*Rapid mineralization rate (1/day)	0.0370	-	0.0283	-
	*Slow mineralization rate (1/day)	0.0025	-	-	-
	*Denitrification rate (1/day)	0.0068	0.0058	0.0026	0.0030
Suresh nagar	*Rapid mineralization rate (1/day)	0.0265	-	0.0382	-
	*Slow mineralization rate (1/day)	0.0018	-	-	-
	*Denitrification rate (1/day)	0.0036	0.0031	0.0016	0.0018

* RISK-N model computed values

Table 5.12 Saturated zone RISK-N model parameters

Parameters	Value	
Average saturated zone thickness or mixing depth (amsl)	Lb nagar	+ 3.0 m
	Madav nagar	+ 1.5 m
	Suresh nagar	+ 2.5 m
Porosity (cm^3/cm^3)	0.40	
Average Darcy velocity (m/yr)	100	
Coefficient of molecular diffusion (m^2/yr)	0.078	
Longitudinal dispersivity of porous media (m)	1.6	
Transverse dispersivity of porous medium (m)	0.67	
Denitrification rate (1/day)	0.0	

Table 5.13 Impact of groundwater NO_3^--N (mg/l) variations on HCO_3^- Concentrations

Location	Seasons	Average groundwater NO_3^--N (mg/l)	Average groundwater HCO_3^- (mg/l)
Lb nagar	Mon- soon	42.55	498
	Non- monsoon	44.39	403
Madav nagar	Mon- soon	15.04	350
	Non- monsoon	9.76	405
Suresh nagar	Mon- soon	10.11	444
	Non- monsoon	7.13	454

Table 5.14 Comparison of estimated groundwater NO_3^--N from RISK-N model and measured groundwater nitrate –nitrogen during July 2002 to June 2003

Location	Measured groundwater NO_3^--N (mg/l) during July 2002 to June 2003			Groundwater NO_3^--N (mg/l) obtained from RISK-N model (monthly average)	
	Max.	Min.	Avg.	k_d=0.001	k_d = 0
Lb nagar	55.0	34.0	44.0	22.3	37.0
Madav nagar	19.0	8.0	12.69	8.46	12.0
Suresh nagar	16.0	5.86	8.83	5.77	8.16

Table 5.15 Isotope values of Groundwater samples in salinity zones

Well location (Polygon No.)	Groundwater Electrical Conductivity (EC) (micro mho/cm)	Groundwater	
		$\delta^{18}O(‰)$	$\delta D(‰)$
L B Nagar (12)	2240	-4.29	-24.76
Sureshnagar (12)	2050	-4.12	-27.84
Suryarao peta (12)	2120	-2.58	-19.75
Vakalapudi (83)	2050	-5.71	-35.92
Endlapalli (5)	2450	-2.41	-14.82
Isukapalli (7)	3710	-1.89	-12.38
Nemam (19)	5920	-1.36	-8.14
Kandarada (45)	2480	-2.32	-14.15
Rameswaram (16)	2240	-4.59	-34.52
Kondevaram (72)	2770	-3.34	-16.10